Oxidized Phosphatidylcholines (OxPCs) as Mediators of Myocardial Ischemia/Reperfusion Injury

By

Aleksandra Stamenkovic

A thesis submitted to the Faculty of Graduate Studies

Of the University of Manitoba in partial fulfillment of the requirements of the degree of

DOCTOR OF PHILOSOPHY

2020

Department of Physiology and Pathophysiology

University of Manitoba

Winnipeg

Abstract

The membrane phospholipid phosphatidylcholine (PC) is highly susceptible to oxidation during myocardial ischemia/reperfusion (I/R) injury. The production of oxidized phosphatidylcholines (OxPCs) results in cardiomyocyte death. However, the mechanism of cell death is unknown. The aim of this thesis is to determine the mechanisms by which OxPC triggers cardiomyocyte cell death during I/R injury and to identify possible therapeutic agent(s) to prevent OxPC-mediated cell death. Isolated cardiomyocytes were treated with increasing concentrations of fragmented OxPCs. Cardiomyocyte viability, bioenergetic response and calcium transients were determined. Cleaved caspase 3 and TUNEL staining were used as apoptosis markers and *High mobility group box 1* (HMGB1) protein as a marker for necrosis. The role of ferroptosis was investigated by addition of ferrostatin-1. Isolated cardiomyocytes were exposed to 1 h ischemia followed by 1 h of reperfusion. Ferrostatin-1 or the antibody to OxPCs, E06, was added at the time of reperfusion. In a porcine model of I/R, the coronary artery was occluded for 1 h by inflation of a balloon inserted in the coronary artery. At reperfusion, the E06 antibody was infused for 1 h. When isolated cardiomyocytes were incubated with five different fragmented OxPCs, 1-palmitoyl-2-(5'-oxo-valeroyl)-*sn*-glycero-3-phosphocholine (POVPC) and 1-palmitoyl-2-(9'-oxo-nonanoyl)-*sn*-glycero-3-phosphocholine (PONPC) had the most potent cardiotoxic effect. POVPC and PONPC also caused a significant decrease in Ca^{2+} transients and net contraction in isolated cardiomyocytes compared to vehicle treated control cells. PONPC and POVPC also depressed indices of cardiomyocyte respiration. Caspase 3 activation, TUNEL staining and nuclear HMGB1 activity were unaffected in cells treated with either POVPC or PONPC. However, glutathione peroxidase 4 (GPx4) activity was markedly suppressed in cardiomyocytes treated with POVPC and PONPC. An inhibitor of ferroptosis,

ferrostatin-1 also suppressed cell death induced by OxPCs. The E06 antibody directed against OxPCs also protected cardiomyocytes and infarct size was reduced in in vivo I/R porcine models. The data support the conclusion that OxPCs induce cardiomyocyte death via ferroptosis in I/R via a disruption of mitochondrial bioenergetics, calcium transients. Cell death was inhibited by ferrostatin-1 and by neutralization of OxPC with E06. These results hold significant promise to provide a new therapeutic approach for myocardial I/R injury.

TABLE OF CONTENTS

Acknowledgements

A big chapter of my life ends here, long and meaningful, difficult but a rewarding one. It has been a chapter that took a lot of strength to go through, and one that would have been hard to accomplish without support and encouragement. It is my great privilege to acknowledge all the people who helped me through this journey and without whom I wouldn't be standing here today. I am indebted to so many for the encouragement, support and for believing in me.

First, I would like to show my sincere and deep gratitude to my supervisor Dr. Grant N. Pierce, for giving me the opportunity to do research in his laboratory and providing invaluable guidance ever since. I could not have imagined myself standing here today if it wasn't for his unlimited support, patience and motivation through my PhD studies and research. I would like to thank him for providing me with the knowledge, his expert advice and constructive feedback. Working under his guidance I learnt that anything is possible particularly when it is done for the right reasons and with care. All of the challenges of being an international student were easier to face knowing I have him by my side, his listening ear, friendly advice, unconditional support and the positive spin he always brings in times of doubt. Therefore, I would like to thank him for all the times he listened to my problems offering friendly advice and encouragement to move forward. I would also like to thank him for making me feel an important part of his laboratory, not just "a student" but a recognized, cared for and valued individual. It was a true honor and a privilege to be a part of his laboratory. Thank you, Gail, Matthew and Tyler for making me feel at home.

Second, I would like to extend my deepest gratitude and appreciation to my co-advisor, Dr. Amir Ravandi, for his constant guidance, encouragement, motivation, and support. His

passion for science has always been inspirational. It has been a privilege and a great learning experience to work by his side, especially on the translational part of the project. I am grateful for his willingness to invest his time in teaching me cath lab skills, his encouragement along the way and positive attitude even when I wasted a few hours of his time by placing catheters in the wrong vessels. Working with him I learnt that once you find your passion and something you believe in, you go and take on the world, without any fear and doubt. I would like to thank him for providing a very pleasant environment to work in.

Besides my advisors, I would like to thank my committee members Dr. Lorrie Kirshenbaum and Dr. Grant Hatch for their support, encouragement, insightful comments and questions which at the time challenged me but expanded my knowledge and made me better at what I do. I would also like to extend my gratitude and appreciation to Dr. Michel Aliani, who was part of the original four, however despite leaving the committee chair, still provided me with support, feedback and a new perspective on my research.

I cannot begin to express my thanks to the members of Pierce lab: Dr. Elena Dibrov, Dr. Kimberley O'Hara, Thane Maddaford, Alex Austria and Dr. Craig Reisch for their patience, guidance and professional and personal support every day for the last 4 years. Special thanks to all of you for offering your expertise, while remaining patient and creating an extremely pleasant environment to work in. Without all of you, this experience would have never been the same. I will never forget the laughs we had during coffee breaks, parties, lab lunches, golf tournaments. Your friendship and support for the last four years have made a tremendous impact on my life and I am honored to have met you all.

I would like to extend my gratitude to all summer students that helped not only with research, but by being there and creating a friendly and fun environment to work in. Special thanks to David Nelson, for the hard work he put in helping the project and all the fun we had.

Closing this chapter would not have been the same without having a close friend by my side. A special thanks goes to my friend, Mihir Parikh. I am extremely grateful for the opportunity to go on the PhD journey together with him. I made a friend for life. Thank you for your support, encouragement and presence in stressful times. All the long talks about the music, comparisons of Serbian and Indian culture, ideas about future research, rehearsing and quoting "Friends" in every possible situation have made work so much more enjoyable. We went through this journey together, won a golf tournament, celebrated 30th birthdays together and I am looking forward to being there for your 60th and 90th. Thank you for being there for me and enriching my life.

I would like to acknowledge the members of the Ravandi lab. I would like to express my endless gratitude to Dr. Andrea Edel for her generous support, not only on the bench but also on a personal level. Working with you was a privilege, tremendous pleasure and the great source of inspiration. I would like to express my deepest and sincere gratitude for all the times you helped me, all the advice you gave me, for every word of encouragement that gave me the strength to keep on going forward. Thank you for welcoming me to your amazing family and all the memories you all have created for me!

I also had great pleasure working with my lab fellows Zahra Solati and Arun Surendran. Thank you for all your help, for all the laughs, talks, debates. You both created an extremely pleasant environment in which to work. It was a pleasure to be a part of the Lipidomics team.

My special thanks are extended to the staff of the Physiology and Pathophysiology Department. I also wish to thank the Faculty of Graduate studies and Dr. Grant Pierce for their financial support.

I would like to thank all the people in the Albrechtsen Research Centre who helped me professionally or personally.

I would like to acknowledge my deepest appreciation and gratitude to my second family Susan, Scott, Sam, Brodie and Everett. Thank you for all your love, care and endless support. Thank you for accepting me for who I am and making me a part of the family. I will always be grateful for the warm meal, a blanket and a safe place to come to when life becomes overwhelming. I am deeply indebted to all of you for all your help and support. Thank you for enriching my life. I feel blessed to have you all in it.

The last, but certainly not the least, I would like to thank my family. My parents, Sladjana and Dragan and my brother Dusan for their endless moral and emotional support throughout the years. Thank you for believing in me and supporting me to follow my own path. Thank you for all the love, care and sacrifice you did to shape my life. I would also like to extend my gratitude to my grandparents, especially my grandpa who was always there to remind me how much he believed in me and how proud of me he is. Thank you all for providing a safe port which I can turn to anytime. For every time you helped me pick myself up and helped me keep on going forward. Thank you in helping creating who I am today.

Acknowledgments of contributions

The vast majority of this study was organized, carried out and analyzed by the author of this thesis. For their contribution I would like to thank the members of the following laboratories: Pierce, Ravandi, Kirshenbaum, Aliani and Fernyhough.

List of tables

List of figures

List of abbreviations

A

AA - arachidonic acid

ACS - Acute coronary syndrome

ACSL4 - Acyl-CoA synthase long-chain family member 4

AdA – adrenic acid

ALA - alpha linolenic acid

AMI – acute myocardial infarction

Apaf-1 - apoptotic protease-activating factor 1

APL - area per lipid

ATP - adenosine triphosphate

AST - aspartate transaminase

B

C

Ca^{2+} - calcium

CAD - coronary artery disease

CAVS - calcific aortic valve stenosis

CK-MB - creatine kinase-MB

CL - cardiolipin

CMR – cardiac magnetic resonance

CVD - cardiovascular disease

D

DFO - deferoxamine

DMT1 - divalent metal transporter 1

DMPO - 5,5-Dimethyl-1-pyrroline N-oxide

DISC - death inducing signaling complex

DOX - doxorubicin

E

ECMO - extracorporeal membrane oxygenation

EGR-1 - endothelial growth related-1 transcription factor

ERK ½ - extracellular signal-regulated kinase ½

ESI - electrospray ionization

F

FADD - Fas associated death domain

FasL – Fas ligand

FOXO1 - Forkhead box protein O1

G

GPx4 - glutathione peroxidase 4

GSH - reduced glutathione

GSSG - oxidized glutathione

H

NHE - Na^+/H^+ exchanger

HMGB1 - *High mobility group box 1*

H_2O_2 - hydrogen peroxide

h-SOD - human recombinant superoxide dismutase

HUVECs - human umbilical vein endothelial cells

I

ICAM-1 - intracellular adhesion molecule 1

IL-1 - interleukin 1

IL-6 - interleukin 6

IL-8 - interleukin 8

I/R - ischemia/reperfusion

IRP1 - iron regulatory protein 1

IRP2 - iron regulatory protein 2

J

K

KLF2 - Krüppel-like factor 2

KO - knockout

KODiA-PC - 1-palmitoyl-2-(5-keto-6-octenedioyl)-sn-glycero-3-phosphocholine

L

LA - Linoleic acid

LAD - left anterior descending

LC - liquid chromatography

LDH - lactate dehydrogenase

LDL - low-density lipoprotein

LIP – labile iron pool

LOX - lypoxygenase

LPC – lysophosphatidylcholine

LPCAT3 - lysophosphatidylcholine acyltransferase 3

LPE - lysophosphatidylethanolamine

LPS – lipopolysaccharide

LV – left ventricle

M

MACCE - major cardiovascular and cerebrovascular events

MALDI - matrix assisted laser desorption ionization

MAPK - mitogen-activated protein kinase

mCL - monolysocardiolopin

MCP1 - monocyte chemotactic protein 1

MDA – malondialdehyde

MI – myocardial infarction

MLKL - mixed lineage kinase domain-like protein

MM-LDL - minimally modified LDL

MPTP - mitochondrial permeability transition pore

MS - mass spectrometry

MYC - MYC proto-oncogene protein

MVO – microvascular obstruction

N

NCX - Na^+/Ca^{2+} exchanger

NF-*κ*B - nuclear factor-κB

NHE - Na^+/H^+ exchanger

NMR – nuclear magnetic resonance

NNCM – neonatal cardiomyocytes

NOX - NADPH oxidases

Nrf2 - nuclear factor-erythroid 2-related factor 2

NSTEMI - non-ST-segment elevation myocardial infarction

NO - nitric oxide

O

$O_2^{\cdot -}$ - superoxide anion radical

$^{\cdot}OH$ - hydroxyl radical

$ONOO^{\cdot}$ - peroxynitrate anion

OxLDL - oxidized LDL

OxPAPC - oxidized PAPC

OxPC - oxidized phophatidylcholine

P

PAF-AH - platelet activating factor acetylhydrolase

PAF-R - platelet-activating factor receptor

PAPC - 1-palmitoyl-2-arachidonoyl-*sn*-3glycero-3-phosphocholine

PARP (Poly(ADP-Ribose) polymerase)

PAzPC - 1-palmitoyl-2-azelaoyl-*sn*-glycero-3-phosphocholine

PC – phosphatidylcholine

PCI - percutaneous coronary intervention

PE – phosphatidylethanolamine

PEIPC - 1-palmitoyl-2-(5,6-epoxyisoprostane E_2)-*sn*-glycero-3-phosphatidylcholine

PFKFB3 - 6-phosphofructo-2-kinase/fructose-2,6-biphosphatase 3

PHKG2 - phosphorylase kinase G2

PIP - phosphatidylinositol phosphate

PKC - protein kinase C

PONPC - 1-palmitoyl-2-(9'-oxo-nonanoyl)-*sn*-glycero-3-phosphocholine

POPC - 1-palmitoyl-2-oleoyl-sn-glycero-3-phosphocholine

POVPC - 1-palmitoyl-2-(5'-oxo-valeroyl)-*sn*-glycero-3-phosphocholine

PS - phosphatidylserine

PUFA - polyunsaturated fatty acids

PUFA-CoA - polyunsaturated fatty acid-acyl-CoA

Q

R

RET - reverse electron transport

RIPK1 - receptor –interacting protein kinase 1

RNS - reactive nitrogen species

ROS - reactive oxygen species

RSL3 - RAS selective lethal

S

SERCA - sarcoplasmic reticulum Ca^{2+} pump ATP ase

SOD - superoxide dismutase

SPECT - single-photon emission computed tomography

STEMI - ST segment elevation myocardial infarction

T

TF - tissue factor

TfR1 - transferrin receptor 1

TNF-α - tumor necrosis factor α

TRADD - tumor necrosis factor α associated death domain

TRAIL - TNF-related apoptosis inducing ligand

TRFR1 - TNF-α receptor 1

TRPC5 - transient receptor potential 5-containing channels

U

UA – unstable angina

V

VCAM - vascular cell adhesion molecule expression

VEGFA - vascular Endothelial Growth Factor A

VDAC 2/3 - voltage dependent ion channel 2/3

VSMCs - vascular smooth muscle cells

CHAPTER I: Review of literature

Cardiovascular disease

Cardiovascular disease (CVD) represents the leading global cause of death with 17.6 million deaths in 2016 [1]. This number is expected to grow to 23, 6 million by 2030 [1]. It is the number one cause of death in the United States with 840,678 deaths in 2016 [1] and second leading cause of death in Canada [2]. In Europe 3.9 million people die due to CVD each year [3]. Coronary artery disease (CAD) was a leading cause of death attributable to CVD in 2016, accounting for 43.2% of deaths [1].

Acute myocardial infarction (AMI)

CAD occurs as a result of atherosclerosis which is a chronic disease characterized by endothelial dysfunction, lipid infiltration and accumulation, and smooth muscle cell proliferation in the arterial wall leading to formation of atherosclerotic plaque. Unstable plaques are vulnerable to spontaneous rupture, erosion or fissure leading to thrombosis and occlusion, occluding blood flow and resulting in ischemic symptoms. Myocardial ischemia is defined by an imbalance between oxygen supply and demand in heart myocardium. MI is the progression of ischemia in which myocardial cells die without recovery [4]. MI represents the leading cause of morbidity and mortality in the United States and contributes with more than $11 billion in annual hospitalization costs [1].

Even with advanced therapies and pharmacology the 30-day mortality rate in the acute MI has decreased recently to 12% [5]. However, improved survival leads to increase of patients who are at risk for development of heart failure [6] [7].This highlights the need for further therapies to minimize the morbidity and mortality of acute myocardial infarction.

Acute coronary syndrome (ACS)

Acute coronary syndrome (ACS) is an umbrella term for clinical symptoms of acute myocardial ischemia and it includes unstable angina (UA), myocardial infarction (MI) (with or without ST-segment elevation). Partially occluded coronary arteries present without the ST-segment elevation and therefore are classified as UA or NSTEMI (non-ST-segment elevation myocardial infarction) based on whether or not the elevation of cardiac troponin is present and the damage occurs [8]. Complete occlusion of the arteries presents with the ST-segment elevation and prominent positive T waves on ECG, elevated troponin levels and tissue injury and is therefore classified as STEMI (ST-segment elevation myocardial infarction). The location of ST elevation on ECG depends on the ischemic myocardial region [9]. According to the American Heart Association report, 38% of patients presenting with an ACS have STEMI [10]. The major cause of STEMI is atherosclerotic plaque rupture or erosion, which causes the occlusion of the epicardial coronary artery and transmural ischemia [11]. The final infarct size depends on the size of the ischemic area at risk, the duration of the occlusion, and the magnitude of the collateral blood flow. The decrease in mortality and improvement in prognosis in STEMI patients in the last few decades is largely due to current therapeutic strategies which aim to decrease the duration of the ischemia by reperfusion. Early primary percutaneous coronary intervention (PCI) is the preferred treatment for patients with STEMI since studies showed significant reduction in morbidity and mortality compared to thrombolytic therapy [12]. However, the mortality and heart failure after STEMI remains high [13]. Within the first year following PCI there was a high event rate with 24.4 % major cardiovascular and cerebrovascular events (MACCE), 18.6% worsening or re-hospitalization for heart failure and 5% mortality [14]. In addition, other studies have reported 5% at 90 days, 6% at 1 year and 14% at 3 years for all-

cause mortality [15-17]. The measurement of the left ventricular ejection fraction was found to be the most powerful predictor of survival following PCI [18]. In addition, analyses of 10 randomized clinical trials showed that infarct size, measured by cardiac magnetic resonance (CMR) or technetium-99m sestamibi single-photon emission computed tomography (SPECT) within 1 month after primary PCI is strongly associated with all-cause mortality and hospitalization for heart failure within 1 year [19].

Early reperfusion of the occluded artery is the major goal of therapy for STEMI patients. In the late 1970s thrombolytic therapy to dissolve coronary thrombus was used to restore the blood flow to the heart muscle and reduce mortality. Later in the 1980s, balloon angioplasty and later the use of stent were introduced as methods for opening the occluded vessels. These types of interventions, referred to as PCIs were associated with short term reduction in mortality, reinfarction and stroke in STEMI patients compared to fibrinolytic therapy [20]. Reperfusion therapy has reduced long term in hospital mortality with PCI or reperfusion in general (40%).

Myocardial ischemia/reperfusion injury

Despite the advancement in pharmacological and interventional therapies, myocardial ischemia reperfusion injury still remains the leading cause of morbidity and mortality worldwide. Partial or complete occlusion of the artery by an atherosclerotic plaque leads to deprivation of oxygen and nutrients to the distal myocardium [8]. The main aim of therapeutic approaches is early reperfusion. Even though timely reperfusion, either by thrombolytic therapy or primary PCI is the most effective way of reducing the myocardial damage in STEMI patients, reperfusion itself can induce cardiomyocyte cell death and this phenomenon is called reperfusion injury. It is responsible for more than 50 % of final infarct size [21].

Morphological features of the reperfused myocardium are cardiomyocyte membrane disruption, mitochondrial swelling and disruption, karyolysis, microvascular destruction, inflammation and interstitial hemorrhage [22, 23]. Infarct size is a clinically useful endpoint in clinical trials and an important prognostic tool as a recent meta analyses from 10 randomized clinical trials showed [19]. When measured within 1 month from PCI, infarct size strongly correlates with all-cause mortality and hospitalization for heart failure within 1 year [19]. The final infarct size depends on several factors: the duration of coronary occlusion, the size of the ischemic area at risk and the extent of the residual collateral blood flow and microvascular dysfunction [24]. A post-infarction reduction in left ventricular ejection fraction is a major cause of chronic heart failure worldwide [25].

Clinically, myocardial I/R injury is associated with four conditions: myocardial stunning, reperfusion arrhythmias, no-reflow phenomenon and lethal reperfusion injury.

Myocardial stunning is reversible contractile dysfunction that occurs on reperfusion despite the restoration of blood flow. Despite the most up to date reperfusion strategies, such as PCI, systolic and diastolic stunning still occurs in STEMI patients [26, 27]. It occurs as a consequence of the effects of oxidative stress and Ca^{2+} overload on myocardial contractile apparatus [28, 29]. This has been supported by studies that showed that administration of antioxidants reduces myocardial stunning [30, 31]. The occurrence of myocardial stunning may worsen hemodynamic conditions in patients who are already unstable. Additionally, repeated episodes of myocardial stunning can cause chronic contractile dysfunction and longer recovery times [32].

Reperfusion arrhythmias occur in patients undergoing reperfusion therapy with an occurrence rate of 88.7% in patients undergoing thrombolytic therapy and 83.3% in patients

undergoing PCI therapy [33]. This represents the major comorbidity of myocardial infarction. The most common types of reperfusion arrhythmias are ventricular ones, ranging from premature ventricular contractions, sustained or non-sustained episodes of ventricular tachycardia, accelerated idioventricular rhythm and ventricular fibrillation. They were shown to predict larger infarct size despite the optimal microvascular reperfusion [34, 35].

Microvascular obstruction (MVO) or no reflow phenomenon occurs when the myocardium remains with poor perfusion even though the blood flow in the epicardial artery has been restored. MVO is a major independent predictor of morbidity and mortality and the major contributor to infarct size [36]. It occurs in 10-30% of patients with a reperfused STEMI [37, 38]. Measured by cardiac magnetic resonance, presence and extent of MVO are strongly associated with mortality and heart failure hospitalization within 1 year [39]. Early MVO is an independent factor for prognosis of adverse outcomes such as recurrent ischemic symptoms, heart failure and repeated hospitalization within 5 years [40] . Different mechanisms have been proposed so far to contribute to MVO: 1) the embolization of debris from the culprit atherosclerotic plaque [41]; 2) vasoconstriction induced by vasoconstrictor substances released from the culprit lesion [42, 43]; 3) platelet and platelet/leukocytes aggregates released from the culprit lesion [44]; 4) physical destruction of the microvascular endothelium [45]; 5) extravascular compression of microcirculation due to edema in the surrounding myocardium [46]. Different approaches are currently used to reduce microvascular obstruction. Antiplatelet agents, coronary vasodilators and statins administered before the PCI reduce the MVO [47-53]. Distal protective devices had no effect on outcomes whereas devices for aspiration provided protection in patients with an MI [41].

Lethal reperfusion injury is defined as reperfusion-induced death of cardiomyocytes that were viable at the time that reperfusion was initiated. In other words, there are cardiomyocytes that are viable at the end of ischemia, but they are fragile and whether they survive or not would depend on the reperfusion conditions. Both experimental studies and clinical trials have shown that lethal reperfusion injury is responsible for more than 50% of the final infarct size [21]. The major contributors are oxidative stress, Ca^{2+} overload, opening of the mitochondrial permeability transition pore (MPTP) and hypercontracture [21]. Currently there is no available therapy for lethal reperfusion injury.

Therapeutic strategies for reducing myocardial I/R injury

An effective therapeutic strategy for myocardial I/R injury currently does not exist. However, different approaches that could be categorized as either mechanical or pharmacological have been tested in the past. Two of the major mechanical approaches are ischemic preconditioning and ischemic post conditioning.

Ischemic pre-conditioning was first tested in 1986 by Murray et al who reported that brief cycles of occlusion before the ischemic insult leads to a reduction in infarct size in dogs [54]. However, this approach could not be applied in clinical settings in patients undergoing STEMI. Therefore, the concept of ischemic post conditioning was introduced for the first time by Zhao [55] in 2003 in canine hearts. They reported a significant reduction in the infarct size (44%) after introducing three cycles of 30 s left anterior descending (LAD) artery occlusion and 30 sec of reperfusion followed by 3h reperfusion [55]. The first clinical study to examine the effects of post ischemic conditioning was done by Staat et al. in 2005 who found a 36% decrease in infarct size in the post ischemic conditioning group [56]. Larger clinical studies examining the same

pattern of post conditioning showed no difference [57], [58]. The ongoing DINAMI-3 (Danish Study of Optimal Acute Treatment of Patients with ST-segment elevation Myocardial Infarction-3) study is looking into effects of post conditioning in 2000 patients who will be allocated into 3 groups: primary PCI, postconditioning and deferred stenting. The primary outcome of the study will be all-cause mortality or heart failure at 2 years (NCT01435408).

Another form of conditioning of myocardium that has been proved successful in animal models is the remote conditioning, in which several brief ischemic periods are introduced in a distant organ [59]. A small clinical trial including 333 STEMI patients, reported greater myocardial salvage when the remote conditioning was applied (4 cycles of 5 min inflation and 5 min brachial cuff deflations) before PCI compared to the control group who received PCI treatment only [60]. A larger ongoing clinical trial, CONDI-2 (Effect of Remote Ischemic Conditioning on Clinical Outcomes in STEMI Patients Undergoing pPCI) will confirm whether remote ischemic preconditioning could be an effective therapy for STEMI patients (NCT02342522).

Hypothermia has been reported as an effective therapy for reducing the extent of ischemic injury in animal models [61, 62]. However, its application in clinical settings is limited due to a lack of cooling procedures capable of achieving the targeted temperature rapidly enough. The CHILL-MI (Rapid endovascular catheter core cooling combined with cold saline as an adjunct to PCI for the treatment of acute myocardial infarction) study showed that despite an inability to reach the target temperature, in 75% of patients before the reperfusion, there was no decrease in myocardial infarct size [63].

One of the promising pharmacological agents in treatment of STEMI patients is cyclosporine A. It inhibits the MPTP pore opening and in a small pilot trial it has been shown to reduce infarct size when administered before PCI [64]. The ongoing CIRCUS (Cyclosporine

and Prognosis in Acute MI Patients) trial will give further insight on the effects of cyclosporine administration on mortality, hospitalization for heart failure and left ventricular remodeling at one and three years following the treatment (NCT01502774).

The effects of different beta blockers on infarct size have been studied in both pre-clinical studies as well as in patients with STEMI, with contradictory results. Intravenous administration of atenolol showed no effects on infarct size [65]. Administration of metoprolol before the reperfusion showed promising effects on infarct size in pre-clinical trials [66, 67]. This opened the possibility for a few clinical trials which led to contradictory results. In METOCARD-CNIC (Effect of early metoprolol on infarct size in ST-segment-elevation myocardial infarction patients undergoing primary PCI: the Effect of Metoprolol in Cardioprotection During an Acute Myocardial Infarction) trial which included 270 patients, infarct size, measured by CMR was significantly smaller in the metoprolol group [68]. On the contrary, the much larger COMMIT (ClOpidogrel and Metoprolol in Myocardial Infarction Trial) trial that included 45,852 patients, reported reduced rates of ventricular fibrillations and reinfarction, however, no effect on mortality was observed [69]. A meta analyses of randomized clinical trials on clinical outcomes with beta blockers administration in patients with STEMI reported that in 60 trials including 102,003 patients beta blockers were effective in reducing the mortality in pre-reperfusion time. Furthermore, their administration before reperfusion in reperfusion era did reduce the infarct size and angina, without any effects on mortality [70].

Another approach to treat myocardial I/R injury has been attempted by targeting glucose metabolism. The IMMEDIATE (Immediate Myocardial Enhancement During Initial Assessment and Treatment in Emergency Care) study showed that administration of glucose/insulin/potassium (GIK) during transfer to the hospital in patients with suspected acute

coronary syndrome, led to a reduction in infarct size measured by CMR [71]. Glucagon-like peptide is an incretin hormone involved in glucose metabolism and therefore investigated as a therapy for diabetes [72]. This hormone maintains glucose homeostasis by preventing glucagon secretion and promoting insulin secretion and its receptors were found in the heart tissue among others [73]. Glucagon-like peptide and its analogs lead to a decrease in infarct size in animal models of myocardial I/R injury [74-77]. Exenatide is a synthetic glucagon-like peptide analogue which was tested in STEMI patients. Intravenous administration of exenatide 15 minutes before the procedure and maintenance for 6 hours after the procedure showed the salvage of the heart measured by CMR compared to placebo [78]. The mechanism of its action includes the activation of the glucagon –like receptor 1, which leads to activation of cAMP and cGMP and inhibition of apoptosis [79].

Pathophysiology of myocardial I/R injury

Experimental studies have identified several factors that mediate myocardial I/R injury: intracellular calcium overload, rapid restoration of physiological pH, inflammation and oxidative stress.

Intracellular Ca^{2+} overload

During ischemia changes in pH, as well as an increase in oxidative stress will result in an intracellular accumulation of Ca^{2+}. The depolarization of the plasma membrane leads to the opening of L-type Ca^{2+} channels leading to a further increase in the intracellular Ca^{2+} concentration. Oxidative stress and a consequent decrease in -adenosine triphosphate (ATP) production lead to a reduced Ca^{2+}-pump ATPase (SERCA) activity [80, 81]. The major role of

SERCA is to remove Ca^{2+} from the cytosol into sarcoplasmic reticulum. Therefore, its reduced activity will contribute to cytosolic Ca^{2+} overload. Intracellular Ca^{2+} overload and rapid re-establishment of physiological pH leads to the opening of the MPTP. The restoration of mitochondrial membrane potential leads to Ca^{2+} entry into the mitochondria through the Ca^{2+} uniporter which also contributes to further MPTP opening. Experimental studies which have used pharmacological antagonists of the sarcolemmal Ca^{2+} channel [82] or Ca^{2+} uniporter [83] administered at the onset of reperfusion were successful in reducing the infarct size by 50%. However, clinical trials that have used calcium channel blockers have failed to show beneficial effects [84].

Rapid restoration of physiological pH

The lack of oxygen during ischemia can switch cardiomyocyte metabolism to anaerobic respiration. This results in lactic acid accumulation leading to a decrease in intracellular pH less than 7.0. In order to restore pH Na^+/H^+ exchanger (NHE) will be activated to extrude H^+, however this leads to intracellular accumulation of Na^+ [85]. Na^+ overload activates the Na^+/Ca^{2+} exchanger (NCX), which will result in intracellular Ca^{2+} overload [85]. Over expression of the NCX will augment cardiomyocyte injury [86]. Upon reperfusion, rapid restoration of pH by lactate washout contributes to reperfusion injury by opening the MPTP and producing hypercontracture [87]. MPTP is a non-selective channel on the inner mitochondrial membrane. Its opening leads to mitochondrial membrane depolarization, uncoupling of oxidative phosphorylation and ultimately to ATP depletion and cell death [88, 89]. Using acidic buffer during reperfusion improved heart function [90] and reduced the size of a MI [91]. Therefore, a more recent study examined if a slower normalization of pH following reperfusion could be an

efficient therapeutic intervention. Therapeutic hypercarpnia was used as a post conditioning strategy in I/R injury in rats. This study showed that inhalation of 20 % CO_2 led to a reduction in infarct size [92]. It prevented mitochondrial damage by inhibiting mitochondrial permeability pore opening and preserving mitochondrial membrane potential [92].

Inflammation

Inflammation is a process required for healing following a myocardial infarction. Cardiomyocytes and endothelial cells secrete chemoattractants such as cytokines, ROS, which will draw neutrophils to the injured area within the first 6 hours of myocardial reperfusion. Their migration to the myocardial tissue is facilitated by adhesion molecules where neutrophils release oxidants and proteases [93]. It is still unknown whether the inflammatory response during I/R injury is simply a response or whether it actively participates in cardiomyocyte cell death. Animal studies targeting a decrease in inflammation during I/R injury were largely positive, reporting up to 50% reduction in MI size [94-96]. Different approaches were used to decrease inflammation following myocardial infarction including: antibodies against CD-18 (beta chain) of neutrophil adherence glycoproteins [95], P-selectin glycoprotein ligand-1 on neutrophil-endothelial cells interaction [94], neutrophil depletion [97], monoclonal antibodies against intracellular adhesion molecule 1 (ICAM-1) [96], losartan, an angiotensin II receptor blocker, [98], anti-inflammatory annexin protein [99] and a pain reliever, sumatriptan, shown to have anti-inflammatory properties [100]. Alternatively, clinical studies targeting inflammation using adenosine (AMISTAD), which inhibits neutrophil and monocyte activation [101], pexelizumab, an immunosuppressive, humanized monoclonal antibody [102], FX06 which is a naturally

occurring peptide derived from fibrin shown to prevent leukocyte migration, [103] have shown no impact on clinical outcomes.

Oxidative stress

Oxidative stress occurs when there is imbalance between the generation of reactive oxygen species (ROS) and the activity of the antioxidant defense system [104]. ROS are chemically reactive molecules produced in all aerobic cells [105, 106]. Various techniques such as alpha-phenyl N-tert-butyl nitron spin trap probes [107], nitron 5,5-Dimethyl-1-pyrolineN-oxide (DMPO) [108] and electron spin resonance spectrometer were used since the early 1980s and 1990s to measure ROS production and release in I/R injury. Their levels increased during myocardial I/R injury [109] and the major ROS species which increased at reperfusion includes hydrogen peroxide (H_2O_2), superoxide anion radical $O_2^{\cdot -}$, hydroxyl radical ($^{\cdot}OH$), peroxynitrate anion ($ONOO^{\cdot}$) [109]. The major sources of ROS in the heart during I/R injury are: xanthine oxidases, NADPH oxidases (NOX), mitochondrion and uncoupled eNOS [110-112]. Moreover, the excess production of ROS during reperfusion has been considered as a crucial factor of cardiomyocyte cell death, responsible for 50% of the final infarct size [21].

NOX use NADPH as an electron donor to catalyze reduction of O_2 that results in a production of $O_2^{\cdot -}$. The detrimental effect of NOX- derived ROS has been shown in human I/R injury [113]. In murine hearts, the knockout (KO) of NOX1 and/or NOX2 gene is protective, suggesting the detrimental role of NOX in I/R induced damage [114]. The production of $O_2^{\cdot -}$ increases during reperfusion in myocardium. Once produced, it can react with nitric oxide (NO), which is a molecule with multiple physiological roles including the regulation of endothelial vasodilation, antioxidant effect and the inhibition of platelet and neutrophil action [115, 116].

However, once it reacts with $O_2^{\cdot -}$, NO can also have a detrimental effect since it leads to a production of $ONOO^-$ which is cytotoxic [117]. $ONOO^-$ production increases as a consequent of increased NO and $O_2^{\cdot -}$ concentrations in I/R injury [118]. Superoxide anion dismutase can reduce the damage formed by $O_2^{\cdot -}$ and leads to a production of hydrogen peroxide (H_2O_2). However, through the Fenton reaction , in presence of Fe^{2+} or Cu^{2+} , H_2O_2 can be converted to hydroxyl radical ($OH^{\cdot}$) and hydroxyl anion radical (OH^-), both of which are more potent radicals than $O_2^{\cdot -}$ and H_2O_2.

Xanthine oxidase is an enzyme present in the vascular endothelium and cardiomyocytes, and its action leads to the generation of $O_2^{\cdot -}$, H_2O_2 and $OH^{\cdot}$ [110]. During ischemia, the conversion of xanthine dehydrogenase to xanthine oxidase is increased [119]. Moreover, there is an increase in the production of hypoxanthine, which is produced by adenosine triphosphate (ATP) degradation and serves as a substrate for the xanthine oxidase [119]. Once reperfusion is introduced, the abundance of hypoxanthine, xanthine oxidase and oxygen will lead to a burst in superoxide production.

NO synthase are a family of enzymes responsible for the conversion of amino acid l-arginine to L-citrulline and NO. In the absence of substrate, endothelial NOS becomes uncoupled which leads to a production of $O2^{-\cdot}$ instead of NO [111, 112, 120].

Mitochondria are cellular organelles in which the main energy production occurs through the process of oxidative phosphorylation. This process involves the transfer of electrons through Complex I, II, III and IV to oxygen which is the final recipient of the electrons. During I/R, these complexes are severely affected. The lack of oxygen during ischemia leads to an impaired function of the electron transport chain which further leads to a large production of ROS which was detected in animal models as well as in patients undergoing coronary revascularization

[121]. Electron leakage through complexes I and III are the major sites of $O_2^{\cdot -}$ production in mitochondria [122]. Alteration of electron transport during ischemia through complex I as well as the accumulation of succinate, the substrate for the complex II, contributes significantly to oxidative stress during reperfusion. Upon reperfusion, the accumulated succinate is hydrolyzed by complex II at a maximal rate generating an excess pool of electrons which by the process of Reverse Electron Transport (RET) flow backwards through complex I [123]. This process further leads to a production of superoxide by NADPH dehydrogenase [124-126]. The increased production of ROS causes injury to the mitochondrial membrane, membrane depolarization, an uncoupling of oxidative phosphorylation and altered respiration [127]. Changes in membrane structure will lead to a release of cytochrome c, caspase activation and cell death [128].

Mitochondrial transplantation as a cardioprotective approach during I/R injury has been given attention in the last decade since the first *in-vivo* study using this approach produced an increase in ATP content, a decrease in cardiomyocyte loss, a reduction in infarct size and an improvement in myocardial function [129]. The isolation of functional mitochondria from the remote tissue which is unaffected by ischemia and its delivery into the ischemic zone before reperfusion is believed to improve functional recovery and prevent cell loss. This treatment has been successfully carried out in 2016 in 5 pediatric patients who were on extracorporeal membrane oxygenation (ECMO) support due to myocardial dysfunction caused by I/R injury [130]. In all patients, ventricular function was improved and 4 of them were successfully separated from the ECMO machine. The patients did not have adverse complications such as arrhythmias, scarring and intramyocardial hematoma [130].

Oxidative stress caused by the increased production of ROS causes alterations of various cellular components. It is well documented that oxidative stress leads to a modification of

phospholipids and proteins through the process of lipid peroxidation and oxidation of thiol group [131]. In this way, the structure and function of the membrane is altered as well as the function of cellular proteins. In early 1990s, Ambrosio et al studied perfused rat hearts to demonstrate that radical-induced membrane lipid peroxidation occurs during reperfusion [132]. They showed that the levels of malondialdehyde (MDA), a marker of lipid peroxidation increases in reperfused heart but not in hearts subjected only to ischemia or I/R treated with human recombinant superoxide dismutase (h-SOD) [132]. Mammalian cells contain several thousand different lipid species [133], many of which are involved in the initiation, progression and execution of cell death [134]. Early studies in this field showed that lipid peroxidation products are present in the sarcolemma, mitochondria and sarcoplasmic reticulum during myocardial ischemia reperfusion injury, suggesting that membrane phospholipids are a class of cellular molecules that are highly susceptible to oxidation [135].

ROS production also leads to DNA damage and cell death [21]. Free radical production during reperfusion also results in an intracellular accumulation of calcium (Ca^{2+}) by affecting the function of various components of Ca^{2+} handling system. They decrease Ca^{2+} efflux by depressing the function of sarcolemmal Ca^{2+} pump ATPase [136] and increase Ca^{2+} influx by depressing Na^{+}/K^{+} ATPase function [137]. Furthermore, oxidative stress depresses the function of SERCA, which is responsible for import of Ca^{2+} from the cytosol into the sarcoplasmic reticulum [138, 139]. ROS increases the activity of the ryanodine channel by inducing its S-nitrosylation and S-glutathionylation, which contributes to intracellular Ca^{2+} overload during I/R [140].

The antioxidant system includes various enzymes and substances that act to protect against oxidative damage. There are different mechanisms suggested through which antioxidants

exhibit their function such as: a)an inhibition of the formation of the ROS; b) scavenging ROS and their precursors; c) attenuating the catalysis of ROS by binding to metal ions; d) increasing endogenous antioxidant production. The most extensively studied antioxidants are superoxide dismutase (SOD), catalase, glutathione peroxidase ad vitamin E. SOD catalyzes the dismutation of the superoxide anion radical ($O_2^{\cdot -}$) to H_2O_2 which is further converted to H_2O and O_2 by catalase or glutathione peroxidase. For this, glutathione peroxidase requires the presence of reduced glutathione (GSH) resulting in the formation of oxidized glutathione (GSSG) at the end of the reaction. The oxidized form is then recycled to GSH by glutathione reductase which requires NADPH for its action. In the past, studies that used different approaches showed the importance and the contribution of glutathione peroxidase in myocardial I/R injury. The studies that used glutathione peroxidase inhibitors such as maleic acid diethyl ester or buthionine sulfoxamine in both rat and feline heart produced an impaired recovery of the systolic function following ischemia [141-143]. Moreover, if there was a deficiency of selenium (which is required for the glutathione peroxidase function), researchers found an increased susceptibility to oxidative damage as well as depressed contractile function following I/R injury [144]. Transgenic mice overexpressing glutathione peroxidase were resistant to I/R injury as demonstrated by a reduction in infarct size and an improved recovery of contractile force, suggesting its detrimental role in the protection against oxidative damage [145].
Glutathione peroxidase has recently attracted research attention because one of the family members, GPx4, may have an important role in a recently described form of cell death called ferroptosis. This will be discussed in more detail later in this treatise.

Oxidative stress not only causes direct changes in organic molecules, it also affects genes by modifying transcriptional factors. The most studied transcriptional factor is nuclear factor-κB

(NF-kB). When its inhibitory subunit gets activated by phosphorylation in presence of ROS, it binds to DNA and promotes the transcription of genes for interleukin 6 (IL-6), which further affects tumor necrosis factor α (TNF-α) and tumor necrosis factor β (TGF-β) [146]. These molecules are responsible for the extracellular matrix remodeling in the heart and fibrosis, which both lead to alterations in electrophysiological properties of the heart.

ROS accumulation also leads to an activation of nuclear factor-erythroid 2-related factor 2 (Nrf2). It is found in cytosol sequestered by Keap [147]. ROS causes the covalent modification of Keap leading to its dissociation from Nrf2 which can now translocate to the nucleus and promote expression of antioxidant enzymes such as catalase, glutathione peroxidase, glutathione reductase, glutathione transferase, oxygenase-1 [147].

Oxidative stress, due to production of ROS in myocardial reperfusion results in cell injury by alteration of intracellular molecules including lipids. The most abundant class of phospholipids in biological membranes is phosphatidylcholine (PC) which is highly susceptible to oxidation. Oxidation of PC leads to a production of bioactive compounds which were recently recognized to be responsible in cardiovascular pathologies.

Oxidized phosphatidylcholine (OxPC)

General characteristics

Phospholipids represent a class of polar lipids found in biological membranes and in the outer shell of circulating plasma lipoproteins [148]. Structurally they contain a glycerol backbone, two fatty acids and a phosphate containing polar head group (Figure 1). According to the head group, they can be clustered into several subclasses. Phosphatidylcholine (PC) is the most abundant class comprising 70% of the total phospholipids in the heart of rat [149].

Phosphatidylethanolamine (PE) was shown to be the second most abundant phospholipid in the rat heart comprising 25% of the total phospholipids [149]. Phosphatidylinositol (PI) and phosphatidylserine (PS) are predominantly cellular, rather than a part of lipoproteins. The sn-1 position in phospholipids can be linked to an acyl residue via an ester bond or an alkyl residue via an ether bond and it usually has a saturated fatty acid bound to it. The sn-2 position is always linked to an acyl residue with a polyunsaturated fatty acid bound to it [150].

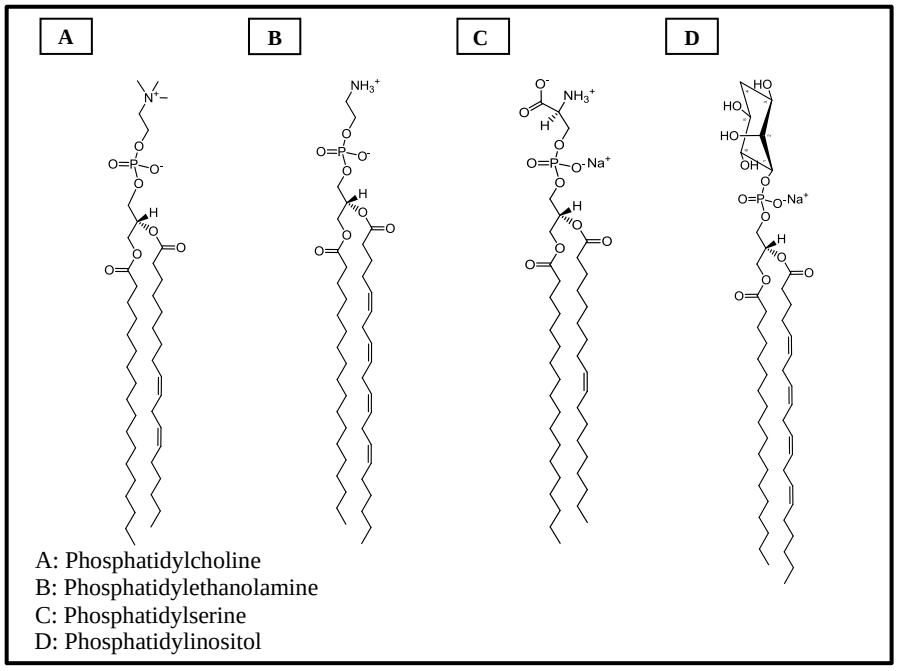

Figure 1.Chemical structures of different phospholipid classes; **A**: Phosphatidylcholine; **B**: Phosphatidylethanolamine; **C**: Phosphatidylserine; **D**: Phosphatidylinositol; Stamenkovic A, Pierce GN, Ravandi A. Oxidized lipids: not just another brick in the wall. Can J Physiol Pharmacol. 2019 Jun;97(6):473-485. *Reprinted with permission*

Phospholipids have various physiological roles. They represent the major building blocks for the permeability barrier of all cells and organelles, thereby maintaining homeostasis. They are involved in signaling processes and provide precursors for signaling molecules [151]. Phospholipids also regulate membrane protein activities [152].

The presence of a polyunsaturated fatty acid in the sn-2 position makes these molecules highly prone to oxidation. This reaction can be facilitated by non-enzymatic free radical modification of the sn-2 fatty acid or under certain physiological conditions enzymes such as lipoxygenase or cyclooxygenase could be involved [153]. Oxidation of the polyunsaturated fatty acid results either in fragmentation of the sn-2 fatty acid chain or the addition of an oxygen molecule to the sn-2 fatty acid residue [150, 154] (Figure 2).

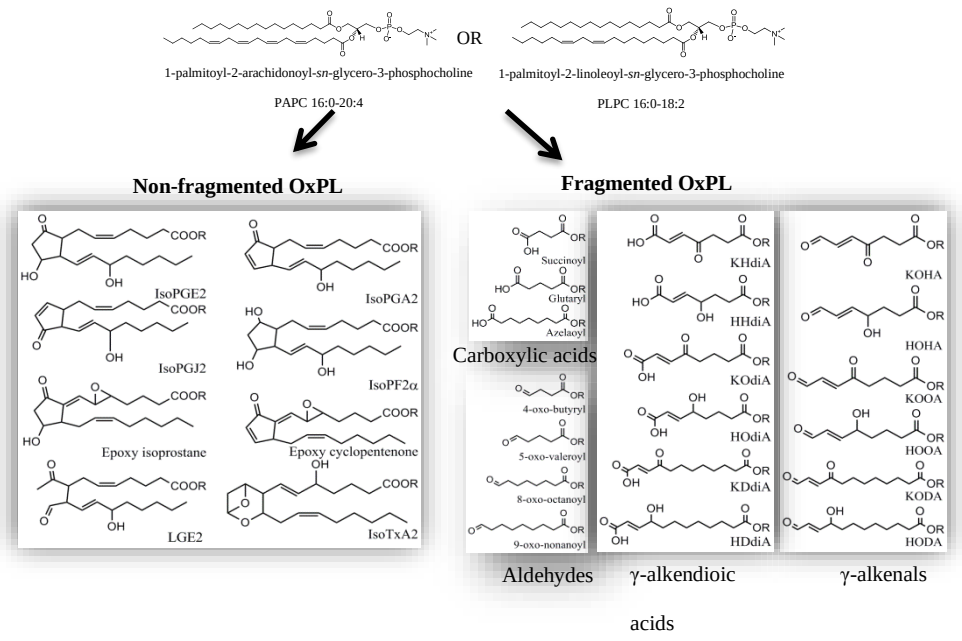

Figure 2. Lipid peroxidation products – representative non- fragmented and fragmented fatty acyl moieties that can be produced following oxidation of sn-2 polyunsaturated fatty acids

(PUFA) Stamenkovic A, Pierce GN, Ravandi A. Oxidized lipids: not just another brick in the wall. Can J Physiol Pharmacol. 2019 Jun;97(6):473-485. *Reprinted with permission*

Just as the structural characteristics of different phospholipids will result in different physiological functions for each of the phospholipids, phospholipids acquire novel roles upon oxidation that are not characteristic of their precursors. Similarly within different oxidized phospholipids, the large variety of chemical structures, the degree of modification and the physical characteristics of the different oxidized phospholipids will produce different biological actions in different tissues (Figure 3). Because PC is highly prone to oxidation [155], the screening studies have shown that the most commonly identified class of oxidized phospholipids is restricted to OxPC, and because of the growing evidence of their involvement in cardiovascular pathologies, the focus of this thesis, therefore, is on oxidized phosphatidylcholine.

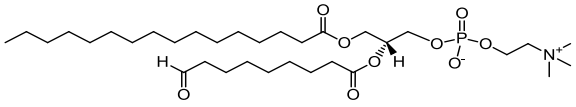

1-palmitoyl-2-(9'-oxo-nonanoyl)-*sn*-glycero-3-phosphocholine (PONPC)

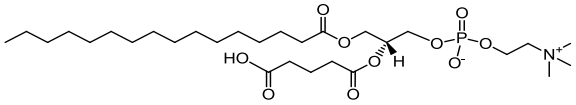

1-palmitoyl-2-glutaryl-*sn*-glycero-3-phosphocholine (PGPC)

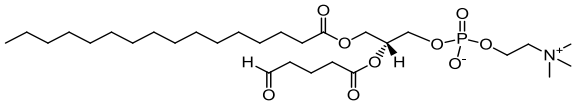

1-palmitoyl-2-(5'-oxo-valeroyl)-*sn*-glycero-3-phosphocholine (POVPC)

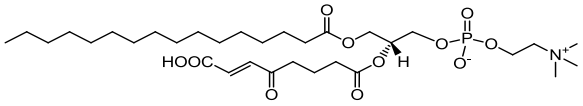

1-palmitoyl-2-(5-keto-6-octenedioyl)-sn-glycero-3-phosphocholine (KODiA-PC)

Figure 3. Chemical structures of the most common fragmented OxPC species involved in CVD Stamenkovic A, Pierce GN, Ravandi A. Oxidized lipids: not just another brick in the wall. Can J Physiol Pharmacol. 2019 Jun;97(6):473-485. *Reprinted with permission*

Generation

Lipid peroxidation has recently been described to play a major role in non-apoptotic cell death. Cell death is associated with an accumulation of lipid hydroperoxydes in membranes. The most common electrophiles involved in lipid peroxidation are ROS and reactive nitrogen species (RNS). Both are highly produced in the most important cardiovascular pathologies, atherosclerosis [156] and I/R injury [157]. Due to high energy demand, cardiomyocytes are rich in mitochondria, which are the major site of ROS production [158]. The most important oxygen radicals involved in different diseases are the hydroxyl radical (•OH), the superoxide anion radical (O_2^-), singlet oxygen ($^1O_2$) and hydrogen peroxide (H_2O_2) [159]. Oxidative phosphorylation within mitochondria leads to a large production of the superoxide anion $O_2^{\bullet-}$ [160]. ROS production can also be enhanced through Fenton chemistry. The Fenton reaction refers to a chemical reaction between hydrogen peroxide and ferrous iron resulting in the production of reactive species that can oxidize intracellular molecules [161]. Polyunsaturated fatty acids (PUFAs) esterified on the sn-2 position of membrane phospholipids are highly susceptible to enzymatic or non-enzymatic oxidation, resulting in the production of primary products of lipid peroxidation, lipid hydroperoxydes. The primary products of lipid peroxidation can decompose and form the secondary products, low and high molecular aldehydes [162]. Aldehydes can interact with cellular components like amines, amino acids and proteins, forming covalent products [163]. These aldehydes can in turn further promote the induction of cell death

pathways [164]. Non-enzymatic lipid peroxidation consists of three major steps: initiation, propagation and termination. The initiation step involves the abstraction of hydrogen from the polyunsaturated phospholipid chain by free radicals. As a result, the carbon centered radical is formed and it is able to react with molecular oxygen to form peroxyl radicals. Hydrogen abstraction is irreversible and it commits the phospholipid to a reaction with the oxygen. In the propagation phase oxygen is added to a carbon centered radical. This step is reversible, fast an diffusion controlled as it depends on how much oxygen gets to the radical. As a result peroxyl radicals are formed. Peroxyl radicals can further abstract the hydrogen from other phospholipids propagating a chain reaction. The half-life of peroxyl radicals can be from milliseconds to seconds, allowing different reaction pathways to occur [165]. The final step is a termination step which occurs either when two radicals react to form a stable product or when antioxidants are able to stop the reaction [166]. OxPC can be divided into two groups. The non-fragmented group which consists of species that have the same number of carbon as the precursor. They undergo cyclization, rearrangement and further oxidation following the initiation step of lipid oxidation, resulting in formation of OxPCs with functional groups such as hydroperoxides, hydroxydes, keto- and epoxy groups [167]. The second group of OxPCs consists of the species with the shorter sn-2 chain than the precursor, resulting in formation of hydroxide and carbonyl groups, highly reactive and capable of interacting with cellular components leading to an injury [168].

Enzymatic oxidation of PUFAs can be achieved by two different groups of enzymes. Lipoxygenases are the only group of enzymes that can oxidize phospholipid esterified PUFAs [169, 170]. In contrast, free fatty acids can be oxidized by lipoxygenases, cyclooxygenases and cytochrome P450 [171, 172].

Biophysical properties

The biological activity of OxPC is high due to its structure. The two groups of truncated OxPCs, carboxylic acids and aldehydes, are the most extensively studied. The presence of the aldehyde or carboxylic group at the sn-2 position allows these molecules to interact not only with the receptor, but also to incorporate within the membrane and interact with membrane bound proteins. This can change their function or alter the lipid bilayer organization. While carboxylic acids can interact with other biomolecules only physically, aldehydes are involved in a chemical reaction through formation of a Schiff base with α and ε-amino groups of amino acids(lysine, valine, lysine methyl ester) in proteins and aminophospholipids [150]. The conformation of the sn-2 chain within the membrane is also different for those two groups. The sn-2 chain of carboxylic acid is negatively charged and stretches out into the water phase, whereas the sn-2 chain of aldehydes is electroneutral and stays in the hydrophilic-hydrophobic part of the membrane [173]. As a consequence of their structure, OxPCs can lead to: a) a decrease of the lipid order; b) lowering of phase transition temperatures; c) lateral expansion and thinning of the bilayer; d) increased lipid mobility; e) augment flip-flop; f) water defects; g) changes in lateral phase organization and h) disintegration of the membrane [174].

The structural dynamics of the membrane as well as the lateral organization of membranes are altered by the presence of two specific OxPC specie: PONPC and PAzPC (1-palmitoyl-2-azelaoyl-*sn*-glycero-3-phosphocholine) [175]. Truncation of the sn-2 position leads to disturbances in the lipid bilayer. However, most important is the chemical nature of the truncated chain as truncated OxPCs lead to an increase in hydration of the carbonyl region of POPC (1-palmitoyl-2-oleoyl-sn-glycero-3-phosphocholine) as well as its mobility, but the effect was stronger with aldehyde (PONPC) than with carboxylic acid (PAzPC) [176].

Upon addition of PONPC and PAzPC to a POPC bilayer, the flip-flop rate of PS increases [177]. This occurs as a consequence of polarity and mobility changes in POPC due to the addition of PONPC and PAzPC. The main determinant of phospholipid mobility from one leaflet to another is the hydrophobicity of the bilayer [174]. PONPC and PAzPC significantly increase the polarity of the POPC bilayer leading to a decrease in the time for PS to flip-flop from weeks to hours [176, 178]. This also confirms their role in inducing apoptosis in different cell lines.

The orientation of these two lipids within the membrane is also different. Treatment of membranes with up to 25% of PAzPC leads to its reversal into the water phase without membrane disruption. However, PONPC in the same amount does not protrude into the water phase to that extent, but it does cause membrane disruption [173]. Both PGPC (1-palmitoyl-2-glutaryl-*sn*-glycero-3-phosphocholine) and POVPC treatment will result in an increased permeability of the membrane to water.

Lis et al. showed that as the oxidation rate increases, area per lipid (APL) increases while bilayer thickness decreases [179]. The same results were reported by another group, where the effects of POVPC and PGPC on endothelial cells were studied. This study confirmed the decrease in bilayer packing and increased water penetration, but also showed that both POVPC and PGPC result in increased endothelial cell stiffness, with PGPC having a more profound effect [180].

The presence of an aldehyde group at the sn-2 position is responsible for the wide range of biological roles of OxPCs. Aldehyde groups can interact with proteins and aminophospholipids forming Schiff bases [163] and leading to disturbances in membrane and protein structure and function [181]. Studies with fluorescently labeled analogs of POVPC and

PGPC, showed that in vascular smooth muscle cells (VSMCs), PGPC is up taken by the cell and transferred into lysosomes, whereas POVPC stays trapped in the membranes for a while before being transported inside the cell, due to the formation of covalent bonds with proteins and aminophospholipids [182].

Cleavage:

Platelet activating factor acetylhydrolase (PAF-AH) is an enzyme that hydrolyzes acyl sn-2 residue of PAF. This family of enzymes consists of one isoform found in plasma and two intracellular isoforms (Ib and II). Intracellular isoform II and plasma isoform can not only degrade PAF, but also fragmented OxPCs. The early studies showed that plasma isoform has a high specificity towards the modified sn-2 chains, whereas it is not specific towards sn-1 and sn-3 residues within the phospholipid [183], therefore it represents an effective system for clearance of OxPCs and preventing the damage caused by these active biomolecules. The study done by the same group showed the enzyme has a preference for the substrate depending on the sn-2 chain length. They showed that aldehyde with 5 carbons on sn-2 position (POVPC) was the most specific substrate for the enzyme [184]. As the carbon chain length increases the efficiency of the enzyme decreases and is lowest for the 9 carbon aldehyde (PONPC) [184]. PAzPC content increases in ApoE -/- animals fed high fat diet. It has been shown in these animals that the clearance of exogenous PAF was slowed down, suggesting that the enzyme has been occupied by increased levels of OxPCs. The same study showed that the fluorescent PAF as well as PAzPC primarily accumulated in the liver and lungs [185].

Detection:

The quantification of OxPCs in blood plasma and their association with diseases has been the most commonly determined by using the E06 antibody immune assay. This IgM antibody binds to phosphorylcholine group in OxPCs, but not to their unoxidized precursors [186]. E06 immune assay is ratiometric assay as it measures amount of OxPCs per LDL particle. One of the major advantages of this approach for measuring OxPC levels in plasma is the fact that E06 antibody binds both free OxPCs, as well as the ones bound to proteins and it cannot discriminate between different oxidized species, therefore giving the total OxPC content in plasma. On the other hand, individual OxPC species have different roles, therefore this assay is unable to provide the information on association of individual OxPCs species with specific pathologies. Another disadvantage of this method is the interference of plasma proteins. It has been shown that the pretreatment of oxidized LDL (OxLDL) with human plasma reduces binding of E06 by 30% [187]. Another method for identification and quantification of individual OxPC species widely used is liquid chromatography coupled to mass spectrometry. This method allows the quantification of wide spectrum of OxPC species. Recent advances in development of soft ionization methods such as electrospray ionization (ESI) and matrix assisted laser desorption ionization (MALDI) allowed for a simplified analyses of high molecular weight biomolecules, such as OxPCs in complex matrices. Both methods have been widely used for the analyses of OxPCs and are the gold standard for identification and measurement of OxPCs in biological fluids.

Biological activity of OxPCs

OxPC can have both, beneficial and pathophysiological functions based on the organ they are generated in and their specific chemical structure. For example, PAPC (1-palmitoyl-2-arachidonoyl-*sn*-3glycero-3-phosphocholine) and POVPC have an anti-inflammatory effect [188-190] through an inhibition of lipopolysaccharide (LPS)-induced neutrophil-endothelial adhesion as well as an up-regulation of E-selectin through Nuclear Factor κB (NF-κB) [188, 191]. Low concentrations of oxidized PAPC (OxPAPC) injected in mice did not cause IL-6 production but it inhibited LPS-induced production of cytokines suggesting their dual, concentration-dependent role [192]. Direct binding of KODiA-PC (1-palmitoyl-2-(5-keto-6-octenedioyl)-sn-glycero-3-phosphocholine) to LPS prevents its binding to MD-2 which is a TLR4 co – receptor, together with CD14 and LPS-binding protein [193, 194]. OxPAPC can also be protective against oxidant-induced toxicity by increasing glutathione levels [190]. In addition, PONPC, which belongs to the fragmented group of OxPCs, is responsible for a feedback mechanism which will limit any pro-inflammatory effects by activation of phospholipase A_2 [189].

Far greater research attention has been paid to the association of OxPCs with a large and ever increasing number of pathophysiologies. Atherosclerosis [154, 195, 196], lung disease [197, 198], neurodegenerative disease [199], non-alcoholic steatohepatitis [200] and chronic alcohol consumption [201] have all been associated with OxPCs. The pathway of their action in different cell types is still largely unknown. However, through the improved separation, identification and quantification of specific oxidized phospholipids via powerful new mass spectrometry (MS) techniques, our understanding of their pathogenic role in different tissues is increasing rapidly.

Oxidized Phospholipids in CVD

Oxidized phosphatidylcholine has so far been recognized to have a biological activity in progression of cardiovascular pathologies such as atherosclerosis, calcific aortic valve stenosis and reperfusion injury.

Atherosclerosis

An extensive amount of evidence from animal studies and discussed above demonstrates that chronic inflammation in atherosclerosis is followed by the production of OxPCs that are involved in different stages of atherosclerotic plaque formation and progression.

Atherosclerosis represents a chronic non-communicable disease characterized by lipid deposition, inflammation and hardening of the walls of medium to large sized arteries. Because atherosclerosis is a major determinant of ischemia and reperfusion injury and the resultant myocardial infarction, it is important and relevant to discuss in some detail in this review.

Atherosclerosis is characterized by a chronic inflammation of the arterial walls via increased oxidative stress [202]. In the last few decades, OxPCs have been recognized to be involved in the formation and progression of the atherosclerotic plaque. An increased concentration of OxPCs has been identified in the atherosclerotic plaque of animals [203]. The most abundant species of OxPCs in rabbit atherosclerotic lesions are oxidized PAPC, POVPC and PEIPC (1-palmitoyl-2-(5,6-epoxyisoprostane E_2)-*sn*-glycero-3-phosphatidylcholine) [203]. They have also been found in both plasma [204] and plaque [205] of patients with CAD. Analyses of plaques released from the lesions and captured with distal devices in coronary, carotid artery and saphenous vein graft led to an identification of fragmented OxPCs in the plaque, specifically POVPC [206]. Different types of OxPCs are involved in each step of atherosclerosis including monocyte recruitment [207], endothelial dysfunction [191, 196],

vascular smooth muscle cell proliferation [208], changes in vascular smooth muscle cell phenotype [208, 209] as well as macrophage death and plaque rupture [210]. However, in all stages of plaque development, the concentration of hydroperoxides (which are an early oxidation product) and core aldehydes (which are a late oxidation product) in human atheroma was similar. This suggests that oxidation is an on-going process in atherosclerosis [205]. Human atherosclerotic plaque contains nearly 5% OxPCs of the total phospholipid content [211]. OxPC specific antibody E06 showed protective effects against atherosclerosis. Mice with low-density lipoprotein (LDL) KO background overexpressing E06 showed 57%, 34% and 28% reduction in atherosclerosis in aorta following 4, 7 and 12 months respectively [212], whereas the reduction in the aortic root was 55%, 41% and 27% [212]. The major effects of fragmented OxPC species in formation and progression of atherosclerosis are summarized in the Figure 4. The OxPC-apoB100 ratio has been identified as an independent predictor of CAD [213].

Oxidized phosphatidylcholine is involved in formation and progression of atherosclerotic plaque directly, by affecting endothelial cells, macrophages, vascular smooth muscle cells and indirectly by promoting inflammation through their effect on platelets.

Endothelial cells

Endothelial cells form a permeability barrier [214], control vascular tone by secretion of vasoactive substances [215], alter the inflammatory status [216] and modulate thrombosis in response to different stimuli [217, 218]. Oxidative stress and inflammation can cause endothelial dysfunction [219], an early event in atherosclerosis [220, 221].

POVPC, PGPC and lysophosphatidylcholine (lysoPC) increase endothelial cell permeability in a dose dependent manner, which is considered to be the initial step of

atherosclerosis [222]. OxPAPC and its derivatives POVPC, PGPC and PEIPC can activate endothelial cells through their presence in minimally modified LDL (MM-LDL) [203]. OxPC species work through various receptors on endothelial cells leading to the formation and progression of atherosclerosis [223].

OxPAPC treatment of human aortic endothelial cells for 4 hours induces an activation of more than 1000 genes [224], many of which regulate inflammation. The vast majority of these genes (80%) are regulated by a PEIPC component of OxPAPC [225] which acts on the endothelial cells through the prostaglandin E2 receptor [226]. OxPAPC also induces the synthesis of interleukin 8 (IL-8) through JAK/STAT activation [207]. IL-8 is a chemoattractant that regulates neutrophil migration [227] and is crucial for the recruitment and entrapment of monocytes in the subendothelial space [228]. Its expression is increased in atherosclerosis [229], presumably with some involvement from OxPAPC.

Expression of adhesion molecules on the endothelial cells leads to monocyte recruitment and binding to endothelial cells. The mechanism involves activation of NF-κB by interleukin 1 (IL-1), LPS and TNF-α. Once activated, NF-κB will lead to expression of adhesion molecules that will bind neutrophils and monocytes [150]. OxPCs are involved in the expression of crucial adhesion molecules leading to progression of atherosclerosis. OxPAPC, POVPC and PEIPC can stimulate the binding of monocytes to endothelial cells [203]. POVPC and PGPC are the most important activators of endothelial cells [191] exhibiting different roles on different adhesion molecules. For example, PGPC promoted E-selectin and vascular cell adhesion molecule expression (VCAM) expression that promoted neutrophil – endothelial interaction [196]. PGPC activates peroxisome proliferator activating receptor (PPARy) in the nucleus of monocytes leading to monocyte maturation, expression of CD36 and OxLDL uptake [230]. This ultimately

led to foam cell formation [231]. PGPC also stimulates the expression of tissue factor (TF) in endothelial cells that activates a rise in cytosolic Ca^{2+} leading to thrombosis [232]. In human umbilical vein endothelial cells (HUVECs), OxPAPC induced an increase in TF expression through a NF-κB independent pathway [232].

In addition to its role in promoting inflammation, OxPAPC can also have beneficial effects as it acts through the NRF2 (nuclear factor E2-related factor 2) which regulates resistance to oxidation in cells [233]. OxPAPC increases the nuclear and cytosolic levels of NRF2 in endothelial cells [234]. OxPAPC treatment leads in changes in the expression of the main regulators of endothelial function: Vascular Endothelial Growth Factor A (VEGFA), Krüppel-like factor 2 (KLF2), 6-phosphofructo-2-kinase/fructose-2,6-biphosphatase 3 (PFKFB3), MYC proto-oncogene protein (MYC) and Forkhead box protein O1 (FOXO1) through NRF2 regulated miR-93 in HUVECs[234].

OxPAPC also increased cytosolic Ca^{2+}, activated protein kinase C (PKC), extracellular signal-regulated kinase 1/2 (ERK 1/2), and mitogen-activated protein kinase (MAPK), leading to an activation of endothelial growth related-1 (EGR-1) transcription factor and nuclear factor of activated T-cells (NFAT) [232]. Conversely, POVPC inhibits the expression of E-selectin that is triggered by PGPC, LPS or TNF-α [188] through a PKA-dependent pathway, resulting in down-regulation of NF-κB dependent transcription [191]. Treatment of EC with POVPC leads to an increase in expression of fibronectin connecting segment-1 consequently increasing monocyte binding [191]. POVPC also inhibited endothelium dependent relaxation in rabbit thoracic aorta [235]. Recent study confirmed the important role of POVPC in endothelial cells and early steps of atherosclerosis. In HUVECs, POVPC inhibited cellular proliferation and migration, and decreased NO production while increasing O^{2-} generation. Apoptosis of ECs was induced by

POVPC by inhibition of BCl-2 expression while increasing the expression of Bax and cleaved caspase 3 [236].

Monocytes/Macrophages

Lipid uptake by monocyte-derived macrophages that leads to formation of foam cells is one of the first steps of atherosclerosis [237]. Oxidized phospholipids induce monocyte binding to endothelial cells and synthesis of monocyte-specific chemoattractants such as monocyte chemotactic protein 1 (MCP1) [231]. OxPAPC promotes the expression of connecting segment 1 (CS1) in endothelial cells [196]. This is required for binding of α4β1 monocyte integrin [196]. OxPAPC and its components POVPC and PEIPC act through prostaglandin receptor EP2 [226] leading to an increase in cAMP which will further activate R-Ras. R-Ras mediated activation of PI3K results in activation of α5β1 integrin leading to monocyte/endothelial binding [196]. POVPC stimulates HUVEC cells to bind monocytes and this action is mediated by protein kinases A and C, as well as p38 MAPKs. POVPC has also induced the activation of lipoxygenases [238]. Inhibition of lipoxygenases led to a decrease in monocyte endothelial cell binding caused by POVPC and MM-LDL [239]. There is evidence showing that OxPCs are also involved in CD36 mediated formation of foam cells. CD36 is a scavenger receptor on macrophages that binds lipids and induces foam cell formation [240]. It is suggested that the OxPCs within OxLDL mediate the binding of OxLDL to the CD36 receptor in order to ultimately induce foam cell formation and the eventual atherosclerotic plaque [240].

Cell death through pathways like apoptosis is also thought to be an important component of atherosclerosis. OxPCs have been implicated in apoptosis and other cell death pathways relevant to atherosclerosis. For example, *in vitro* exposure of macrophages to POVPC and PGPC

led to apoptosis [210]. PGPC was more potent than POVPC at inducing membrane loss and formation of apoptotic blebs [210]. Formation of apoptotic blebs can be pro-inflammatory [241]. The possible site of action of oxidized lipid is platelet-derived, platelet-activating factor receptor (PAF-R). In human monocytes/macrophages, POVPC induced an increase in intracellular Ca^{2+} flux as well as a several fold increase in IL-8 gene expression [238]. In mouse macrophages, POVPC led to an activation of procaspase-1 within the inflammasome resulting in activation of Il-1β ultimately contributing to inflammation [242]. Recent study shows that exposure of macrophages to OxPAPC results in hyperinflammation [243]. By upregulation of several glutamine transporters, OxPAPC favors the utilization of glutamine over glucose. Glutamine accumulation and utilization as a main energy substrate by macrophages in atherosclerotic lesions was previously reported [244]. Moreover, OxPAPC leads to increase in mitochondrial respiration as well as oxaloacetate accumulation, both of which stimulate the production of Il-1β which contributes to inflammation [243].

Vascular smooth muscle cells (VSMCs)

OxPCs may induce a progression of atherosclerosis through functional and structural changes in VSMCs. Fragmented OxPCs like PGPC and POVPC induced VSMC can induce VSMC proliferation *in vitro* [208]. Connexin 43, a gap junction protein, is an important marker of atherosclerosis. Its expression and function changes during the progression of atherosclerosis [245]. Reduced expression also correlates with VSMC proliferation [246]. POVPC induced VSMC proliferation at the same time as it reduced the expression of connexin 43 through an increase in connexin phosphorylation at serine (pS) 279/282 *in vivo* and *in vitro* [246]. PGPC and

POVPC also enhanced VSMC migration by stimulation of Ca^{2+} entry through transient receptor potential 5 (TRPC5)-containing channels [247].

POVPC and PGPC can also induce a change in VSMC phenotype from contractile to synthetic (as shown by a reduced *in vivo and in vitro* expression of α actin and myosin heavy chain [195] and an increase in collagen synthesis). Both of these compositional changes are critical steps in the development of atherosclerosis. Collagen is an important component of an atherosclerotic plaque. Type VIII collagen is up-regulated in the diseases associated with vascular remodeling [248]. POVPC has induced the expression of the α1 chain of Type VIII collagen and fibronectin [195]. In mice overexpressing E06 antibody there was 44% reduction in necrotic core area, with the increased collagen deposition, resulting in more stable plaque [212].

Balloon angioplasty is a primary intervention for coronary artery occlusion. Smooth muscle cell hyperplasia and vascular remodeling leads to neointimal hyperplasia following balloon angioplasty as the form of wound healing. Inflammation plays an important role in neointimal hyperplasia. Hyperlipidemic $ApoE^{-/-}$ mice develop greater neointima formation, proliferation and inflammation upon vascular injury [249, 250]. In these $ApoE^{-/-}$ mice, concentrations of lysoPC and unsaturated PCs were increased. *In vitro* incubation of Apo $E^{-/-}$ VSMC with PGPC resulted in a stimulation of proliferation [208].

Apoptotic cell death is commonly found in VSMCs during atherosclerosis [251]. Sphingomyelinases are involved in stress signaling and the initial stages of apoptosis [150]. PGPC and POVPC can activate sphingomyelinases in VSMCs [150] and induce apoptosis in VSMC [252]. Apoptotic blebs are increased in patients with atherosclerosis and these dead cells can further promote inflammation [241]. Apoptotic blebs are rich in POVPC. Both apoptotic blebs and membrane vesicles can stimulate endothelial cells to bind monocytes. E06 is a

monoclonal antibody able to bind OxPCs but not their native precursors [253]. Pre-incubation of membrane vesicles with E06 prevented monocyte adhesion to endothelial cells caused by POVPC [241].

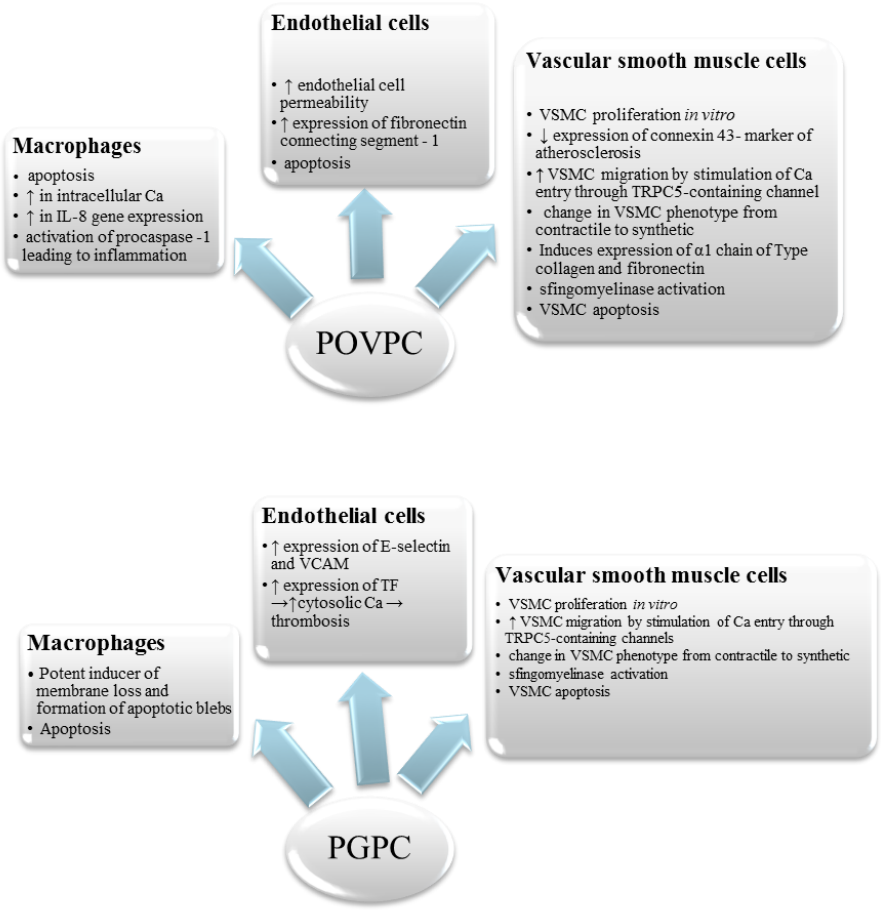

Figure 4. Pathophysiological role of fragmented OxPC species (POVPC and PGPC) in different cell types involved in formation and progression of atherosclerosis ; Stamenkovic A, Pierce GN, Ravandi A. Oxidized lipids: not just another brick in the wall. Can J Physiol Pharmacol. 2019 Jun;97(6):473-485. *Reprinted with permission*

Platelets

OxLDL itself induces platelet aggregation and mobilization through an increase in the expression of P-selectin. However, in combination with thrombin, this action is significantly enhanced and it is mediated through PAFR [254]. Truncated OxPCs also induce platelet activation through PAFR and through the CD36 receptor. Platelet activation by OxPCs is induced by increasing the intracellular concentration of calcium ions, upregulation of P-selectin expression, changes in platelet shape, activation of glycoprotein IIb/IIIa and stimulation of aggregation [254, 255]. An additional site of action of OxPCs on platelets is the CD36 scavenger receptor that has a role in fatty acid uptake [256]. The group of OxPCs that binds to CD36 with high affinity was identified to have γ-hydroxy(or oxo)-α,β-unsaturated carbonyl group on the sn-2 position and is known as $OxPC_{CD36}$ [257]. One of the members of this group known as KODA-PC can activate fibrinogen receptor on the platelets and induce expression of P-selectin that leads to formation of a platelet-monocyte aggregation [258].

Calcific Aortic Valve stenosis

Calcific aortic valve stenosis (CAVS) is a cardiovascular disorder which prevalence is increasing with the prognosis of 4.5 million people suffering from it by 2030 [259]. The reason for this is the increase in life span and aging of the population. Calcific aortic valve stenosis and CAD share the risk factors for development [260]. Moreover the etiology of CAVS is in many ways similar to that of atherosclerosis. The first step in initiation of CAVS is lipid deposition [261, 262] which is followed by endothelial dysfunction, oxidative stress and inflammation [263]. Currently, there is no therapy for prevention or regression of CAVS and the only treatment is aortic valve replacement. Most of the patients are not eligible for this intervention

due to increased frailty that develops by the time the procedure is needed. Taking this in consideration, it is crucial to investigate potential biomarkers for early prognosis or possible target for the regression of the disease. One of the independent, genetically determined risk factors for the presence of the CAVS is lipoprotein(a) (Lp[a]) [264-267]. Lp(a) is the main carrier of oxidized phospholipids [268, 269] and the study that included 220 patients showed that its elevated levels together with the elevated levels of OxPL-apoB correlate with the faster progression of aortic stenosis [264]. MS analyses of the fragmented OxPC species in human stenotic valves showed that the most prevalent group was aldehydes with PONPC being the most prevalent, followed by carboxylic acids among which the PAzPC was the most abundant [270]. Moreover, in LDL-/-/ E06scFv mice, 49% reduction in mean aortic valve pressure gradient , compared to LDL-/- mice was reported after 12 months of high cholesterol diet [212]. This implies that OxPCs are involved in pathophysiology of AS and that targeting these molecules can be a possible therapeutic approach.

Reperfusion injury

Plasma levels of fragmented OxPCs were elevated in patients after coronary surgery with cardiopulmonary bypass [204]. OxPCs are elevated in different stages of plaque development in patients with coronary heart disease [205, 271]. Moreover, analyses of plaques released from the lesions and captured with distal devices in coronary, carotid artery and saphenous vein grafts have identified fragmented OxPCs in the plaque, specifically POVPC [206]. We have recently shown that fragmented OxPC species such as POVPC and PONPC are increased in both *in vitro* and *in vivo* rat models of I/R injury in the heart [272] and in neonatal cardiomyocytes (NNCM). Recent findings showed the detrimental biological activity of OxPCs in myocardial reperfusion

injury. Using mass spectrometry, OxPC levels were measured both *in vitro* and *in vivo* in rats. Following I/R in NNCM the levels of four fragmented OxPCs: PONPC, POVPC, PGPC and PAzPC were found to be significantly increased [272]. Oxidatively fragmented PCs, POVPC and PGPC, were elevated in adult rat cardiomyocytes after 30 min of ischemia followed by reperfusion [273]. Furthermore, the analyses of rat myocardium following 1h of ischemia and 24h of reperfusion *in vivo* showed also significant rise in fragmented OxPC species [272].

Not only that endogenous levels of OxPCs increase during and I/R insult, but exogenous addition of OxPCs showed cardiotoxic effect in NNCM [272]. However, recent study showed the OxPC induced cardiomyocyte cell death occurs though mitochondria. Due to high energy demands of the heart, cardiomyocytes are rich in mitochondria which dysfunction during I/R leads to ROS production which further promotes lipid peroxidation. MS analyses of mitochondrial fraction of cardiomyocytes undergone I/R showed significant increase in production of fragmented OxPCs compared to control [272]. Also, an increase of PONPC and POVPC were shown when mitochondrial fraction after I/R was compared to the other cell membranes. Furthermore, it was shown that POVPC and PONPC lead to an opening of mitochondria permeability pore in a concentration dependent manner [272].

Natural IgM antibody, E06 binds PC group on OxPL and it was previously shown to inhibit the pro inflammatory effects of OxPL by blocking the uptake of OxPL by macrophages [253, 274, 275]. The addition of E06 antibody *in vitro* attenuated cardio toxic effects of POVPC by 74.6% and PONPC induced cell death by 74.7%. Moreover, in the mouse model of E06 overexpression exposed to I/R the infarct size was decreased compared to Ldlr-/- mice, suggesting the possible pharmacological target for the reduction of I/R injury [272]. Moreover, omega-3 fatty acid, alpha linolenic acid (ALA), was protective against OxPCs in I/R injury. Pre-

treatment of isolated adult rat cardiomyocytes with ALA for 24h before I/R lead to a significant decrease in POVPC and PGPC amounts compared its respective control [273].

This injury can be attenuated by E06, an IgM antibody against OxPCs [272]. However, the mechanism through which OxPCs induce cell death during I/R injury in cardiomyocytes is largely unknown.

OxPCs as biomarkers of disease

OxPCs are found in such high concentrations during so many pathologies *in vitro* that they may have importance as biomarkers [276]. In plasma, 85% of OxPC is bound to the apo(a) part of Lp(a) [269]. In a prospective population based study, the incidence of cardiovascular events in 765 patients was estimated between 1995 and 2005 was correlated to levels of OxPL/apoB in their plasma.

Two independent studies confirmed the generation and release of OxPL/apoB from atherosclerotic plaque following ACS [277] and PCI [278]. While in patients with stable CAD and control group, followed for 7 months there was no significant difference in OxPL/apoB levels, in patients with an ACS there was an immediate rise in OxPL/apoB levels by 54% with tendency of going towards the baseline in the next 7 months [277]. Moreover, the study that supports these findings showed the immediate rise in OxPL/apoB levels following PCI by 36% followed by the decrease to the baseline levels in the next 6h [278]. In 504 patients, 60 years or younger, that underwent clinically indicated coronary angioplasty, elevated levels of OxPL/apoB were found to be in correlation with the presence and severity of CAD, as well as independent predictor of CAD, especially in patients younger than 60 [213].

The first study to show the predictive value of OxPL/apoB levels in death, myocardial infarction, stroke and transient ischemic attack and revascularization of general population was Bruneck study (Table 1.) [279]. This study showed that patients in the highest OxPL/apoB tertile have the highest risk of cardiovascular events. Moreover, it showed that independent from the Framingham Risk Score, OxPL/apoB levels were able to predict 10 year CVD event rates [279]. The EPIC-Norfolk study confirmed the results obtained in the Bruneck study. 763 patients and 1379 healthy matched controls, both, men and women, aged 45-79 were followed for 6 years and a correlation was observed between OxPL/apoB and a higher risk of CAD, particularly in the highest tertiles of OxPL/apoB [280].

Table 1. Clinical studies showing the importance of oxidized phosphatidylcholine in cardiovascular disease. Stamenkovic A, Pierce GN, Ravandi A. Oxidized lipids: not just another brick in the wall. Can J Physiol Pharmacol. 2019 Jun;97(6):473-485. *Reprinted with permission*

Year	Author	Title	Number of patients	Outcome	Ref
1999	Wu et al.	Autoantibodies to OxLDL are decreased in individuals with borderline hypertension	146	OxPL/apoB ratio is increased in hypertension and that could reflect vascular changes	[281]
2001	Penny et. al	Improvement of coronary artery endothelial dysfunction with lipid-lowering therapy: heterogeneity of segmental response and correlation with plasma-oxidized low density lipoprotein	29	OxPL/apoB ratio correlates with the severity of endothelial dysfunction and is the most powerful independent risk factor	[282]
2003	Tsimikas et al	Temporal increases in plasma markers of oxidized low-density lipoprotein strongly	66	OxLDL levels increase after MI	[277]

		reflect the presence of acute coronary syndromes			
2004	Tsimikas et al	PCI results in acute increases in oxidized phospholipids and lipoprotein(a): short-term and long-term immunologic responses to oxidized low-density lipoprotein.	141	Following PCI OxPL/apoB levels increase, but return to baseline after 6 h	[278]
2004	Tsimikas et al	High-dose atorvastatin reduces total plasma levels of oxidized phospholipids and immune complexes present on apolipoprotein B-100 in patients with acute coronary syndromes in the MIRACL trial	2341	80 mg per day of atorvastatin increases OxPL/apoB ratio	[283]
2004	Silaste et al	Changes in dietary fat intake alter plasma levels of oxidized low-density lipoprotein and lipoprotein(a)	37	Increased OxPL/apoB ratio in response to low fat – high vegetable diet	[284]
2005	Tsimikas et al	Oxidized phospholipids, Lp(a) lipoprotein, and coronary artery disease.	504	OxLDL levels associated with coronary artery disease	[213]
2006	Tsimikas et al	Oxidized phospholipids predict the presence and progression of carotid and femoral atherosclerosis and symptomatic CVD: five-year prospective results from the Bruneck study	765	OxPL are strong predictors of presence of femoral and carotid atherosclerosis	[285]
2007	Kiechi et al	Oxidized phospholipids, lipoprotein(a), lipoprotein-associated phospholipase A2 activity, and 10-year cardiovascular outcomes: prospective results from the Bruneck study	765	OxPL/apoB ratio predicts 10-year CVD mortality independently from traditional risk factors, hsCRP, and FRS	[279]

2006	Rodenburg et al	Oxidized low-density lipoprotein in children with familial hypercholesterolemia and unaffected siblings: effect of pravastatin	256	40 mg/day of pravastatin increased the OxPL/apoB ratio in children with FH compared to placebo	[286]
2007	Inami et al	Tea catechin consumption reduces circulating oxidized low-density lipoprotein	40	Catechin decreased levels of OxLDL in plasma	[287]
2008	Ky et al	The influence of pravastatin and atorvastatin on markers of oxidative stress in hypercholesterolemic humans	120	OxPL/apoB levels increased 26% with pravastatin and 20% with atorvastatin	[288]
2008	Choi et al	Relationship between biomarkers of oxidized low-density lipoprotein, statin therapy, quantitative coronary angiography, and atheroma: volume observations from the REVERSAL (Reversal of Atherosclerosis with Aggressive Lipid Lowering) study	214	OxPL/apoB levels increased 39% with pravastatin and 48% with atorvastatin	[289]
2009	Tsmikas et al	Relationship of oxidized phospholipids on apolipoprotein B-100 particles to race/ethnicity, apolipoprotein(a) isoform size, and cardiovascular risk factors: results from the Dallas Heart Study	3481	OxPL/apoB levels varied according to race/ethnicity, and are largely independent of cardiovascular risk factors	[290]
2010	Tsmikas et al	Oxidation-specific biomarkers, lipoprotein(a), and risk of fatal and nonfatal coronary events	2160	The highest tertiles of OxPL/apoB associated with the higher risk of CAD events	[280]
2009	Budoff et al	Aged garlic extract supplemented with B vitamins, folic acid and L-arginine retards the progression of subclinical atherosclerosis: a	60	OxPL/apoB levels increased with aged garlic extract and predicted the lack of coronary artery calcium progression	[291]

		randomized clinical trial.			
2010	Ahmadi et al	Relation of oxidative biomarkers, vascular dysfunction, and progression of coronary artery calcium	60	OxPL/apoB levels increased with aged garlic extract and correlated with the improved vascular function	[292]
2010	Faghihnia et al	Changes in lipoprotein(a), oxidized phospholipids, and LDL subclasses with a low-fat high-carbohydrate diet	63	Low-fat high-carbohydrate diet increased OxPL/apoB levels	[293]
2015	Byun et al	Relationship of oxidized phospholipids on apolipoprotein B-100 to cardiovascular outcomes in patients treated with intensive versus moderate atorvastatin therapy: the TNT trial	1503	In patients with stable CHD, OxPL/apoB levels predict secondary MACE. This is mitigated by 80 mg atorvastatin	[294]
2015	Capoulade et al	Oxidized Phospholipids, Lipoprotein(a), and Progression of Calcific Aortic Valve Stenosis	220	Elevated levels of OxLDL/apoB are associated with aortic stenosis progression and need for valve replacement	[264]
2016	Leibundgut et al	Acute and long-term effect of PCI on serially-measured oxidative, inflammatory, and coagulation biomarkers in patients with stable angina	125	OxPL/PLG and plasminogen decreased significantly immediately after PCI, rebounded to baseline, peaked at 3 days and slowly returned to baseline by 6 months	[295]
2016	Yeang et al	Effect of therapeutic interventions on oxidized phospholipids on apolipoprotein B100 and lipoprotein(a)	591	Niacin decreased OxPL/apoB levels while ezetimibe/simvastatin (E/S) and combination E/S with niacin significantly increased the levels of OxPL/apoB	[296]
2016	van der Valk et al	Oxidized Phospholipids on Lipoprotein(a) Elicit Arterial Wall Inflammation and an Inflammatory Monocyte Response in Humans	30	Elevated Lp(a) leads to an increase in arterial inflammation and enhanced peripheral blood mononuclear cells trafficking to the arterial wall; Lp(a) contains OxPL	[297]
2017	Byun et al	Oxidized Phospholipids on Apolipoprotein B-100 and	4385	Elevated OxPL/apoB levels predicted recurrent stroke and first major coronary events in	[298]

	Recurrent Ischemic Events Following Stroke or Transient Ischemic Attack	patients with prior stroke or transient ischemic attack.

Cardiomyocyte cell death during I/R injury

Apoptosis

Apoptosis has been shown to occur in I/R injury *in vitro, in vivo,* in different animal models and in human hearts. Evidence shows that it plays an important role in the determination of the infarct size, extent of left ventricle (LV) remodeling as well as the development of early symptomatic heart failure following an AMI.

According to the Nomenclature Committee of cell death apoptosis is defined as a caspase dependent form of cell death which can be controlled genetically [299]. Apoptotic cell death is initiated and executed through two different pathways: extrinsic and intrinsic. Extrinsic pathway is triggered by stress signaling molecules such as TNF-α, TNF-related apoptosis inducing ligand (TRAIL) and Fas ligand (FasL), which bind to their receptors: TNF-α receptor 1 (TNFR1), TRAIL receptor 1/2 (TRAILR1/2), and Fas, respectively. Receptor activation then leads to a recruitment of Fas associated death domain (FADD) and procaspase 8 which form a complex known as death inducing signaling complex (DISC) which activates caspase 8. Caspase 8 then induces activation of effector caspases: 3, 6 and 7, leading to apoptotic cell death. Intracellular stress such as oxidative stress, Ca^{2+} accumulation and DNA damage lead to an opening of mitochondrial outer membrane permeabilization pore (MOMP) which is followed by cytochrome c release into the cytosol. Cytochrom c interacts with the apoptotic protease-activating factor 1 (Apaf-1) to form apoptosome which leads to the activation of caspase 9.

So far, apoptosis has been shown to occur in I/R injury *in vitro, in vivo,* in different animal models and in human hearts. Evidence shows that it plays an important role in determination of the infarct size, extent of LV remodeling as well as the development of the early symptomatic heart failure following an AMI.

Activation of Fas receptor by FasL leads to apoptosis and Lee et al showed that this receptor is an important mediator of cardiomyocyte apoptosis in an *in vivo* model of I/R injury [300]. The levels of Fas and FasL have been shown to increase in patients with acute MI [301]. However, multiple clinical trials showed no correlation between the levels of soluble Fas receptor, Fas ligand and the infarct size in MI patients. There was no correlation between the FasL levels in plasma and LV remodeling measured by echocardiography up to one year post MI [302]. Moreover, in study that included STEMI patients, the levels of FasL and Fas were measured prior to PCI and 24h after the procedure. Infarct size and LV dysfunction were evaluated at 5 days and 4 months after the STEMI. There was no correlation between the FasL and Fas levels and infarct size or LV dysfunction, suggesting that this particular part of apoptotic pathway cannot be used a biomarker to predict outcomes post MI [303].

Tumor necrosis factor alpha (TNF-α) is an inflammatory cytokine shown to induce apoptosis in rat cardiomyocytes during I/R injury [304]. Its effect in the heart during I/R injury depends on the concentration as well as the receptor it binds to. Low concentration was shown to improve myocardial function, whereas the high concentration has a cardiotoxic effect [305] primarily when acting through TNFR1 receptor as shown in murine model [306]. The levels of TNF-α and its receptors increase in patients with AMI and can be used to predict the infarct size, LV dysfunction and prognosis. TNF- α serum levels measured in 42 STEMI patients, before, one and 6 days after the successful PCI, increased and correlated with the infarct size [307]. Moreover, this study showed that the infarct size on day 6 could be predicted by serum values of TNF- α measured on day 1 after the PCI [307]. Levels of TNFR1 and TNFR2 increase in STEMI patients are associated with the LV dysfunction and infarct size [303]. Despite the predictive value of TNF- α shown in different studies, a double-blind, parallel group, randomized

controlled clinical trial in which TNF-L antagonist was used in patients with an acute MI showed no benefits to this patient population [308].

One of the executioners of apoptosis, caspase-3 overexpression in mice was shown to increase the infarct size and susceptibility to die after I/R [309]. Moreover, the downregulation of caspase-3 improved cardiac function by decreasing the infarct size and decreasing the apoptotic index of cardiomyocytes [310]. The caspase-3 fragment p17 was measured in STEMI patients initially and 3 months PCI. It was found that there was a fourfold increase in the acute state of MI [311].

Evidence in literature shows that apoptosis occurs at the reperfusion stage of I/R injury. Even though reperfusion is necessary since it will lower the number of cardiomyocytes undergoing cell death, it has been shown that in rat model of I/R injury it promotes apoptosis in non-salvageable myocytes . In rats subjected to continuous ischemia, apoptosis occurred after 2.5 hours, whereas exposure to 45 min to ischemia followed by one hour of reperfusion accelerated apoptosis only in reperfused myocardium [312].

De Mossac et all found that in adult rat cardiomyocytes, 1 h of hypoxia leads to caspase 3 activation and release of cytochrome c into the cytosol [313]. Moreover, in Langendorf model of I/R in rabbits' hearts, it's been shown that cytochrome c is released into the cytosol as early as 15 minutes into reperfusion and 30 minutes after induction of ischemia [314].

Necrosis

Unlike apoptosis, necrosis is viewed as un unregulated, accidental and irreversible form of cell death. It is characterized by the membrane discontinuity and swelling, ultimately leading to membrane rupture and loss of cell structure [315, 316].

It has been recently suggested that necrosis can be regulated and that form of cell death was named necroptosis. Unlike necrosis, necroptosis is programmed cell death, highly regulated and can be prevented [317-319]. Morphologically, necroptosis cannot be distinguished from necrosis since is characterized by the cell disorganization, cytoplasm vacuolation, swelling of the plasma membrane which results in rupture and release of the intracellular content which further leads to an inflammatory response [320, 321].

The initiation of necroptosis involves recruitment of receptors associated with apoptosis such as Fas, TNF and Trail. Activation of these receptors leads to recruitment of caspase-8 and execution of extrinsic apoptotic pathway. However, when caspase-8 is inhibited, the activation of the same receptors will lead to execution of necroptosis through receptor –interacting protein kinase 1 (RIPK1), RIPK3 and mixed lineage kinase domain-like protein (MLKL) [322, 323]. Ligands such as Fas, TNF, LPS activate RIPK3which then leads to phosphorylation of MLKL and its activation [324]. Phosphorylation of the MLKL causes its translocation to the inner leaflet of the plasma membrane where it binds to phosphatidylinositol phosphates (PIPs) [325], ultimately leading to a disruption of the cell membrane organization and compromises the integrity of the cell [326, 327].

The best described form of necrosis is the one induced by tumor necrosis factor alpha and Fas binding to their receptors. This leads to a formation of the membrane associated Complex I which consists of: 1) tumor necrosis factor α associated death domain (TRADD) or Fas associated death domain (FADD); 2) RIP1; 3) TNFR-associated factors (TRAF) 2 and 5 and 4) cellular inhibitors of apoptosis protein 1 (cIAP1) and 2 [328]. The first step of necroptosis is deubiquitination of RIP1 which leads to its deletion from complex-1 and its destabilization [323]. Once released from Complex I, RIP1 combines with TRAD, FADD , RIP3and caspase-8 to form

Complex II [329]. As long as caspase-8 is inhibited RIP and RIP3 will remain active, combine together to form necrosome which is involved in downstream signaling cascade, leading to necroptosis [330]. Necroptosis induced by TNFα is known as extrinsic necroptosis. However, it can also be induced by intracellular signals such as ROS [331]. ROS were found to promote necroptosis by phosphorylation of RIP1 and therefore inducing the formation of necrosome [322].

There is evidence in the literature suggesting the involvement of necrosis in myocardial I/R injury. Exposure of H9c2 cardiomyocytes to 30 minutes of hypoxia followed by 2,4,6 and 8 hours of reoxygenation lead to an increase in expression levels of RIP3 [332]. The same group showed that silencing RIP3 increases cell viability during hypoxia/reoxygenation and decreases the levels of LDH, proving the involvement of RIP3 in cell death process in cells [332]. The role of RIP3 in mediating necroptosis in I/R injury was also confirmed in another study which showed that not only RIP3 induces myocardial necroptosis by forming complex with RIP1 and MLKL, but also triggers it through phosphorilation of CaMKII, which ultimately leads to a mPTP pore opening [333]. Moreover, RIPK3 was shown to induce the mPTP pore opening by inducing ER stress, accompanied with increased intracellular Ca^{2+} levels and xanthine oxidase expression. The RIPK3 genetic ablation decreases the ER stress, blocks Ca^{2+}overload and XO-ROS-mPTP pathway, promoting the survival of cardiomyocytes during I/R [334] . Necrostatin-1, the inhibitor of necroptosis was shown to cause an increase in left ventricular systolic pressure when administered intracoronary in isolated rat hearts, however it does not lead to a significant decrease in infarct size [335]. On the other side, in an *in vivo* model of murine LAD ligation, the venous administration of necrostatin-1 (3.5 mg/kg) 5 minutes prior reperfusion lead to a

significant decrease in infarct size compared to a control group [319]. These effects of necrostatin-1 are due to decrease in RIP1/RIP3 phosphorylation [319].

Ferroptosis

Ferroptosis is an iron mediated form of regulated cell death caused by accumulation of lipid-based ROS when the GSH-dependent lipid peroxide repair systems are compromised [336]. The name "ferroptosis" comes from Greek word "ptosis" meaning "a fall" and "ferrum", which is a Latin word for iron, suggesting the importance of this metal in execution of this form of cell death [337, 338]. Ferroptosis represents a regulated form of cell death that is morphologically, biochemically and genetically distinct from apoptosis, necrosis and autophagy [338]. In 2012 Dixon et al. used phenotypic small molecule screening to identify the key inducers of ferroptosis, one of which was erastin [338]. They found that erastin inhibits cysteine import, depriving that way the cell of cysteine which is necessary for the synthesis of glutathione [338]. Moreover, erastin as a class 1 ferroptosis inducer binds to and inhibits voltage dependent ion channel (VDAC) 2/3, leading to cell death [339]. Erastin was shown to cause cardiomyocyte cell death [340] despite the fact that system Xc^- is not expressed in the heart [341], suggesting that its effects are due to blockage of VDAC in the heart rather than system Xc^- inhibition. Recent study done in isolated perfused mouse heart showed that Liproxtatin-1, an inhibitor of ferroptosis reduces the extent of I/R injury by reducing the levels and the oligomerization of VDAC1, but does not affect VDAC2/3 [342].

System Xc^- inhibition deprives cells of cysteine causing glutathione depletion which will then lead to inactivation of GPx4 [343], selenium dependent enzyme, the only member of peroxidase enzyme family able to convert phospholipid hydroperoxides to lipid alcohols [344]. Moreover, another molecule called RAS selective lethal (RSL3) has been identified as an inducer

of ferroptosis [345], which acts by directly inhibiting GPx4. Treatment of HT-1080 fibrosarcoma cells with erastin leads to intracellular ROS production and accumulation which can be suppressed by co-treatment with iron chelator deferoxamine (DFO) [338]. There is enough evidence in the literature to support the necessity of iron for the execution of ferroptosis. Addition of iron, but not divalent metal ions such as Cu^{2+}, Mn^{2+}, Ni^{2+}, Co^{2+}, to the medium potentiates erastin induced cell death [338]. Not only that iron overload has been shown to induce ferroptosis *in vitro*, but Wang al showed that the administration of the iron in mice containing defect in system Xc^-enhances ferroptotic cell death [346]. Furthermore, iron availability, regulated by phosphorylase kinase G2 (PHKG2), to lypoxygenases which are responsible for PUFA oxidation was recognized as crucial for ferroptosis to occur [347]. Ferroptotic cell death can be inhibited by iron chelators, lack of iron in the cell, or knockdown of transferrin or its receptor [338, 343, 345, 348, 349].

Treatment of BJeLR cells with erastin showed morphological features such as mitochondria which are smaller than normal with increased membrane density, detected by electron microscopy [338]. There were no morphological changes observed which are associated with: staurosporin treatment, such as chromatin condensation, margination, hydrogen peroxide treatment, such as plasma membrane rupture and organelle swelling, or rapamycin induced formation of double membrane vesicles [338]. Moreover, Dixon et al tested various death inhibitors and their potential to modulate erastin induced cell death. They found that apoptosis, necrosis and autophagy inhibitors were unable to modulate erastin induced cell death [338].

Through high-throughput screening Ferrostatin-1 was identified as an inhibitor of ferroptosis [338]. Ferrostatin-1 acts as a lipid ROS scavenger and is potent in preventing

ferroptosis, but is unable to prevent cell death caused by staurosporine or hydrogen peroxide [338].

Ferroptosis has been described recently as a form of cell death in renal I/R injury (43). Moreover, treatment with inhibitors of ferroptosis, ferrostatin-1 and its analogue compounds, were protective in acute renal failure [350]. Angeli et al also tested the *in vivo* efficacy of ferroptosis inhibitors, which were able to attenuate cell death in hepatic I/R injury [351].

Ferroptosis is an iron mediated form of cell death caused by the accumulation of lipid peroxidation products [338]. Iron driven lipid peroxidation of phospholipid esterified polyunsaturated fatty acids has been recognized to play a major role in ferroptotic cell death [352]. Iron toxicity in patients with CAD is still controversial, however, clinical data shows that myocardial hemorrhage in patients who have undergone percutaneous reperfusion therapy is associated with residual iron following myocardial hemorrhage and is responsible for left ventricular remodeling [353]. Circulating and intracellular iron availability contribute to ferroptosis. Iron concentration and homeostasis are regulated by several key components, such as: iron regulatory proteins (IRP1 and IRP2), transferrin receptor 1 (TfR1), divalent metal transporter 1 (DMT1), H and L ferritin subunits and ferroportin [354]. Iron storage has been shown to increase sensitivity of cells to ferroptosis [338]. Circulating iron is transported inside the cell by binding to transferrin receptor 1 (TfR1) and the expression of transferrin increases susceptibility to ferroptosis [338]. Erastin induced ferroptosis can be prevented by chelation, confirming that iron is necessary for the ferroptosis to occur [338]. Moreover, in an ex vivo model of myocardial I/R injury, DFO was shown to be protective [355].

The exact intracellular site where ferroptosis occurs is still not completely explored. However, there is evidence in the literature that the possible site where ferroptosis occurs is

endoplasmic reticulum. Stockwell and his group have utilized an imaging technique known as stimulated raman scattering (SRS) microscopy coupled with small vibrational tags to visualize ferrostatin in live cells [356]. They found that ferrostatin accumulates in specific subcellular regions including lysosomes, mitochondria and endoplasmic reticulum, but not plasma membrane and nucleus. They treated fibrosarcoma cell line (HT-1080 cells) deprived of mitochondria with erastin or RSL3 and a serial dilution of Ferrostatin-1, and showed that ferr-1 was more potent following mitophagy, indicating that mitochondria are not required for ferroptosis. Further evidence that ferroptosis does not occur in mitochondria was obtained in study done by the same group showing that ROS generated by mitochondrial electron transport chain do not contribute to ferroptosis as the cells lacking mitochondrial DNA are still sensitive to ferroptosis [338]. Knockdown of Gpx4 -/- in mice kidneys lead to an increase in PL oxidation products: PC, PE and CL suggesting that mitochondria and other cellular compartments contribute to lipid peroxidation. However, mitochondria targeted antioxidants were far less efficient in saving Gpx4 cells than untargeted ones, suggesting that mitochondria is not the crucial site of lethal signal production [351]. Postmitophagy cells show greater endoplasmic reticulum abundance and ferr-1 potency increases further, suggesting the involvement of ER in ferroptotic cell death [356]. Moreover, Kagan et al showed that accumulation of lipid hydroperoxides, one of the hallmarks of this form of cell death, predominantly occurs in the endoplasmic reticulum [352].

Role of lipid peroxidation in ferroptosis

Both inhibition of glutathione synthesis through prevention of cysteine uptake or direct inhibition of GPx4 will lead to an iron-mediated formation and accumulation of lipid

peroxidation products [134]. The major substrates for ferroptosis are PUFA rich membrane phospholipids [336, 352] (Figure 1). Biological membranes consist of several classes of phospholipids. Whereas the sn-1 position in phospholipids can be linked to an acyl residue via an ester bond or an alkyl residue via an ether bond and it usually has a saturated fatty acid bound to it, the sn-2 position is always linked to an acyl residue with a PUFA bound to it [150]. Having PUFAs positioned on the sn-2 position results in phospholipids being highly susceptible to oxidation. However, a study using external fatty acids with different saturation levels and chain lengths showed that the level of unsaturation is not what is crucial for ferroptosis, but instead the position of the double bond is critical, since the ω6 fatty acids led to a 5-10 fold increase in cell death compared to ω3 fatty acids [357].

Several groups have independently shown that phospholipid hydroperoxides are involved in ferroptosis. Oxidative lipidomic analyses of kidneys lacking the GPx4 enzyme showed significant accumulation of several classes of phospholipid hydroperoxides: PC hydroperoxides, PE and cardiolipin (CL) [351]. Moreover, the accumulation of lysophosphatidylcholines (LPC), lysophosphatidylethanolamines (LPE) and monolysocardiolopin (mCL) was detected in ferroptosis [351]. Linoleic (LA) and arachidonic (AA) acids stimulate ferroptosis whereas oleic acid has an inhibitory effect [343]. Two enzymes involved in phospholipid metabolism have been identified as important in ferroptosis, further confirming the involvement of phospholipids in this form of cell death. Acyl-CoA synthase long-chain family member 4 (ACSL4) is an enzyme that catalyzes the formation of polyunsaturated fatty acid-acyl-CoA (PUFA-CoA), with the preference for AA, facilitating the esterification of PUFA into phospholipids [358].

Both genetic ablation and chemical inhibition of ACSL4 increased the resistance to RSL3 (class II inhibitor of ferroptosis) -induced ferroptosis [357]. Furthermore, ACSL4 deficient cells

were resistant to RSL-induced cell death but not to inducers of other forms of cell death [357], suggesting that phospholipids play a crucial role in the execution of ferroptosis. In ACSL4 deficient cells, the levels of free oxygenated PUFAs were higher than esterified oxygenated PUFAs in comparison to the wild type cells [352] . The supplementation of ACSL4 and wild type cells with AA led to a 13% increase in RSL induced ferroptosis in ACSL4 deficient cells compared to a 24% increase in wild type cells [352] which clearly demonstrates the involvement of phospholipids and not the free oxygenated PUFAs in the execution of ferroptosis. AA and adrenoic acids containing PE, recognized by Kagan et al. to play a major role in ferroptosis, were depleted in ACSL4 deficient cells [357].

Lysophosphatidylcholine acyltransferase 3 (LPCAT3) is another enzyme involved in phospholipid remodeling. LPCAT3 catalyzes the insertion of an acyl group into lysophosphatidylcholine. The knockdown of LPCAT3 in mouse lung epithelial cells increased the resistance to RSL-induced ferroptosis [352] .

Studies including 15-LOX (15-lipoxygenase) have further confirmed an involvement of phospholipids in the execution of ferroptosis. Indeed, inhibition of LOX suppresses the RSL-induced ferroptotic cell death, whereas the same effect was not observed with the inhibition of COX (cyclooxygenase) or CYP450 (Cytochrome 450) [352]. Moreover, the same group showed that in mouse embryonic fibroblasts (Pf1a cells), 15-LOX-induced oxidation of AA and adrenic acid (AdA) esterified PE in the endoplasmic reticulum and this process was required for ferroptosis to occur [352]. 15-LOX activity could be suppressed by an inhibitor of ferroptosis, Liproxtatin-1, which led to a decrease in oxygenated PE *in vivo* [352].

In normal conditions, phospholipid hydroperoxides are reduced by GPx4. Glutathione peroxidase 4 is the only member of a family of 8 enzymatic isoforms that can reduce toxic lipid

hydroperoxides to lipid alcohols in mammalian cells [359]. One of the major features of ferroptotic cell death is the loss of activity of GPx4 [338]. Inhibition of GPx4 leads to the accumulation of lipid peroxidation products and ferroptosis [360, 361]. Under physiological conditions, this is suppressed by GPx4 [134, 343]. Gpx4 is often reported as a regulator of ferroptosis since a class I inducer (erastin) and a class II inducer (RSL3) lead to indirect or direct Gpx4 inhibition [343]. RSL3 inhibits Gpx4 directly and independently of GSH levels [345]. Gpx4 knockdown sensitizes RSL induced ferroptosis, whereas the overexpression leads to increased resistance to RSL-induced ferroptosis [362]. Angeli et al. showed *in vivo* that depletion of Gpx4 in mice leads to acute renal failure, accumulation of oxygenated phospholipids and finally ferroptosis [351]. In addition, the knockdown of Gpx4 also leads to an increase in oxygenated PE species containing AA and AdA [352]. Recent LC-MS/MS analyses showed that the levels of GPx4 are decreased in mice in early and middle stages of an MI, while they increase in late MI. Western blot analyses also confirmed the same trend of changes in protein levels of GPx4. The decreased protein levels of GPx4 are due to downregulation of mRNA levels as shown by qRT-PCR analyses [363]. The mRNA levels of other members of GPx family were increased suggesting that Gpx4 is specifically downregulated and contributes to ferroptosis in MI [363]. In a study done by Kegan et al. chemical inactivation of GPx4 by RSL3 led to a marked decrease of the protein abundance, suggesting that GPx4 activity is needed to prevent its instability or degradation [352].

Ferroptosis and ischemic heart disease

Oxidative stress plays a major role in coronary heart disease. Atherosclerosis is the leading cause of coronary heart disease [364]. Chronic inflammation of arterial walls via

oxidative stress is one of the main characteristics of atherosclerosis [202]. OxLDL deposition within the arterial wall is one of the hallmarks of atherosclerosis [365]. The phospholipid esterified PUFAs like AA and LA in LDL are lipids that are highly susceptible to lipid peroxidation [366]. Phospholipid oxidation leads to progression of atherosclerosis by inducing four of the hallmark phenomena associated with atherogenesis: endothelial dysfunction [191, 196], foam cell formation [224], vascular smooth muscle cell proliferation and their migration [208]. The generation of an atherosclerotic plaque leads to the narrowing of coronary blood vessels which ultimately causes the onset of ischemia. The primary therapy for an ischemic event is rapid reperfusion which, despite its need, will cause further damage via the production of ROS. Phospholipid oxidation products have been recently identified in myocardial I/R injury [273, 367-369]. MS analyses have detected a significant increase in OxPC species following *in vitro* I/R injury [369]. These OxPC species have been predominantly fragmented species: POVPC, PONPC, PAzPC and PGPC [369]. An increase in these OxPC species during reperfusion injury can be of great clinical importance since the exogenous addition of these compounds to cardiomyocytes results in death [369]. These data also further confirm the detrimental role of phospholipids in cell death. However, supplementation with an omega-3 ALA fatty acid led to a decrease in POVPC and PGPC during I/R injury [273].

In addition to lipid peroxidation, free iron is necessary for ferroptosis to occur. This is shown by DFO, an iron chelator, which binds iron and prevents cell death [338]. Iron acts as a pro-oxidant in ferroptosis because the redox iron is responsible for the conversion of hydrogen peroxide to a hydroxyl radical through the Fenton reaction [370]. Enzymes involved in ROS production in cells contain iron or iron derivatives that are essential for enzyme function [371, 372]. Cells also contain a labile pool of redox-active iron (LIP - labile iron pool) [373] in the

cytosol, mitochondria and lysosomes [373]. Lysosomes can contain large amounts of labile iron since they are involved in the uptake of exogenous iron and the recycling of endogenous iron [373]. However, maintaining the pools within a relatively narrow concentration range is crucial for the prevention of iron toxicity. Iron accumulation can occur as a consequence of glutamate depletion which sensitizes iron regulatory protein 1 (IRP1) [355]. Evidence shows that ferroptosis can be prevented by inhibition of NADPH oxidase enzymes [338] suggesting iron involvement in ferroptosis, since it is required for NADPH oxidase function. The inhibition of iron carrying protein-transferrin expression led to a reduction of the rate of cell death, further confirming the importance of iron in ferroptosis [355].

There is ample evidence to support the contention that iron is involved in the progression of ischemic heart disease. Even though iron is an essential metal for hemostasis, excessive amounts of iron can lead to pathologies such as hemochromatosis and hepatic carcinoma [374]. Iron overload in the heart occurs in β-thalasemia and hereditary hemochromatosis leading to a cardiomyopathy (12). The leading cause of morbidity and mortality in these patients is due to arrhythmias and early diastolic dysfunction [375]. Moreover, early studies suggested that iron can be involved in the formation and progression of atherosclerosis [376]. The possible mechanism for this was endothelial dysfunction, up-regulation of NADPH oxidase and monocyte adhesion [377] [378]. Excess iron has also been shown to correlate with an increased risk of acute MI [379]. Magnetic resonance imaging of 48 STEMI patients at 4 days and 5 months after percutaneous reperfusion showed higher levels of residual iron in the infarcted area and LV remodeling [353]. A recent study by Baba et al. confirmed the presence of iron overload in cardiomyocytes during ischemia-reperfusion injury [340] suggesting the possible role of ferroptosis in I/R injury. Exposure of mice to 30 minutes of ischemia followed by 24 h of

reperfusion resulted in increased levels of non-heme iron and increased Ptgs2 mRNA levels [380]. Ferrostatin-1 and DXZ pretreatment reduced the infarct size and also prevented the increase of myocardial enzymes in serum: lactate dehydrogenase (LDH), aspartate transaminase (AST) and creatine kinase-MB (CK-MB) [380]. Moreover, exposure to 30 min of ischemia followed by 4 weeks of reperfusion and ferrosttin-1 treatment lead to a decrease in cardiac remodeling and fibrosis [380]. Finally, desferrioxamine which binds iron, was shown to be protective against myocardial I/R *ex vivo* [355]. It has been recently shown that doxorubicin (DOX) induces carditoxicity through ferroptosis [380]. This group shows that DOX treatment induces the accumulation of Nrf2 in the nucleus, which promotes Hmox1 expression leading to a heme degradation and release of iron in the heart. The importance of iron in mediating DOX induced ferroptosis was further shown in mice fed high iron diet. Compared to a normal iron diet, the high iron one lead to an increased mortality and more severe heart damage [380].

As indicated above, GPx4 is a key regulator of ferroptotic cell death. LC/MS-MS analyses as well as western blot analyses showed downregulation of GPX protein in mouse MI model [363]. RNA-seq analyses showed decreased levels of GPx4 mRNA expression, whereas the mRNA of other GPx family members were increased, probably as a defensive mechanism [363]. Moreover, exposure of H9c2 cells to a cysteine free medium lead to a depletion of intracellular GSH content. This lead to a decrease in cell viability, which could be prevented by Ferr-1 and Lip and did not cause poly(ADP-Ribose) polymerase (PARP) cleavage, suggesting that the form of cell death induced by cysteine deprivation is ferroptosis and not apoptosis [363].

These data suggest that ferroptosis is involved in myocardial I/R injury and that ferrostatin-1 could potentially be a new therapeutic approach for reducing the damage caused by reperfusion.

Chapter II: Rationale and hypotheses

a. Rationale

Myocardial I/R injury is accompanied by a large production of ROS leading to a modification of intracellular molecules. The most vulnerable intracellular molecule is PC, highly susceptible to oxidation. PC molecules acquire roles upon oxidation that are not characteristic of their precursors. In non-cardiac cell lines, OxPCs induce apoptotic cell death. Myocardial I/R injury is followed by concomitant loss of cardiomyocytes. It is possible that myocardial injury is in large part induced by cell death associated with the generation of OxPCs. However, the mechanism of OxPC action in the myocardium remains unknown. Therefore, it is of great importance to understand how OxPC molecules can affect myocytes and whether their inactivation by specific antibodies will reduce the damage in I/R. This can lead to a new therapeutic approach for I/R which currently does not exist.

b. Hypothesis

We hypothesize that OxPCs molecules generated during myocardial I/R injury will correlate with cardiomyocyte dysfunction and that they are potent stimulators of cell death.
We hypothesize that the mode of cell death is through ferroptotic process.
We also hypothesize that antibody-mediated inactivation of OxPCs generated in a MI will attenuate the detrimental effects of OxPCs.

Chapter III: Objectives

The focus of the present study will be to:

1. Determine the effects of various OxPCs in different concentrations on cardiomyocyte viability;
2. Determine the effects of POVPC on cardiomyocyte viability in time dependent manner;
3. Identify CD36 as a possible site of OxPC action;
4. Determine the effects of OxPCs on mitochondrial function;
5. Determine the effects of OxPCs on cardiomyocyte contractile function;
6. Identify the cell death pathway induced by OxPCs in cardiomyocytes;
7. Identify the potential for E06 antibody to prevent cardiomyocyte cell during I/R injury caused by OxPCs.

Chapter IV: Methods

All animal experiments conformed to the Canadian Council on Animal Care (CCAC) guidelines regarding animal experimentation and were approved by the Research Ethics Board of the University of Manitoba.

Cardiomyocyte isolation

Adult rat ventricular myocytes were isolated from 12 week old male Sprague Dawley rats as described previously [273]. Animals were anesthetized with an intraperitoneal injection of a cocktail mixture consisting of ketamine (90 mg/kg) and xylazine (10mg/kg). The heart was removed and cannulated on the Langendorff perfusion system followed by washing with Ca^{2+} free buffer containing 90 mM NaCl, 10 mM KCl, 1.2 mM KH_2PO_4, 5 mM $MgSO_4$•7H2O, 15 mM $NaHCO_3$, 30 mM taurine, and 20 mM glucose for 10 min. Perfusion was then continued for 30 minutes with the buffer containing collagenase (WORTINGTON, Collagenase type II) (0.05%) and 0.2% bovine serum albumin. Ventricles were minced the isolation of individual myocytes by gravitational separation was continued in a 37°C water bath. Cells were then suspended in a series of buffers with increasing Ca^{2+} concentrations (150 μM, 500 μM and 1.2 μM). In a final step, cells were re-suspended in medium (M199 containing penicillin (50 U/ml), streptomycin (50 U/ml)) on laminin coated coverslips and incubated for 1.5-2 h in a CO_2 incubator (5% CO_2 and 95% O_2). The medium was replaced with fresh medium before proceeding with the treatment.

Neonatal cardiomocyte isolation

Neonatal cardiomyocytes were isolated from 1 to 2 day old rat pups. The hearts were excised by mid-line sternotomy after cervical dislocation. Hearts were washed and minced to adequately break up macroscopic structures. To remove red blood cells and debris re-washing with cold filter sterilized phosphate buffered saline (PBS) containing 10 g/L of glucose was done. The heart fragments were enzymatically digested with collagenase (740U), trypsin (370U), and DNase (2880U) (Worthington Biochemical) for three 10-min and three 7-min digestions at 35ºC. Solutions containing digested supernatant were centrifuged into a cell pellet and then a Percoll® (GE Healthcare) gradient of 1.05, 1.06, and 1.082 g/mL was used to separate cell types allowing for the layer rich in myocytes to be isolated. . The cells were then pre-plated on non-coated 150 mm culture plates for 45 min to remove fibroblasts. Purified NNCM (95% pure by sarcomere staining) were then transferred to sterile tissue culture plates at a cell density of 1.75 x 10^6/35-mm plate. Dulbecco's Modified Eagle Medium/Ham's nutrient mixture F-12 (1:1) containing 2 mM glutamine, 3 mM NaHCO3, 15 mM HEPES, and 50 mg/mL gentamycin (DMEM/F12) plus 10% fetal bovine serum (FBS) was used for the overnight incubation of the cells. The following day DMEM/F12 with 10% FBS was changed to serum-free DMEM/F12 (DFSF).

Cell viability assay

Cell viability was assessed using the (LIVE/DEAD® Viability/Cytotoxicity Kit, Life Technologies™) assay kit. Cells were incubated with increasing doses (0.1-10 μM) of fragmented OxPCs : POVPC, PAzPC (1-palmitoyl-2-azelaoyl-sn-glycero-3-phosphocholine), PONPC, KOdiA-PC (1-palmitoyl-2-(5-keto-6-octene-dioyl)-sn-glycero-3-phosphocholine),

KDdiA-PC (1-palmitoyl-2-(4-keto-dodec-3-enadioyl)-sn-glycero-3-phosphocholine), PGPC (1-palmitoyl-2-glutaroyl-*sn*-glycero-3-phosphocholine) and a non-oxidized PC, PSPC (1-palmitoyl-2-stearoyl-sn-glycero-3-phosphocholine), which was used as a control. Commercially available fragmented OxPC standards (Avanti polar lipids, Alabaster, Alabama) were prepared as unilaminar liposomal vesicles. Following 1 h treatment with OxPCs and PSPC, a cell viability assay was performed for 30 minutes. Cells were washed twice with HEPES buffer and fixed with 4% paraformaldehyde. Images were taken on a Nikon Eclipse TE2000S fluorescent microscope. NIS software was used for quantification. Results are presented as the percent of live cells over total. Six fields per coverslip were used and all cell numbers per field were combined representing $n = 1$. These were repeated for each individual experiment ($n = 3$). Cells were counted in a blinded fashion.

Cleaved Caspase 3 detection

Western blot analyses were performed to determine the expression of cleaved Caspase 3 in cardiomyocytes treated with PSPC and POVPC. Following treatment with 10μM POVPC and 10μM PSPC for 1 h, cells were harvested and lysed in RIPA buffer containing protease inhibitory cocktail. Protein content was determined by the BCA protein assay. Proteins were then separated on polyacrylamide gel, followed by transfer onto membranes. Blots were incubated overnight with the primary antibody 1:1000 (Caspase 3, Cell signaling) at 4 °C. HRP-conjugated secondary antibody incubation was carried out for 1 h at room temperature. Blots were then developed by enhanced chemiluminescence (ECL) detection. Western blot data was quantified by normalizing bands to total protein in each lane [381]. Each experiment was repeated n=3 times.

HMGB-1 (High mobility group box 1) detection

The HMGB-1 protein amount in cardiomyocytes treated with 10 µM OxPCs and 10 µM PSPC was determined by Western blot analyses. Following 1 hour treatment, cells were lysed in RIPA buffer containing protease inhibitory cocktail. The BCA protein assay was used to determine protein content. Proteins were then size-fractionated by SDS-PAGE and transferred onto membranes. Blots were incubated overnight with the primary antibody 1:1000 (HMGB-1, Abcam) at 4 °C. HRP-conjugated secondary antibody incubation was carried out for 1 h at room temperature. Blots were then developed by enhanced chemiluminescence (ECL) detection. Western blot data was quantified by normalizing bands to total protein in each lane [381]. Each experiment was repeated n=3 times.

Cardiomyocyte treatment with POVPC and Ferrostatin

Cardiomyocytes were exposed to 1 hour of 10 µM POVPC or 10 µM POVPC and 1µM ferrostatin -1. Following treatment, cell viability was determined by a Live/Dead assay. Cells were then fixed with 4% paraformaldehyde and mounted. Results are presented as percent of live cells over total. Experiment was repeated n=3 times.

Simulated I/R injury

Isolated cardiomyocytes were first incubated for 1 h in a hypoxic chamber with an ischemic buffer modified according to Lucas and Ferrier [382] containing 140 mM NaCl, 8 mM KCl, 1 mM MgCl2, 1.8 mM CaCl2, 6 mM HEPES. The pH was 6.0 and it did not contain glucose. The buffer was bubbled with 100% nitrogen. Following ischemia 1 h of reperfusion was

induced by incubation of cells with Tyrode buffer composed of 140 mM NaCl, 6 mM KCl, 1 mM MgCl2, 1.25 mM CaCl2, 6 mM HEPES (pH 7.4), and 10 mM D-glucose and bubbled with 100% oxygen. At the time of reperfusion, 1 μM ferrostatin-1 (Sigma-Aldrich) or 40μg of E06 antibody (Avanti polar lipids, Alabaster, Alabama) were added. Following treatment a Live/Dead assay was performed to determine cell viability. Cells were then fixed with 4% paraformaldehyde and mounted. Results were presented as percent of live cells over total.

Treatment with a CD36 inhibitor

Pre-incubation of isolated cardiomyocytes with 25 μM sulfosuccinimidyl oleate (SSO-Cayman Chemical), or the same amount of DMSO, for 15 minutes was followed by treatment with 10 μM OxPC for 1 h. Following treatment, a Live/Dead assay was performed and cells were fixed in 4% paraformaldehyde and mounted on slides. Results were presented as a percent of live cells over total.

Tunel assay

Following treatment of cardiomyocytes with 5 μM POVPC and PONPC for 1 h, a Tunel assay was performed as previously described [273]. Apoptosis detection was performed using the ClickiTPlus Tunel Assay with Alexa 488, as per the manufacturer's instructions (Molecular Probes, Burlington, Canada). Cardiomyocytes were fixed in 4% paraformaldehyde for 15 minutes at room temperature. Cells were then washed and permeabilized with 0.25% Triton-X in PBS for 20 minutes. Pre-incubation with TdT reaction buffer for 10 minutes was followed by the incubation with the TdT reaction cocktail for 60 minutes at 37 ºC. Cells were washed two times in 3%BSA in PBS before proceeding to incubation with Clicl-iT Plus Tunel reaction cocktail for

30 minutes at 37 ºC protected from light. Cells were then washed in 3% BSA in PBS. Images were taken on a Nikon Eclipse TE2000S fluorescent microscope. Each experiment was repeated n=3 times.

Mitochondrial stress test

Seahorse Bioscience XF24 Flux Analyzer was used to measure the bioenergetic response of adult rat cardiomyocytes. Following the isolation, cells were seeded in the laminin pre-coated XF plates at a density of 3750 cells per well in media M199 for 1.5 h. The culture medium M199 was then replaced with 675 µl of HEPES buffer containing 10 mM glucose and supplemented with 1 mM pyruvate or the same HEPES buffer containing POVPC or PONPC. Following 1 h treatment in the incubator without CO_2, an automated Seahorse protocol was performed. The protocol consisted of 11 minutes calibration/equibrilation, followed by injection of drugs at optimized concentrations in each of 3 ports (2 min mix, 2 min wait, 2 min measure). The ports were loaded with: FCCP 4 µM, oligomycin 10 µM, a mixture of 4 µM antamycin A and 2 µM rotanone. Following the basal measurements, the first drug to be injected was oligomycin which is an ATP synthase (Complex V) inhibitor. It decreases the electron flow through the electron transport chain, resulting in the reduction in OCR. The second drug to be injected was FCCP which is an uncoupler. It collapses the proton gradient and disrupts mitochondrial membrane potential leading to an uninhibited electron flow through the electron transport chain. As a result the oxygen consumption by Complex IV will reach the maximum. Once the basal and maximal OCR are determined, spare respiratory capacity can be calculated. Spare respiratory capacity is the ability of the cell to respond under stress when the energy demand is increased. The last injection included mixture of rotenone, Complex I inhibitor and antamycin A, Complex III

inhibitor. This leads to a complete inhibition of mitochondrial respiration chain and allows the calculation of nonmitochondrial respiration.

Calcium transient measurements

Isolated cardiomyocytes were loaded with the calcium sensitive dye Fura-2 AM (1 μM), which was used as an intracellular Ca^{2+} indicator. The calcium signal was collected on a PTI Ratiomaster spectrofluorometer as described previously [383]. Adherent cells were loaded with Fura-2 AM for 15 minutes at 37 ºC, washed and then mounted in a Leiden chamber and perfused for one hour with control buffer with or without 0.1 μM PSPC, POVPC or PONPC. Cells were excited at 340 and 380 nm with an emission of 505nm. Cardiomyocyte contractile activity was measured by a video edge-detection system (Crescent Electronics, Sandy, UT) coupled with the camera that captures data at a rate of 60 Hz. Cell length was determined by calibrating the signal with a stage micrometer and recording the results with Felix GX software. Data was collected and recorded for 30 seconds every 5 minutes for up to a total of 60 minutes.

Calcium measurements during I/R with or without addition of ferrostatin-1

Cardiomyocytes adherent on a coverslips were loaded with 2 μM Fura-AM for 15 minutes at 37º C, washed and mounted on a Laiden chamber heated to 37° C with a Medical Systems PDMI-2 Open Perfusion Micro-Incubator (Greenvale, NY). Cells were perfused at the rate of 1 ml/minute with the control perfusate bubbled extensively with 100% oxygen. The control perfusate contained 140 mM NaCl, 6 mM KCl, 1 mM $MgCl_2$, 1.25 mM $CaCl_2$, 6 mM

HEPES (pH 7.4), 10 mM dextrose, and 0.02% BSA. After an initial period of equilibration, the perfusate was changed from the control perfusate to an ischemic solution, modified from Lukas and Ferrier [382]. The ischemic perfusate was bubbled with 100% nitrogen gas for ≥45 min before the experiment was started. The duration of the ischemic perfusion was 30 min after which the perfusion was continued with the control perfusate with or without 1 μM Ferrostatin-1 for 15 minutes.

Phosphatidylcholine hydroperoxyde (PC-OOH) preparation

PC–OOH preparation was conducted as described previously by Roveri et al [384]. PLPC (1-palmitoyl-2-linoleoyl-sn-glycero-3-phosphocholine) at the concentration of 0.3mmol/L was incubated with 0.7 mg of (Cayman Chemical) for 90 min at room temperature. A Sep-Pak C18 cartridge (Waters, Milford MA), pre-conditioned with methanol and equilibrated with water was used to load the mixture following incubation. After one wash with 10ml of water, the sample was collected in 6 ml of methanol. Finally, the sample was dried and reconstituted in 0.5 ml of methanol and stored at -20 ºC.

A 4000 QTRAP triple quadrupole mass spectrometer system with a Turbo V electrospray ion source from AB Sciex (Framingham, MA, USA), coupled to the liquid chromatography system was used to confirm the presence of PC-OOH in the sample following the solid phase extraction (SPE). The separation of PC-OOH was carried out using reverse phase chromatography. The sample was reconstituted in RP eluent consisting of 60:40 acetonitrile:water, 10 mmol/L ammonium formate and 0.1% formic acid immediately prior to injection. Thirty μl of the sample was injected onto an Ascentis Express C18 HPLC column (15 cm × 2.1 mm, 2.7 μm; Supelco Analytical, Bellefonte, Pennsylvania, USA) with separation

by a Prominence UFLC system from Shimadzu Corporation (Canby, OR, USA). Elution was performed using a linear gradient of solvent A (acetonitrile/water, 60:40 v/v) and solvent B (isopropanol/acetonitrile, 90:10, v/v) with both solvents containing 10 mmol/L ammonium formate and 0.1% formic acid. The mobile phase composition that was used is as follows: initial solvent B at 32% until 4.00 min; switched to 45% B; 5.00 min 52% B; 8.00 min 58% B; 11.00 min 66% B; 14.00 min 70% B; 18.00 min 75% B; 21.00 min 97% B; 25.00 min 97% B; and 25.10 min 32% B. A flow rate of 260 µL/min was used for analysis, and the sample tray and column oven were held at 4°C and 45°C, respectively.

Glutathione peroxidase 4 (GPx4) activity assay

GPx4 enzyme activity was measured using a glutathione peroxidase assay kit (Abcam). Isolated cardiomyocytes were treated with 5 µM PSPC, POVPC or PONPC for 1 h. Following treatment, cells were harvested and samples were prepared according to the assay protocol. Fifty µg of protein per sample was incubated with 10 µl of the previously prepared substrate (PC-OOH) and a Plate Reader (FLUOStar Omega Luminometer) was used to measure the enzyme activity. The data was presented as a percentage of control for n=6.

Nuclear magnetic resonance (NMR) analyses of OxPC interaction with PONPC

The mixture of 1 mg of Ferrostatin-1 standard with 0.1mg of PONPC standard in 1:1 chloroform:methanol was incubated overnight at 37 ºC with the constant shaking. For the standard samples, 1µg of standard was measured and dissolved in 550µL of deuterated

chloroform ($CDCl_3$); the mixture is then transferred into a 5mm NMR tube. The reaction sample was dried then reconstituted in $CDCl_3$ and transferred into a 5mm NMR tube. The NMR experiments were conducted on a Bruker Ascend 600 spectrometer, operating at 600.27 MHz for proton nuclei and 150.938 MHz for carbon nuclei. Each sample was run with a probe temperature of 298.0 K within 24 hours of preparation. Seven different scans were run, focusing on NOESY, COSY, and HSQC for analysis. The proton was run with a 65.5k time domain, a 90° pulse width of 10µs, a spectral width of 16ppm, and a relaxation delay of 5s. The number of scans was 32 with 2 dummy scans producing an acquisition time of 4.75mins. The NOESY was suppressed at 2823Hz, with a time domain of 32.7k, a 90° pulse width of 10µs, a spectral width of 16ppm, and a relaxation delay of 5s. The 7.75 min acquisition time was produced by 64 scans and 4 dummy scans. The ^{13}C also had a time domain of 32.7k, but the 90° pulse width was 12µs, the spectral width 240ppm, and the relaxation delay 2s. The number of scans was 7168 with 4 dummy scans producing an acquisition time of approximately 5.5 hours. The ^{13}Cdept135 and ^{13}Cdept90 both had a 65.5k time domain, with a 90° pulse width of 12µs, a spectral width of 240ppm, and a relaxation delay of 2s. However, the ^{13}Cdept135 used 3072 scans with 8 dummy scans for an acquisition time of approximately 2.5 hours, while the ^{13}Cdept90 used 2048 scans and 8 dummy scans for an acquisition time of approximately 1.75 hours. The COSY and the HSQC had a 90° pulse width of 10µs and a relaxation delay of 1.5s, but the time domain had different values for F1 and F2, 2048 and 400, respectively. The COSY had a spectral width of 16ppm for both F1 and F2, and the 32 scans with 16 dummy scans gave an acquisition time of approximately 6 hours. The HSQC had spectral width of 16ppm for F1 and 164ppm for F2, the acquisition time was 22.25 hours due to the 64 scans and 16 dummy scans.

BNip3 knockdown

Short hairpin RNA (shRNA) directed against Bnip3 targeted against exon 3 of Bnip3, with the sequence 5'-CAC CGACA CCACA AGATA CCAAC AGCGA ACTGT TGGTA TCTTG TGGTG TC-3' was designed to knock-down Bnip3 expression in neonatal cardiomyocytes. BLOCK-iT U6 RNAi entry vector kit (Invitrogen) was used to construct adenoviral vectors encoding shRNA-Bnip3 or non-relevant shRNA [385]. Adenoviral vectors encoding a shRNA directed against Bnip3 or control shRNA at a multiplicity of infection of 10 were then used to infect the cells for 24 h in DMEMSF. Cardiomyocytes without or with Bnip3 knock-down were treated with 5μM PSPC,POVPC and PONPC 24 hours following the infection.

Myocardial ischemia/reperfusion injury in a pre-clinical pig model

Animal model: Male swine, 45 to 50 kg, were used for this study. Pigs were anesthetized with telazol/xylazine (2.5mg/kg for telazol and 5mg/kg for xylazine) followed by inhaled isoflurane at the dosage of 5% for the remainder of the study. Animals were intubated with the 9.0 mm endotracheal tube. Temperature was measured and maintained at 37.5 ± 0.5 ºC with the warming blanket.

All animals received an IV heparin bolus (100U/kg) and 1000 U heparin every hour thereafter. The animals were ventilated with room air using volume controlled ventilation (North American Drager; Narkomed2B anesthetic) with tidal volume 10 ml/kg and the respiratory rate adjusted to maintain $PaCO_2$ of 40 mmHg and arterial O_2 saturation > 95% . Surface electrographic tracings (ECG) and other vital signs were continuously monitored by SurgiVet Advisor (V9200, Smiths Medical).

Animals were randomized into a control or E06 group.

Percutaneous coronary occlusion: Vascular access was obtained in the bilateral femoral arteries with the 6-F sheats placed percutaneously. In addition, 8F-sheat was placed in the left femoral vein. The left main coronary artery was engaged with a 6F HS guide advanced from the right femoral sheat with fluoroscopic guidance. Coronary angiography was performed with the injection of Omnipaque contrast. The coronary guide wire was inserted in the left anterior descending (LAD) artery over which a 3.0 mm balloon was advanced distal to the second diagonal branch. The balloon was inflated occluding the flow. Vessel occlusion was verified with intracoronary (IC) contrast injection showing no blood flow beyond the balloon. The vessel remained occluded for 60 minutes after which the balloon was deflated. A brief coronary angiogram was performed to verify the blood flow to the ischemic region. Another micro infusion balloon connected to the injector was inserted to allow for antibody or saline administration. Both were delivered over the first hour of reperfusion, first by injecting the bolus and then allowing for the remaining amount to be injected slowly. Since the IgM E06 antibody infusion has not been studied during IR injury, the dosage for the pigs was calculated from the *in vivo* study which showed that intraperitoneal E06 injection at 2.5 mg/kg resulted in a decrease in plasma OxPC levels [386]. Since the heart of a pig is approximately 200 g, we calculated the starting dosage to be 0.5 mg of the E06 delivered over one hour. Total time of reperfusion was 2 h. Following reperfusion, the balloon was positioned and inflated again and 2% Evans Blue dye was injected into both, left and right coronary arteries. Forty milliliters of 40mM KCl was then administered to stop the heart in diastole. The heart was then removed.

TTC Staining: After the heart was taken out, 5 slices 1 cm thick were made and incubated in 1% TTC mixture at 37ºC for 20 minutes. Following the incubation, pictures were taken and analyzed

by ImageJ software. Arterial, venous and coronary blood samples were taken at indicated time points. Blood was immediately centrifuged at 10,000xg for 10 minutes and plasma was kept at -80ºC until the further analyses were done.

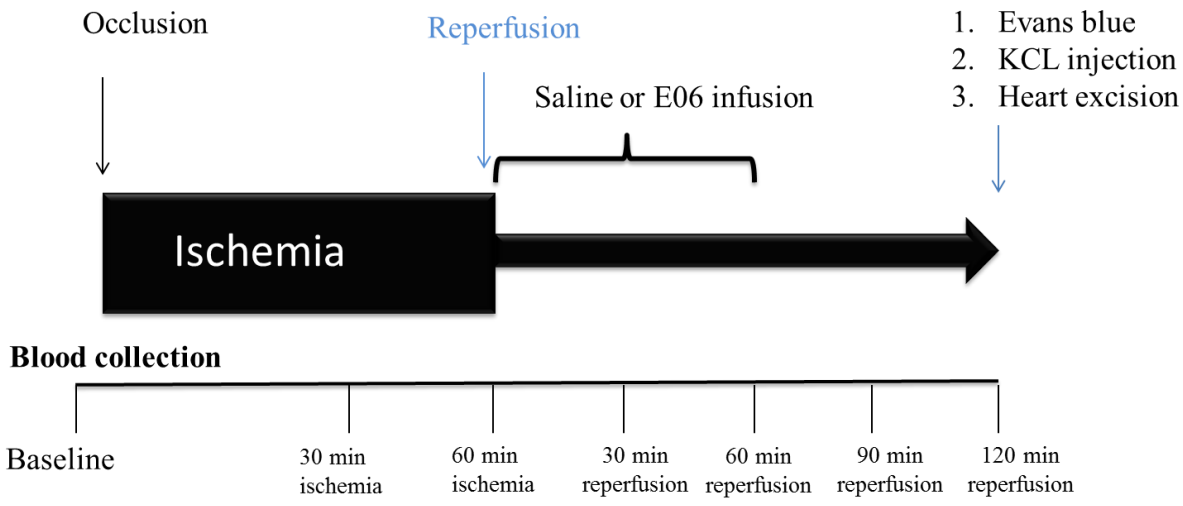

Figure 5. Schematic representation of pig reperfusion protocol

Statistical analysis

One-way analysis of variance (ANOVA) was used to determine statistically significant differences between groups, with the Tukey post-hoc test, using a level of significance set at $P<0.05$. SPSS Software (version 24, IBM Corporation, Armonk, NY, USA) was used for calculations. A T-test was used to identify statistically significant differences when only two groups were compared. All data are presented as ±SEM

Chapter V: Results

Effects of various OxPCs in different concentrations on cardiomyocyte viability

To establish the effects of OxPCs on cardiac cell viability, isolated cardiomyocytes were exposed to various concentrations of different OxPCs. Increasing concentrations (0.1-10 μM) of the unoxidized control phospholipid PSPC did not affect cardiomyocyte viability (Figure 6B). Fragmented OxPCs: KDdiA-PC ($p<0.05$), PAzPC ($p<0.05$) and PGPC ($p<0.01$) caused significant decrease in cardiomyocyte viability only at higher (10μM) concentration (Figure 6B). However, two fragmented OxPCs, POVPC ($p<0.01$) and PONPC ($p<0.001$), induced significant cardiomyocyte death at lower 5μM concentrations (47.42 % POVPC, 55.54% PONPC) (Figure 6B).

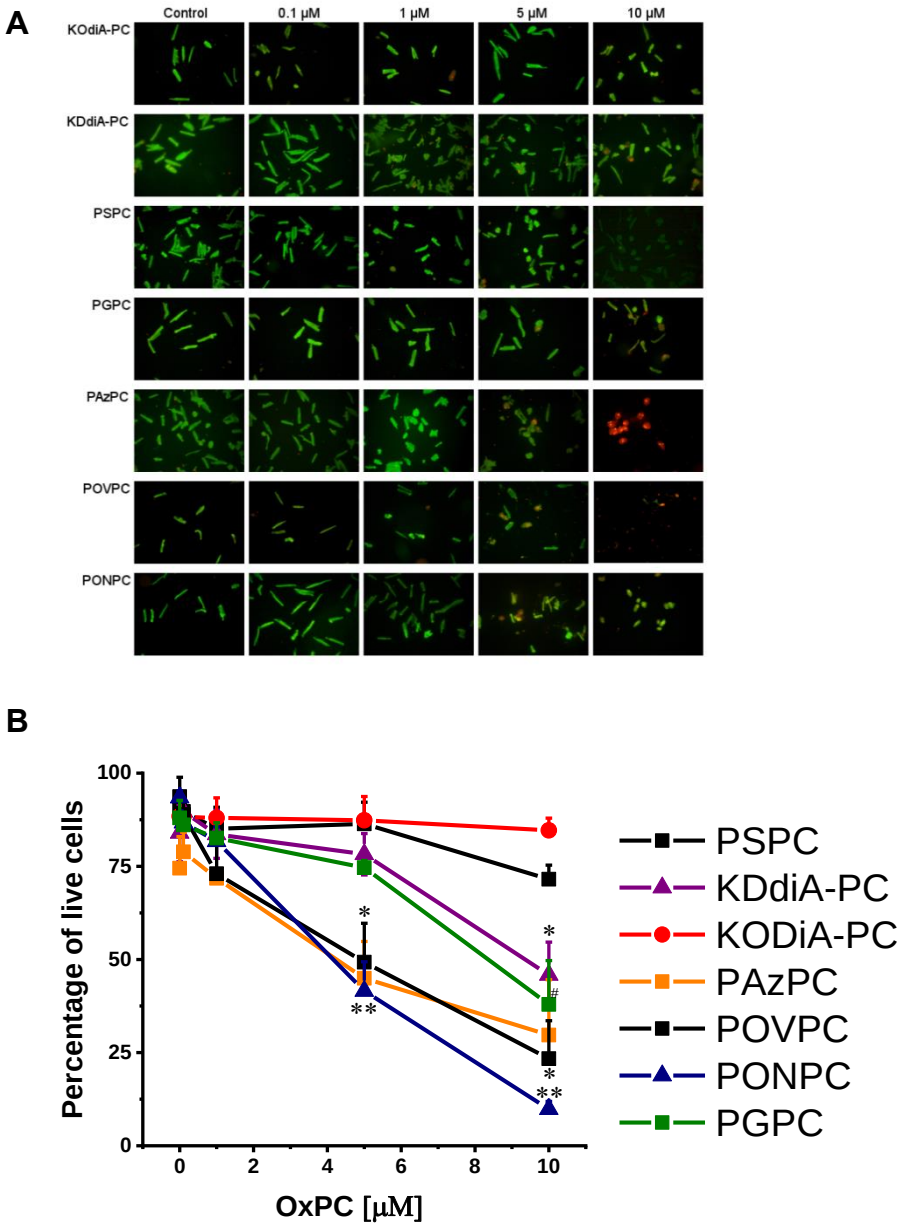

Figure 6. Impact of various fragmented OxPC species and PSPC on cardiomyocyte viability **A:** Representative images of cardiomyocytes treated with various OxPCs and control PSPC in different concentrations **B**. Cardiomyocyte viability after 1 h exposure to different concentrations of a control PSPC and a number of fragmented OxPCs; *Significant compared to

control P<0.05; **P<0.01; ***P<0.001; n=3, ANOVA with post hoc Tuckey test; Green indicates live cells, red indicates dead cells

Effects of POVPC on cardiomyocyte viability as a function of exposure time

Our previous work has shown that POVPC increases during I/R injury [212]. Incubation of cardiomyocytes with 0.1µM POVPC over 4 h led to a decrease in cell viability in a time dependent manner compared to control (Figure 7). POVPC induced a significant decrease in viable cells (10.33%, p<0.05)) after as little as 15 minutes.

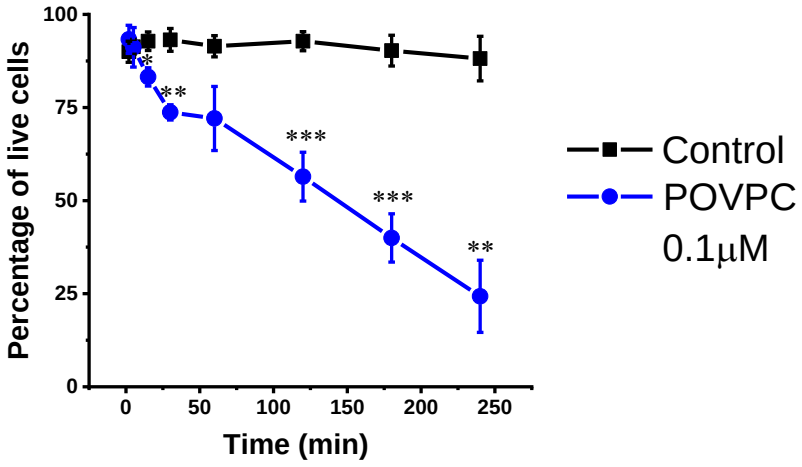

Figure 7. Cardiomyocyte viability following 4 h exposure to 0.1 µM POVPC. Values are mean ±SEM (n=4) *Significant compared to control P<0.05; **P<0.01; ***P<0.001; ANOVA with post hoc Tuckey test

CD36 as a possible site of OxPC action

In previous studies, OxPCs mediated their effects through a CD36-dependent pathway. OxPCs induced platelet aggregation [255] and foam cell formation by binding to the CD36 receptor on macrophages [240]. Sulfosuccinimidyl oleate (SSO) binds to the CD36 receptor and blocks the uptake of OxPC's by macrophages [387]. Therefore, we tested if the CD36 receptor is the possible site of cardiotoxic action of the two fragmented OxPCs, POVPC and PONPC. Pre-incubation of cells with SSO was followed by the addition of POVPC or PONPC. However, pre-incubation with SSO did not prevent cardiomyocyte cell death induced by POVPC or PONPC (n=5 for control; n=4 for POVPC+SSO and POVPC+ DMSO and n=5 for PONPC+SSO and PONPC+DMSO, $P < 0.05$) (Figure 8). This would suggest that these two fragmented oxidized species do not exert their cardiotoxic action via binding to the CD36 receptor.

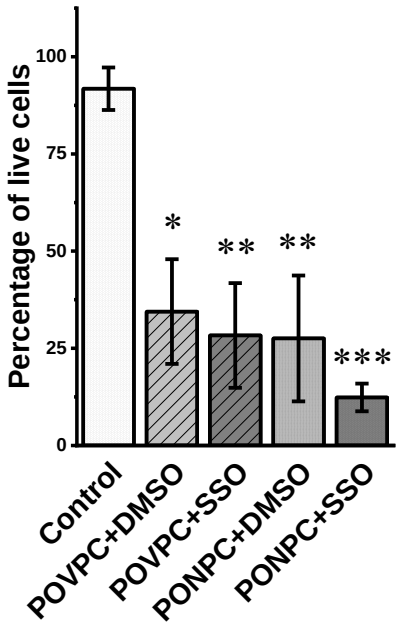

Figure 8. Cardiomyocyte viability following pre-incubation with CD36 receptor inhibitor sulfosuccinimidyl oleate (SSO) followed by addition of POVPC or PONPC *Significant compared to control $P<0.05$; **$P<0.01$; ***$P<0.001$; n=5 for control; n=4 for POVPC+SSO and POVPC+ DMSO and n=5 for PONPC+SSO and PONPC+DMSO; ANOVA with post hoc Tuckey test

Effects of OxPCs on mitochondrial function

To examine the effects of POVPC and PONPC on mitochondrial function we have used the Seahorse Bioscience XF24 Flux Analyzer. We observed a significant decrease in basal respiration in cardiomyocytes treated with 0.1 µM POVPC (46.7% reduction) compared to control, whereas the treatment of cardiomyocytes with 0.1 µM PONPC (40% reduction) shows a trend towards a reduction but this did not quite reach statistical significance (p=0.058) (Figure 9B). Maximal respiration was significantly lower when cells were exposed to PONPC (54%) (Figure 9C). Consequently, a significant reduction in spare respiratory capacity in PONPC treated cells was observed, with a similar trend in POVPC treated cardiomyocytes (Figure 9D).

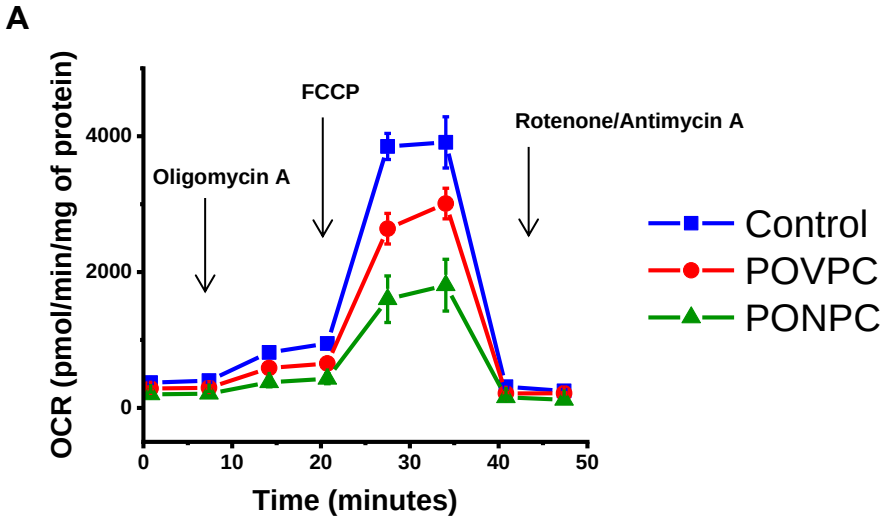

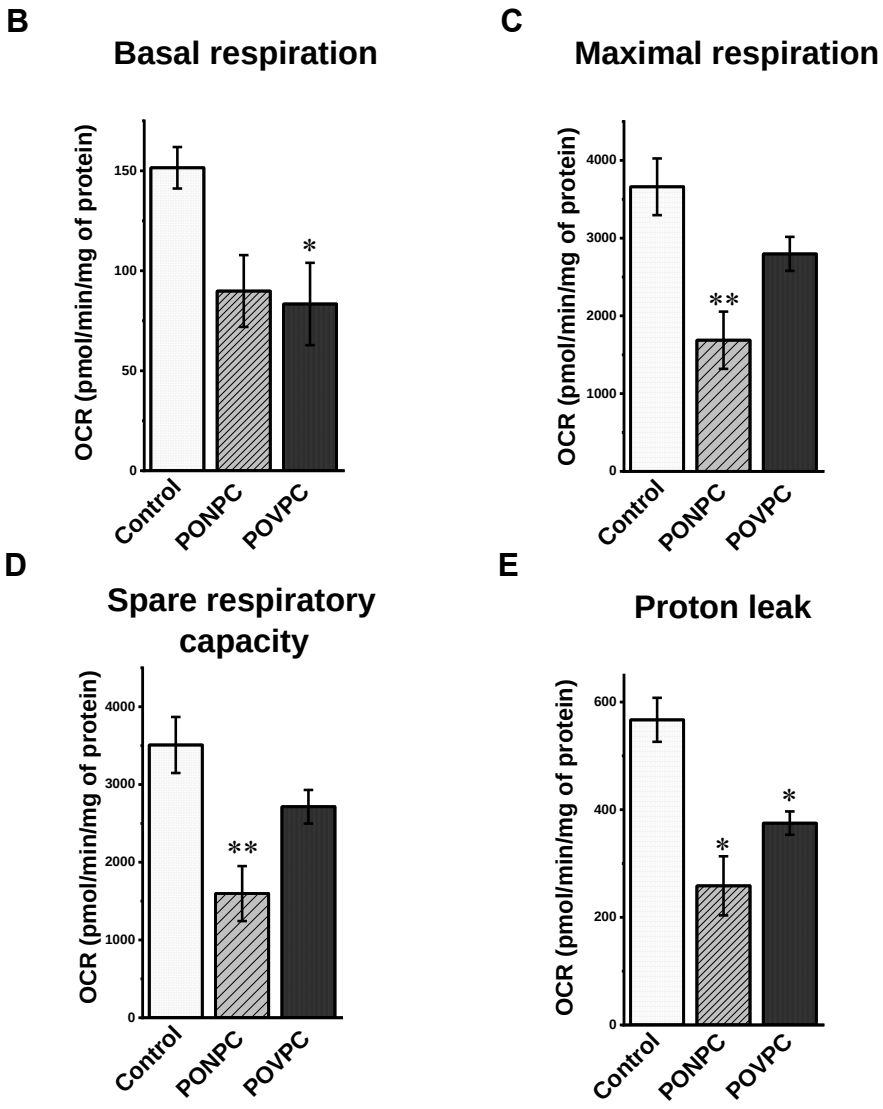

Figure 9. OxPC-induced disruption of mitochondrial respiration. **A**: XF trace in control and cells treated with 0.1 μM POVPC and 0.1 μM PONPC; **B**: Basal respiration normalized according to the protein concentration; **C**: Maximal respiration and **D**: Spare respiratory capacity and **E**: Proton leak normalized to protein concentration; Data are presented as means ± SEM for n=5; *Significant compared to control $P<0.05$; **$P<0.01$; ***$P<0.001$ by one-way ANOVA and Tukey's post-hoc test

Extracellular acidification rate (ECAR) decreased significantly in cardiomyocytes treated with PONPC (53.88% reduction, $P< 0.001$) and POVPC (28.9% reduction, $P<0.05$) compared to control upon oligomycin addition (Figure 10). In addition, a reduction in the ECAR was observed upon the addition of FCCP and Rotenone/Antimycin A in cardiomyocytes treated with PONPC (47.77% and 66.6% reduction respectively, $P<0.001$ for FCCP and $P<0.05$ for Rotenone/Antimycin A) (Figure 10D and E).

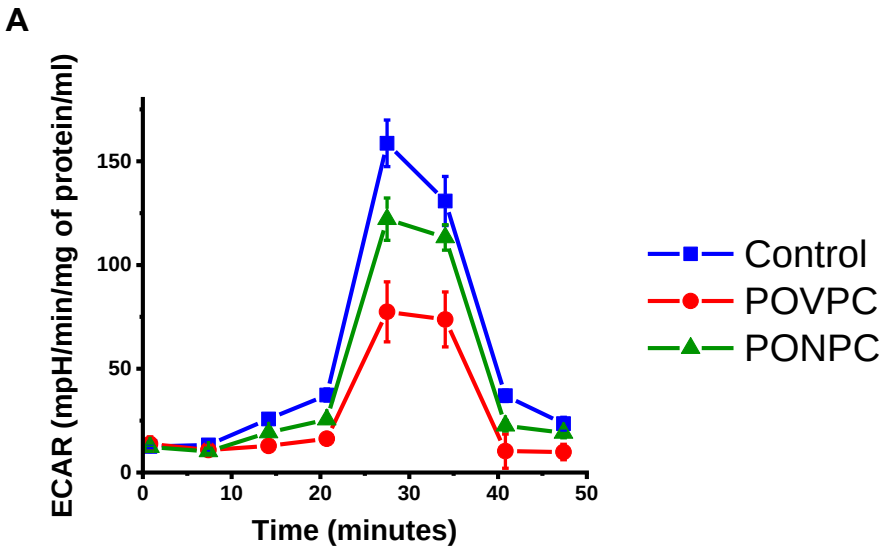

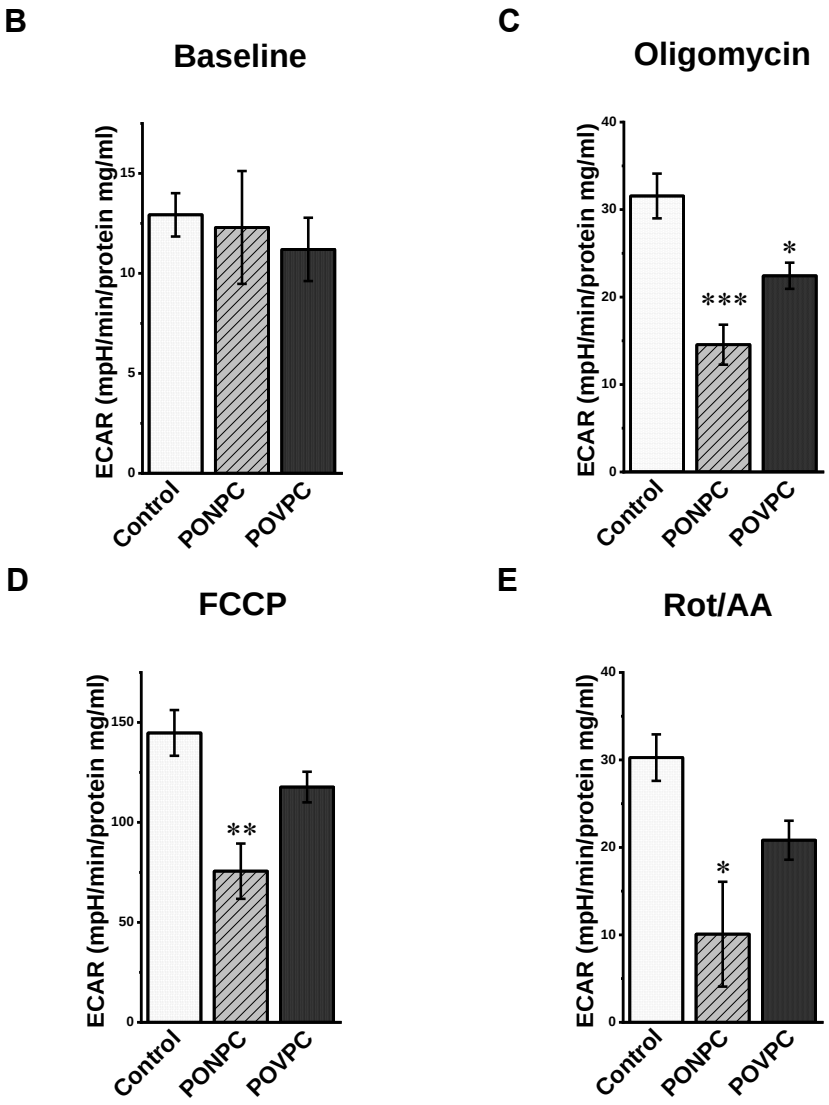

Figure 10. A: Extracellular acidification rate (ECAR) trace in control and cells treated with 0.1 µM POVPC and 0.1 µM PONPC; **B**: ECAR baseline; **C**: ECAR following Oligomycin addition; **D**: ECAR following FCCP addition; **E**: ECAR following the addition of Rotenone/Antimycin A; Data are presented as means ± SEM for n=5; *Significant compared to control P<0.05; **P<0.01; ***P<0.001 by one-way ANOVA and Tukey's post-hoc test

It has been previously shown that mitochondria involvement in ischemia reperfusion injury is mediated through Bnip3 [388]. Exposure of neonatal cardiomyocytes to POVPC and PONPC leads to a significant increase in Bnip3 expression [369]. Moreover, pretreatment of cardiomyocytes exposed to 5 µM POVPC and 5 µM PONPC with the E06 antibody led to a decrease in Bnip3 expression [369]. Bnip3 knock-down cells were more resistant to POVPC compared to wild type cells (*P<0.05) (Figure 11A and B).

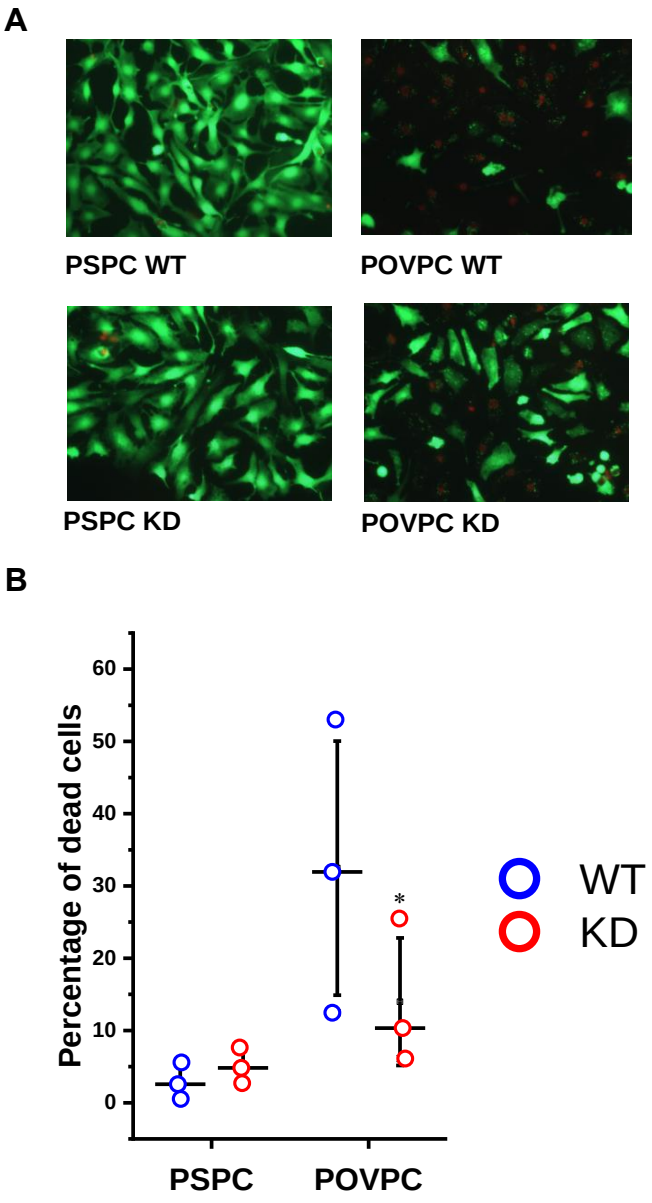

Figure 11. Cell viability of NNCM exposed to 5 µM POVPC and 5 µM PSPC in wild-type and Bnip3KO cardiomyocytes. **A:** Representative images of WT and Bnip3 KO neonatal cardiomyocytes treated with 5 µM of PSPC and POVPC; **B:** Percent cell death in NNCM exposed to POVPC in wild-type and Bnip3KO cardiomyocytes (n=3) SEM; (WT POVPC vs. Bnip3 KD POVPC), *P< 0.05, Student's t test; Yeang C, Hasanally D, Que X, Hung MY, Stamenkovic A, Chan D, Chaudhary R, Margulets V, Edel AL, Hoshijima M, Gu Y, Bradford W, Dalton N, Miu P, Cheung DY, Jassal DS, Pierce GN, Peterson KL, Kirshenbaum LA, Witztum JL, Tsimikas S, Ravandi A. Reduction of myocardial ischaemia-reperfusion injury by inactivating oxidized phospholipids. Cardiovasc Res. 2019 Jan 1;115(1):179-189. *Modified with permission*

OxPCs effect on cardiomyocyte contractile function

The effect of POVPC and PONPC treatment on Ca^{2+} handling and contraction was examined in this study as a potential mechanism for cardiomyocyte damage and cell death. A significant decrease (0.3µm on average) in cardiomyocyte net contraction between 30 and 60 minutes was observed when cells were treated with OxPCs compared to control and PSPC (*P<0.05, **P<0.01) (Figure 12A). Additionally, treatment with 0.1µM POVPC or 0.1µM PONPC caused a significant decrease in Ca^{2+} transients compared to PSPC-treated cells (P<0.05; 28.39% in POVPC and 24.17% reduction in PONPC group) (Figure 12B).

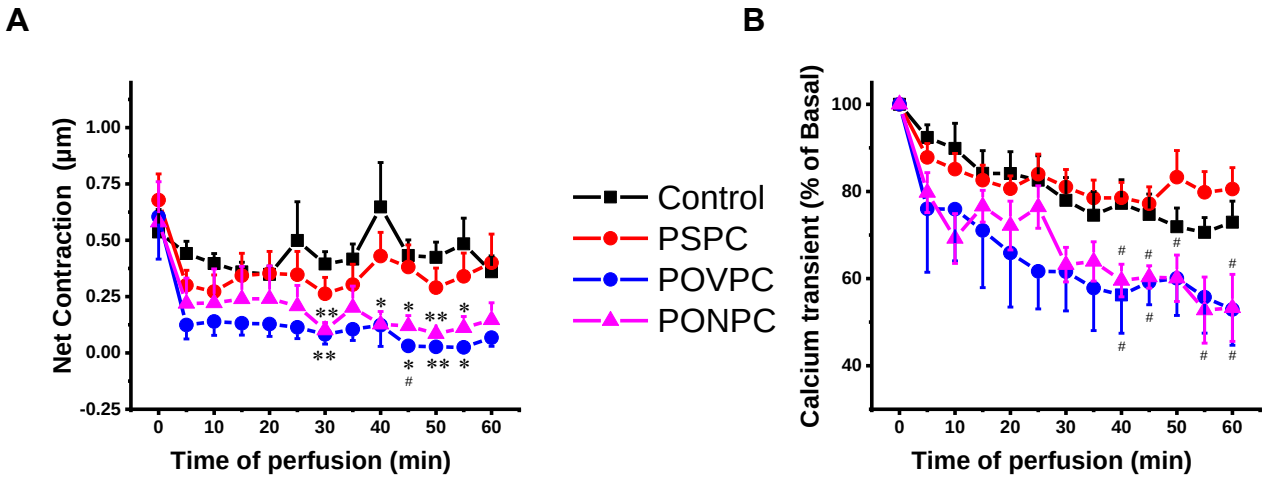

Figure 12. Impact of OxPC on cell contraction and calcium transients **A**: Net contraction measured in microns from cardiomyocytes treated with control HEPES perfusion buffer, PSPC, POVPC and PONPC. **B**: Calcium transients of cardiomyocytes represented as a percent of basal following 1 hour treatment with control perfusion buffer, 0.1 µM PSPC (1-palmitoyl-2-stearoyl-*sn*-glycero-3-phosphocholine), 0.1 µM POVPC and 0.1 µM PONPC; Data collected for 30 seconds each 5 minutes over one hour. *P<0.05 compared to control, #P<0.05 compared to PSPC. Mean values ± SEM from a series of experiments. ANOVA with post hoc Tuckey test

Cell death pathway induced by OxPCs in cardiomyocytes

Apoptosis

To investigate the mechanism through which OxPCs induce cell death, western blots were carried out. Cleaved caspase 3 was used as a marker of apoptosis. Isolated cardiomyocytes were treated with 10 µM PSPC and 10 µM POVPC for 1 hour. Staurosporine was used to induce apoptosis as a positive control. In staurosporine-treated cells, cleaved caspase 3 was abundant. However, cleaved caspase 3 was not detected in PSPC and POVPC treated cells (Figure 13A) suggesting that apoptosis is not the cell death pathway through which OxPCs exhibit their cardiotoxic effect. In addition, Tunel assay, meant to detect DNA fragmentation was performed to further confirm these results. As seen in Figure 13B and C, Tunel positive staining was not detected when cells were treated with POVPC and PONPC.

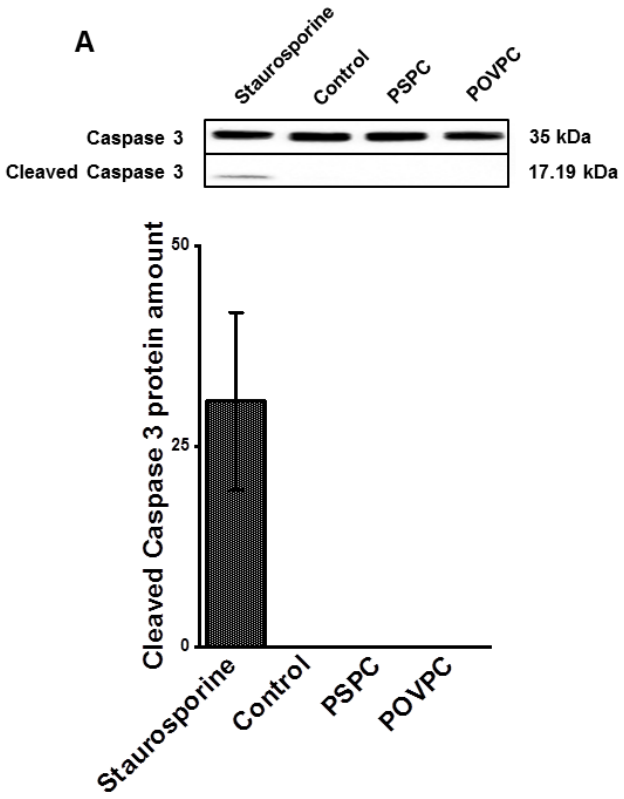

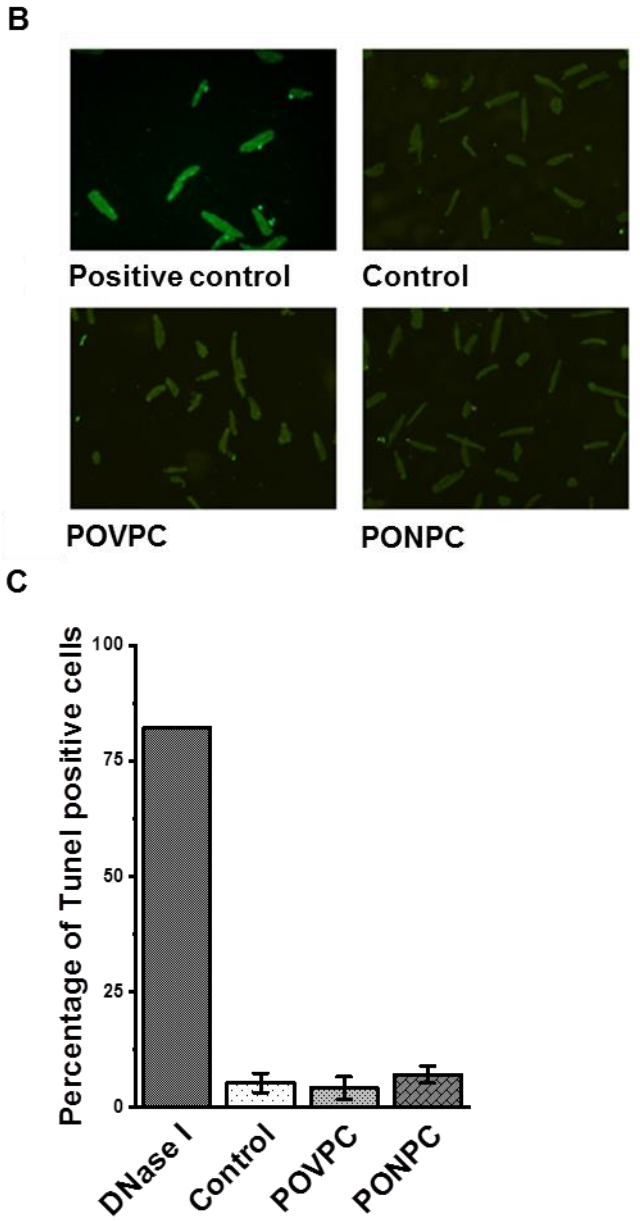

Figure 13. Impact of OxPC on apoptosis in cardiomyocytes **A:** .Cleaved caspase 3 activity in cardiomyocytes treated with 10μM PSPC and POVPC. Normalized protein expression levels were represented as fold change in comparison to control samples (n=3). **B:** Representative pictures of cells treated with POVPC , PONPC, control and positive control stained for Tunel assay; **C:** graphical representation of percentage of Tunel positive cells *P < 0.05 compared to control n=3 Values are mean ±SEM; P<0.05. ANOVA with Tukey post hoc test

Necrosis

Another form of cell death described in myocardial I/R injury is necrosis. Therefore, we tested if POVPC and PONPC induce necrosis in cardiomyocytes. The levels of HMGB1 protein in cells treated with 10 μM POVPC and 10 μM PONPC for 1 hour were not significantly different compared to control (Figure 14.) which suggests that necrosis is not the form of cell death induced by OxPCs.

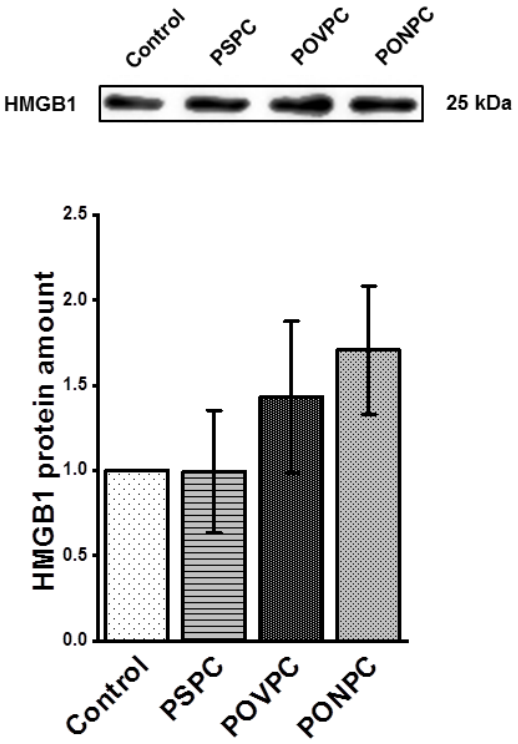

Figure 14. Western blot analyses of HMGB-1 amount in cardiomyocytes as a function of exposure to 10 μM PSPC, POVPC and PONPC for 1 hour. Normalized protein amount levels

were represented as fold change to control samples. Values are mean ±SEM (n=3); P<0.05; ANOVA with Tuckey post hoc test

Ferroptosis

Another potential cell death pathway that may be responsible for OxPC-mediated cell death is ferroptosis [389, 390]. Glutathione peroxidase 4 has been identified as a crucial regulator of ferroptotic cell death [338]. Loss of GPx4 activity leads to ferroptosis [338, 351]. We hypothesized that POVPC and PONPC may lead to inactivation of GPx4 enzyme. Following exposure of isolated cardiomyocytes to 5 µM POVPC and 5 µM PONPC for 1 h, we observed a decrease in GPx4 activity compared to PSPC (Figure 15).

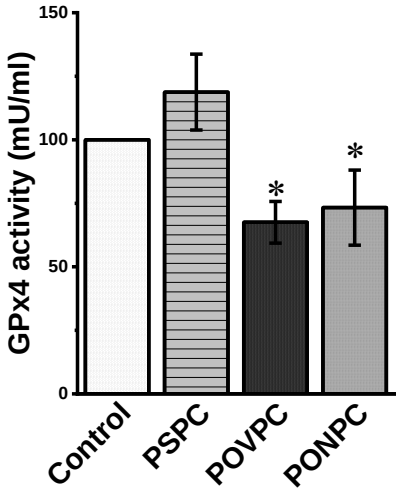

Figure 15. GPx4 enzyme activity as a function of exposure to OxPCs. Values are mean ±SEM (n=6) *Significantly different when compared to PSPC (1-palmitoyl-2-stearoyl-*sn*-glycero-3-phosphocholine) (P<0.05). ANOVA with Tuckey post hoc test

In addition, the effect of ferrostatin on cell viability was tested. Ferrostatin-1 blocks ferroptosis-mediated cell death [338]. Treatment of cardiomyocytes with 10 µM POVPC induced cell death, however, the addition of 1 µM ferrostatin-1 in the presence of POVPC prevented the cardiotoxic effect of POVPC (Figure 16).

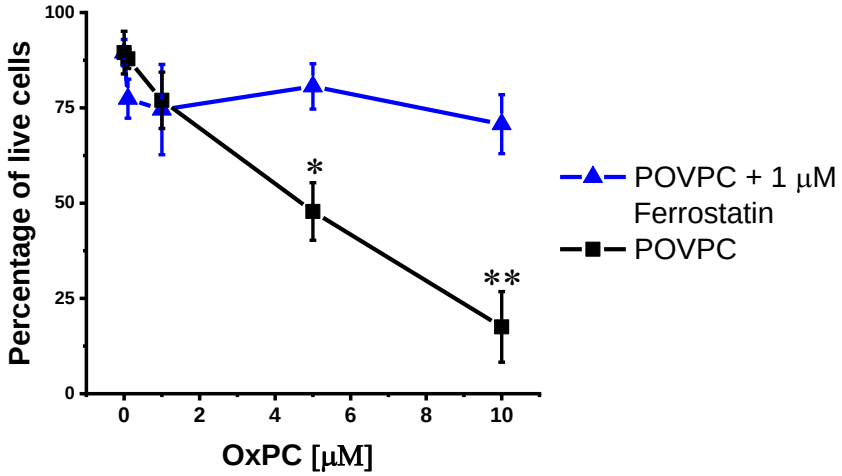

Figure 16. The effects of 1µM Ferrostatin-1 on cardiomyocyte viability following treatment with 10 µM POVPC. Values are mean ±SEM (n=4) and POVPC + ferrostatin-1 (n=3). *P<0.05; **P<0.01 significant compared to POVPC+Ferrostatin-1; T-test

The potential for these results to have implications in I/R injury were further explored. The effects of ferrostatin-1 on cardiomyocyte cell death in I/R was examined. One hour of ischemia followed by one hour of reperfusion led to significant cardiomyocyte death (Figure 17).

However, the addition of 1 μM ferrostatin-1 at the time of reperfusion prevented cardiomyocyte cell death compared to I/R treated cells (Figure 17).

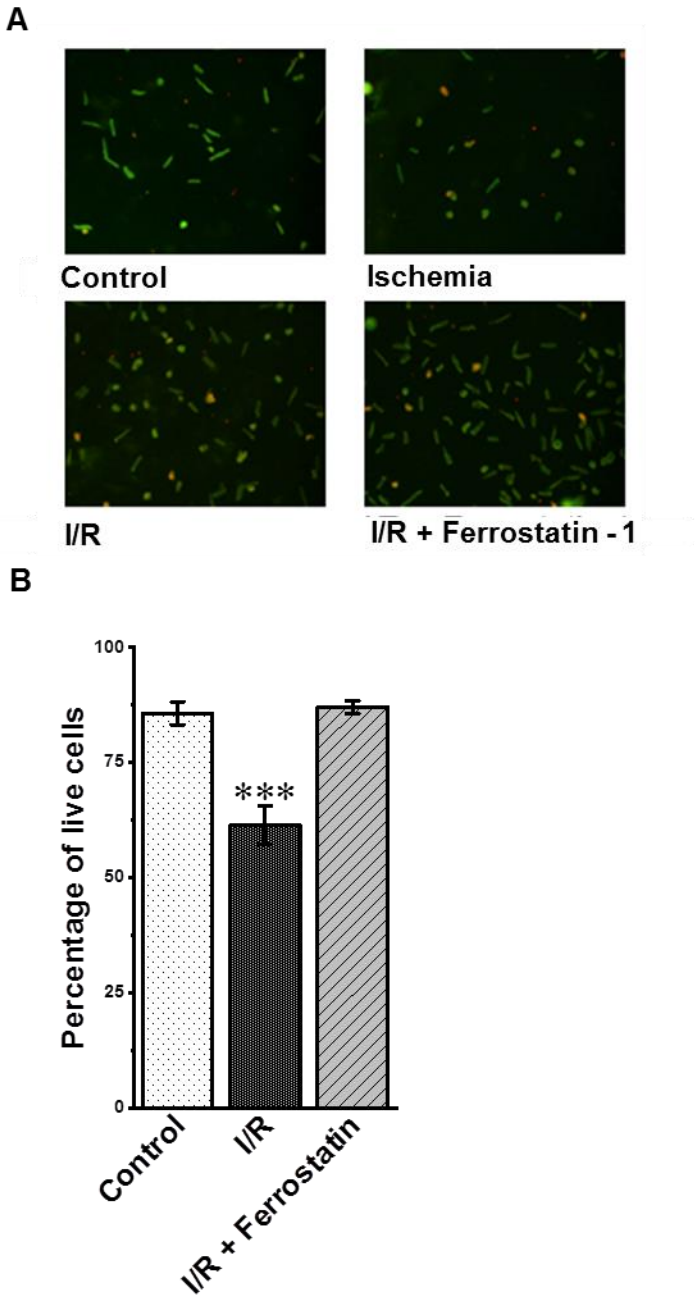

Figure 17. A: Representative images of cardiomyocytes following I/R injury without or with ferrostatin-1**. B:** Cardiomyocyte viability following exposure to I/R with addition of 1 µM ferrostatin-1 at reperfusion. Values are mean ±SEM (n=5); ***Significant compared to control and I/R+ Ferrostatin-1; P<0.001; ANOVA with Tuckey post hoc test

Mechanism of Ferrostatin-1 action

To date, the exact mechanism of ferrostatin-1 action is largely unknown. We used an NMR technique to test whether ferrostatin-1 will interact with PONPC when incubated together. The expected product, as seen in Figure 18, has the ferrostatin-1 attached at the aldehyde carbon. Because of this, the aldehyde peak from the original starting material at 9.74 ppm should not appear in the spectrum of the reaction mixture. Using prediction software, MestReNova 12.0, to predict the expected product, this proton should shift to a position near 7.5 ppm. The disappearance of the aldehyde peak at 9.74 ppm and the observation of the new imine proton peak at 7.5 ppm would provide sufficient evidence that a reaction took place. Another indication that a reaction has taken place can be seen when examining the ferrostatin peaks. The three aromatic peaks of pure ferrostatin are a doublet (d) at 7.44 ppm, a doublet of doublets (dd) at 7.60 ppm, and a doublet at 6.62 ppm, observed from the spectrum of a standard sample. The prediction shows a shift of all three of these peaks when attached to PONPC. The new positions are 7.97 ppm (d), 7.91 ppm (dd), and 7.50 ppm (d), respectively. Because the reaction mixture involved an excess of ferrostatin, there should be no disappearance of the aromatic peaks. However, the appearance of the shifted peaks having a similar integration of the imine proton would also support a completed reaction.

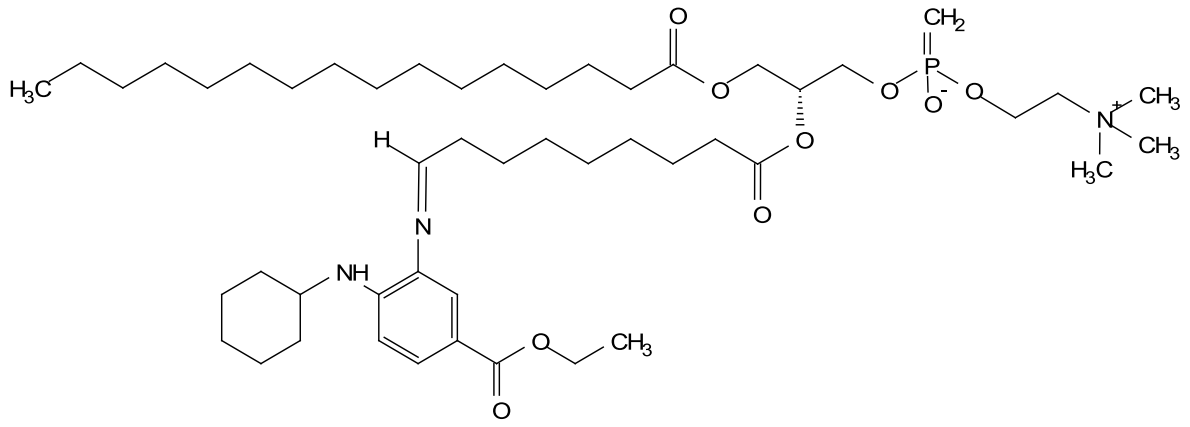

Figure 18. The expected product from the reaction of ferrostatin and PONPC.

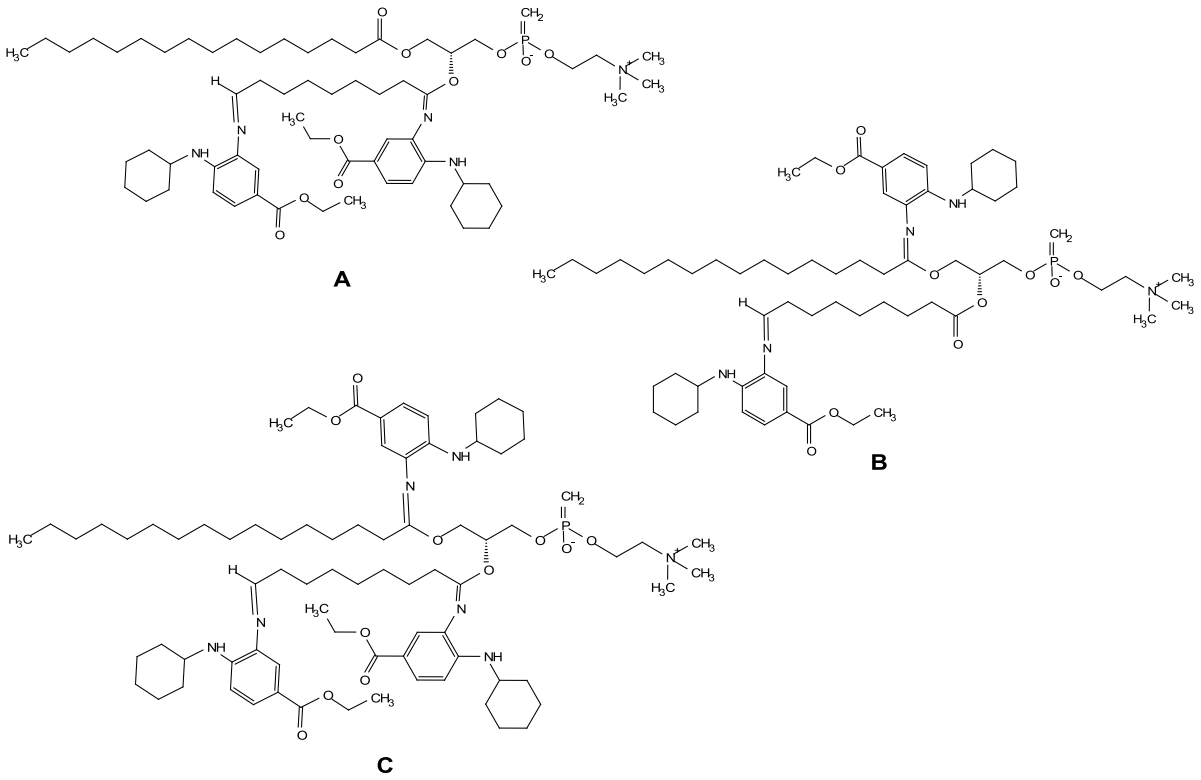

Figure 19. The potential products of multiple additions of ferrostatin-1 to the PONPC chain. **A:** The addition of ferrostatin-1 at both the aldehyde position and the side chain carbonyl. **B:** The

addition of ferrostatin-1 at both the aldehyde position and the backbone carbonyl. **C:** The addition of ferrostatin-1 at all three carbonyls on the PONPC

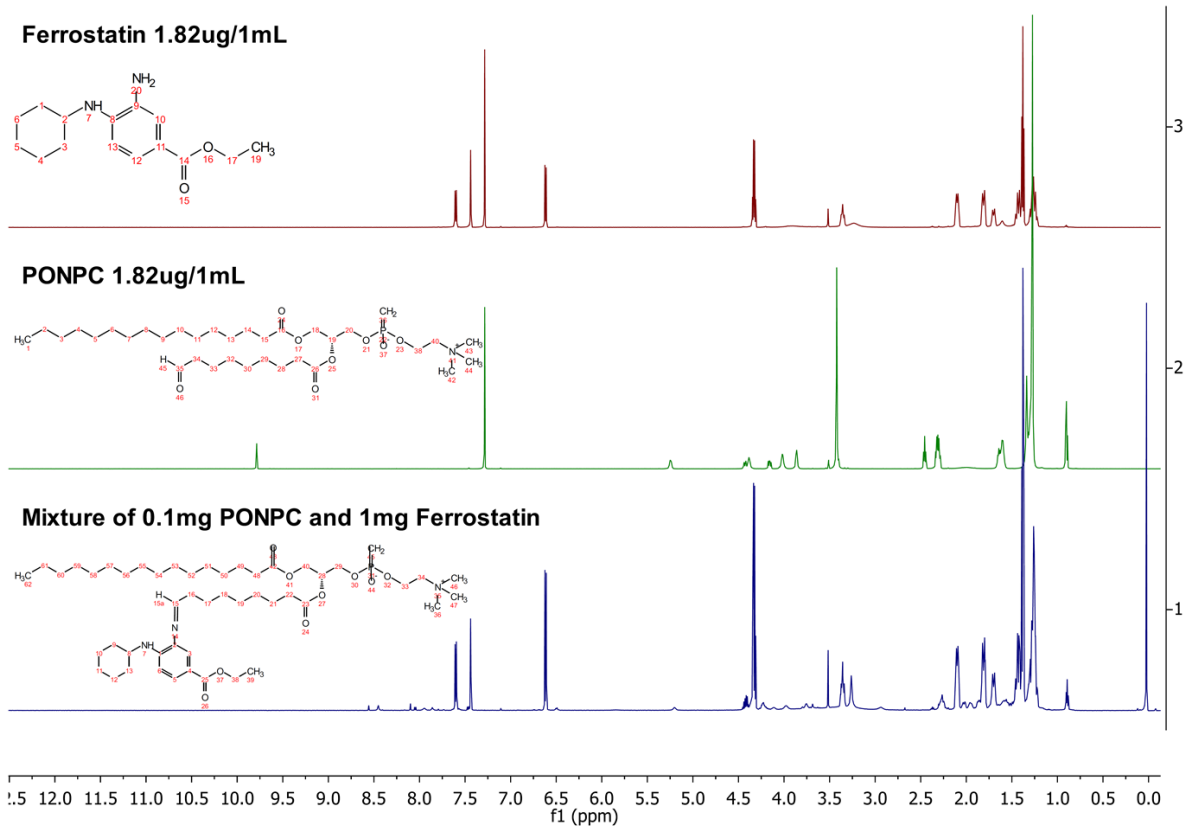

Figure 20. ^{1}H NMR analyses of an OxPC and ferrostatin-1 mixture. ^{1}H NMR spectrum of Ferrostatin-1 standard, PONPC standard and their reaction mixture, plotted as signal intensity (vertical axis) and chemical shift (horizontal axis).

Using Raman scatter microscopy, Gaschler et al. showed the accumulation of ferrostatin-1 in mitochondria, lysosomes and endoplasmic reticulum. In addition, they showed that mitochondria and lysosomes are not required for ferroptosis, suggesting an important role for the

endoplasmic reticulum [356]. In the present study, we have shown the protective effect of ferrostatin during I/R. It then becomes important to address the effect of ferrostatin on Ca^{2+} transients and cardiomyocyte contractility during ischemia/reperfussion injury. First, we addressed the impact of 1µM ferrostatin-1 on beating cardiomyocytes in the absence of the I/R challenge. Thirty minutes of perfusion with ferrostatin-1 did not lead to any significant differences in cardiomyocyte cell length, contraction and diastolic calcium (Figure 21.).

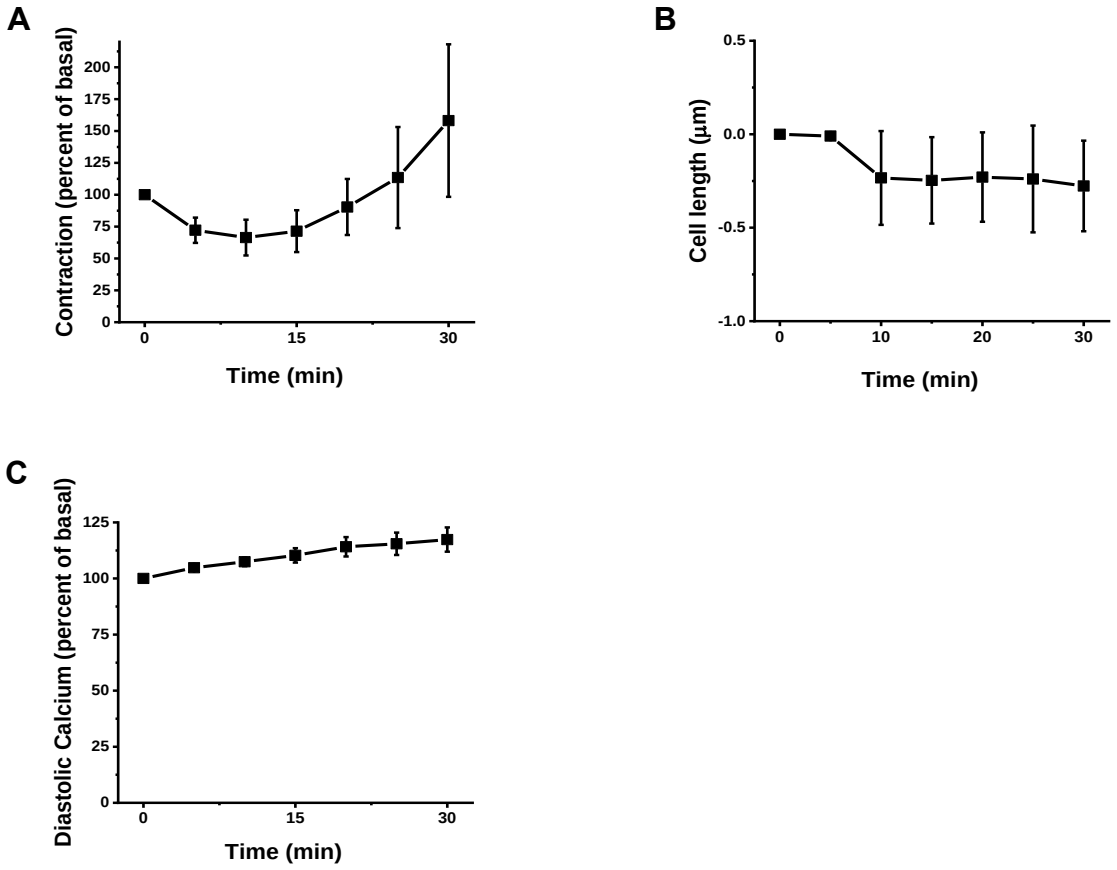

Figure 21. A: Impact of 1µM ferrostatin-1 on contraction of cardiomyocytes over 30 minutes of perfusion. **B:** Effect of ferrostatin-1 on cardiomyocyte cell length; **C:** Effect of ferrostatin-1 on

diastolic calcium in perfused cardiomyocytes; Mean values ± SEM from a series of experiments *Significant compared to baseline ($p<0.05$)

Adding ferrostatin-1 at reperfusion leads to a decrease in diastolic calcium, increase in cardiomyocyte contraction and calcium transients. It also prevents the decrease in cell length compared to cardiomyocytes exposed to I/R only (Figure 22A, B, C and D).

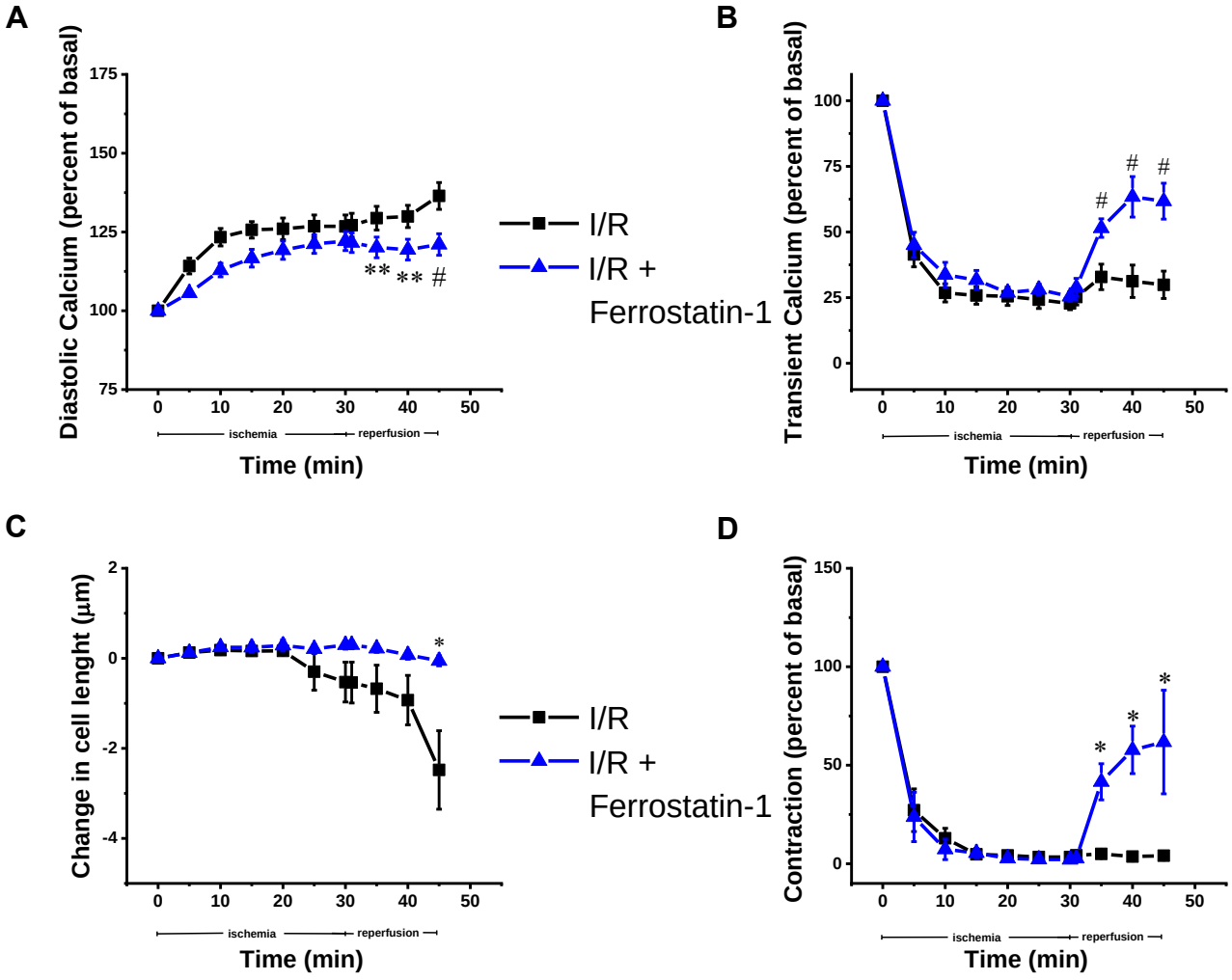

Figure 22. Impact of 1 µM ferrostatin-1 on calcium handling and contraction in isolated cardiomyocytes during I/R injury **A**: Diastolic calcium represented as a percent of basal following 30 minutes of ischemia and 15 minutes of reperfusion with or without the addition of ferrostatin-1 at the reperfusion **B**: transient calcium presented as a percent of basal following 30 minutes of ischemia and 15 minutes of reperfusion with or without the addition of ferrostatin-1 at the reperfusion **C**: change in cell length in cardiomyocytes treated with 30 minutes of ischemia and 15 minutes of reperfusion with or without the addition of ferrostatin-1 at the reperfusion **D:** Contraction presented as a percent of basal in cardiomyocytes treated with 30 minutes of ischemia and 15 minutes of reperfusion with or without the addition of ferrostatin-1 at the reperfusion. Data collected for 30 seconds each 5 minutes; (n=10 for I/R; n=9 for I/R + Ferrostatin-1) *Significant compared to I/R $P<0.05$,**$P<0.01$, #$P<0.001$); Mean values ± SEM from a series of experiments.

E06 potential to prevent cardiomyocyte cell death during I/R injury

These results suggested an involvement of OxPCs in I/R injury. E06 is an antibody that binds and inactivates OxPCs [253]. Following exposure of cardiomyocytes to 1.5 h of simulated ischemia followed by 1 h of reperfusion a decrease in cardiomyocyte viability was observed (Figure 23). However, when 40µg of E06 antibody was added at the time of reperfusion cardiomyocyte cell death was prevented compared to I/R treated cells (Figure 23).

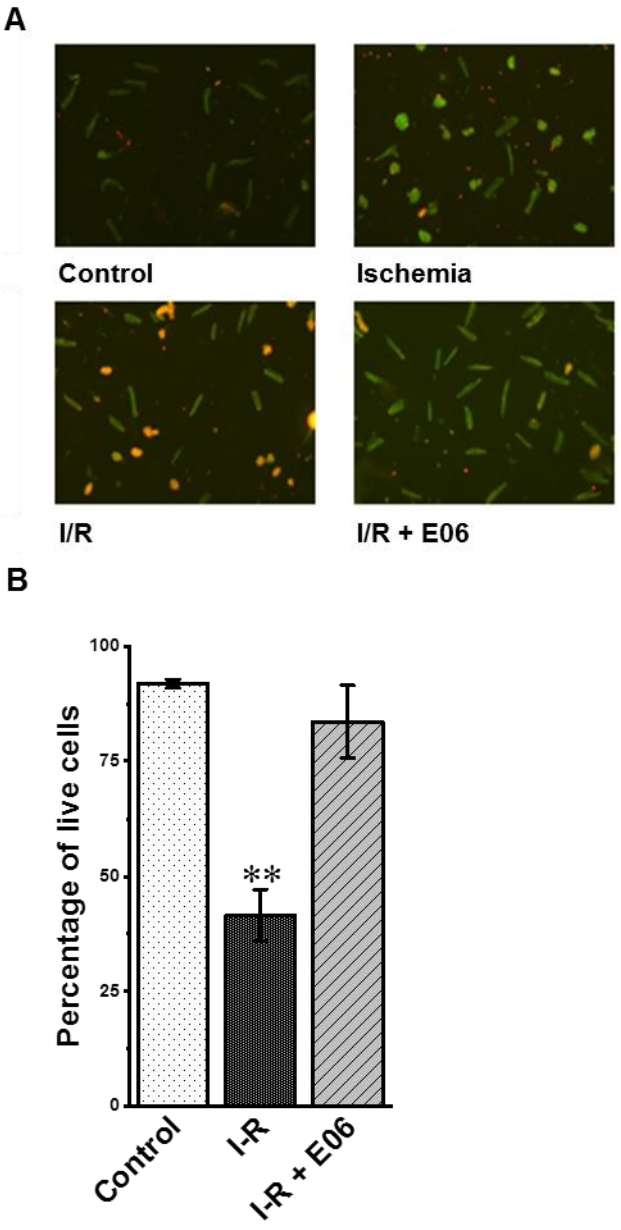

Figure 23. **A:** Representative images of cardiomyocytes following I/R injury without or with E06 antibody**. B:** Cardiomyocyte viability following I/R with addition of E06 antibody; Mean values ± SEM from a series of experiments (n=3). **Significant compared to I/R+E06 ($p<0.01$).

The potential of E06 to prevent cardiomyocyte death during I/R injury in a porcine model

In a pig model of myocardial I/R injury, intracoronary delivery of E06 antibody for 1 hour followed by an additional hour of reperfusion led to a decrease in infarct size expressed as a ratio of area at risk to total area, compared to control (Figure 24). This reduction however, was not statistically significant.

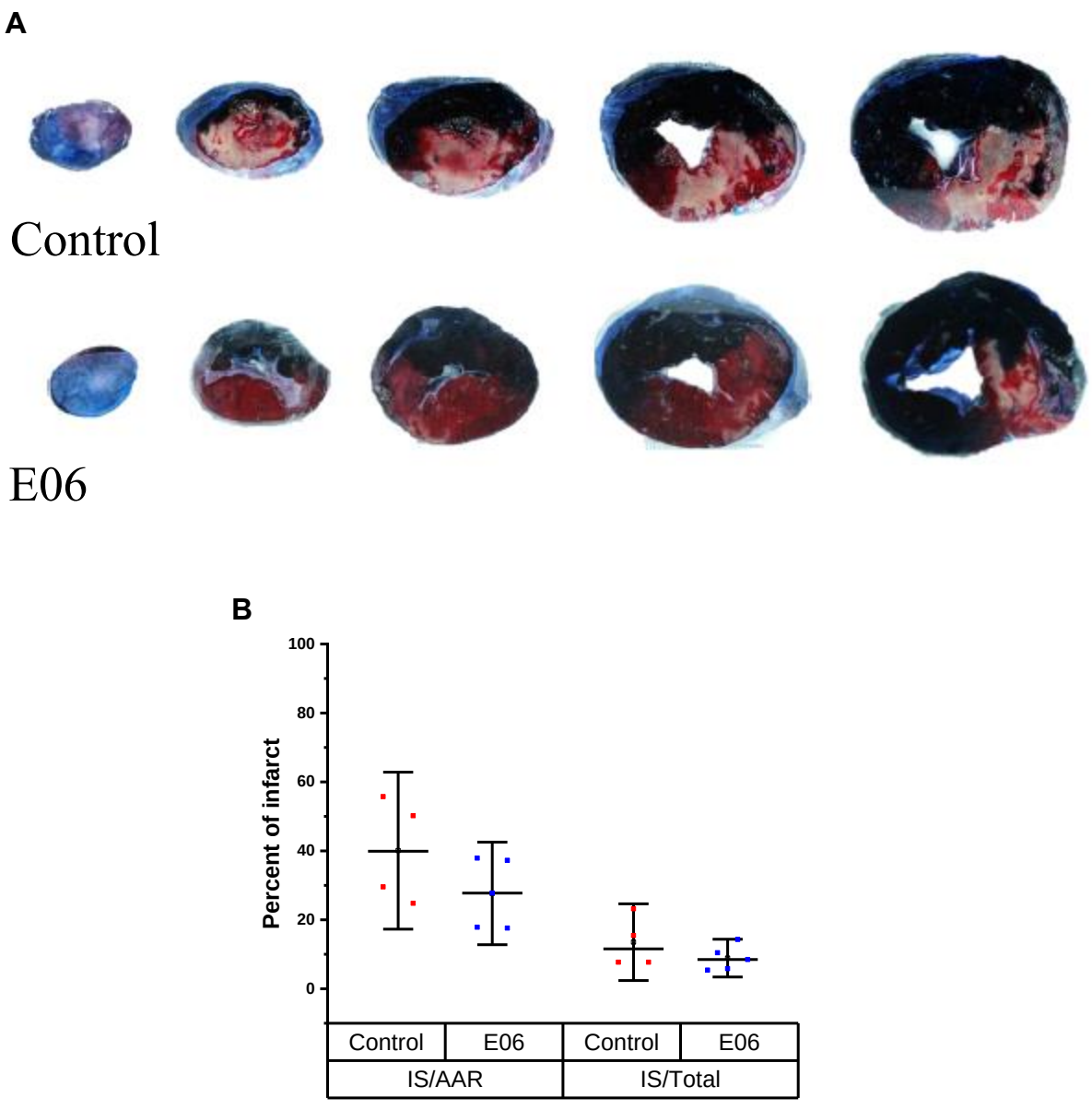

Figure 24. E06 reduced infarct size after I/R injury **A:** Representative photographs of myocardial tissues from the control group and the E06 group after I/R injury. The non-ischemic area is indicated by blue, area at risk (AAR) by red, and the infarct area by white. **B:** Quantification of infarct size in the control group (n=4) and the E06 group (n=5); IS/AAR- infarct size normalized to AAR; IS/Total- infarct size normalized to total ventricle area Results are presented as mean ± SE

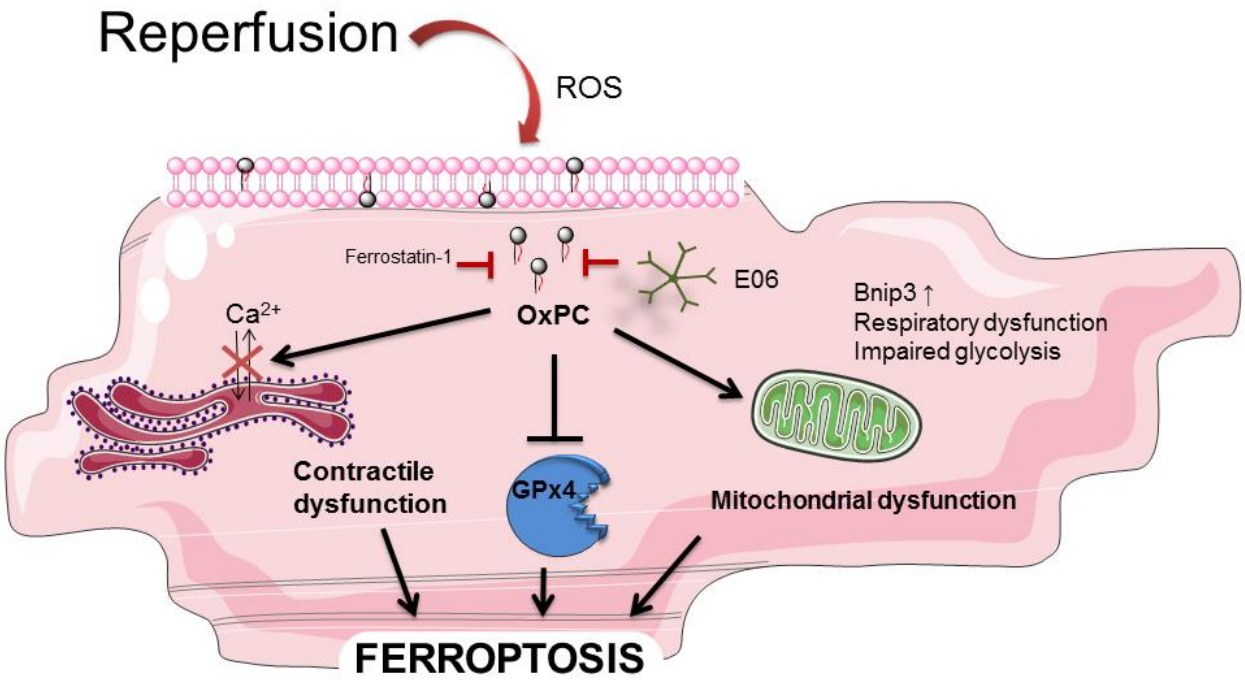

Figure 25. Proposed mechanism describing the role of OxPC (oxidized phosphatidylcholine) during cardiomyocyte reperfusion injury. OxPCs generated during myocardial I/R injury lead to cardiomyocyte cell death through ferroptotic pathway. Fragmented OxPCs decrease the activity of glutathione peroxidase 4 (GPx4) enzyme, which leads to ferroptosis. They decrease mitochondrial functional capacity by reducing basal, maximal respiration, consequently leading to a decrease in spare respiratory capacity. OxPCs affect calcium handling and lead to contractile dysfunction, ultimately causing cell death. Ferrostatin-1, an inhibitor of ferroptosis prevents cardiomyocyte cell death caused by OxPCs. Also, E06, a monoclonal murine antibody specifically binds to OxPCs and prevents their cardiotoxic action.

Chapter VI: Discussion

This study shows for the first time that OxPCs can induce cardiomyocyte cell death and that the mechanism of their cardiotoxic action is through a ferroptotic pathway. The most potent OxPC to induce cardiomyocyte cell death were the fragmented oxidized species POVPC and PONPC. Our findings are important for their pathological relevance due to our previous work that showed a three-fold enrichment of PONPC and POVPC in isolated rat hearts exposed to I/R injury compared to control hearts [369].

Simulated I/R injury in neonatal cardiomyocytes led to a significant increase in the production of fragmented OxPC species, specifically the levels of PONPC, POVPC, PAzPC and PGPC were increased. In addition, exposure of rat myocardium to 1 h of ischemia followed by 24 h of reperfusion caused a three fold enrichment of POVPC and PONPC. According to those results, the physiological concentration of the OxPCs in the rat myocardium is 9-150 μg/mg of wet tissue weight or 3μM [369]. We show here for the first time that oxidized PCs induce cell death in an adult rat cardiomyocyte in a concentration (Figure 6) and time (Figure 7) dependent manner. We have tested different OxPCs species, identified previously to be increased in I/R, within the physiological range of concentrations for each one of them - from 0.1 μM to 10 μM. Although, the carboxylic acids PGPC (Figure 6) and PAzPC did cause cell death in higher concentrations (10 μM), our further focus was on the fragmented aldehydes POVPC and PONPC (Figure 6), which caused significant cell death (Figure 6). This finding has a pathological relevance as our previous work showed three-fold enrichment of POVPC and PONPC in both isolated cardiomyocytes and perfused rat hearts subjected to I/R compared to control [369]. Incubation of cardiomyocytes with 0.1 μM of POVPC over 4 h led to a decrease in cardiomyocyte viability in time dependent manner compared to control (Figure 7). Our lab has

also shown that in STEMI patients, aldehyde containing OxPCs significantly increase in reperfusion. There was 2 fold increases in POVPC and 5 fold increase in PONPC in plasma of STEMI patients 48h following reperfusion. The concentration of POVPC was 0.5µM (0.3ng/ml of plasma) and PONPC 3.6 µM (2.36 ng/ml), which both correspond to concentrations used in this study. To date, therefore, we have shown that OxPCs are generated during myocardial I/R and the ones that are found to be abundant have a cardiotoxic effect on isolated cardiomyocytes. Therefore, investigating the mechanism of their action and addressing the possible mechanisms to attenuate the OxPC induced cardiomyocyte cell death might lead to a new approach to prevent myocardial I/R injury.

In order to examine the mechanism of their action, first we needed to address whether their action is endogenous or exogenous to the cardiomyocyte. We have previously shown that there is an increase in OxPCs in mitochondria in cardiomyocytes subjected to I/R [369]. However, here we show that exogenous addition of purified OxPC standards to isolated cardiomyocytes leads to their cell death. This would suggest that in addition to the generation of dangerous OxPCs within the cell, the presence of OxPCs in the extracellular milieu is threatening to the viability of the cardiomyocyte as well. It would also suggest that there may be a mechanism of interaction that could involve entry of OxPCs into the cell. Therefore, one of the aims of this study was to determine if this interaction of exogenous OxPCs with the cardiomyocytes is receptor mediated.

CD36 is a receptor present in many mammalian cells including cardiomyocytes [391] It is known to recognize different classes of ligands including modified phospholipids [240, 392, 393] and free fatty acids [256, 394, 395]. This suggests that CD36 may be a reasonable target to propose as a receptor for OxPCs. The terminal aldehyde or carboxylic acid, a ketone or alcohol

in the γ position, and a double bond in the β sn-2 position of truncated OxPCs can all serve as high affinity ligands for the CD36 receptor [396]. Early studies in this area showed that POVPC –bovine serum albumin (BSA) was able to inhibit the uptake of CuOxLDL in macrophages, suggesting that POVPC binds to a CD36 receptor [186]. Sulfosuccinimidyl oleate (SSO), an irreversible CD36 inhibitor, prevents OxLDL uptake by macrophages [387] which is mediated by OxPCs [240]. However, in our study, pre-incubation of cardiomyocytes with SSO did not prevent cell death induced by POVPC and PONPC (Figure 8), suggesting that in cardiomyocytes CD36 is not a receptor through which those fragmented aldehydes exert their biological action. One of potential concerns about this experiment was that SSO was found to be a potent inhibitor of mitochondrial respiration chain [397]. In isolated mitochondria, the respiration chain was inhibited by 50 μM and 70μM SSO [397]. However, the concentration of SSO used in this study on intact cells was lower (25 μM) and on its own it did not cause cell death, therefore the toxic effect we report here is attributed to OxPCs and not SSO. Our results are in accordance with previous work done by Moumtzi in VSMCs[182], which showed that OxPCs with an aldehyde moiety entered the cell by covalently binding to plasma membrane amino acid and sulfhydryl groups allowing for transfer across the membrane [182].

In addition to the role extracellular OxPCs may play in cardiomyocyte injury, our previous work has shown that OxPC content within cardiomyocytes and rat hearts is increased in I/R injury [369]. Additionally, there is a significant increase in OxPC content in the mitochondria of cardiomyocytes subjected to I/R injury compared to control [369]. Our results are in accordance with previously reported decrease in PC content in mitochondria of rats hearts subjected to I/R [398]. This loss could be attributed to the generation of oxidized PC species. As mitochondria are considered to be the major powerhouse of cardiomyocytes producing >95%

of energy in form of ATP [399], one of the aims of the present study was to examine the effect of OxPCs on mitochondrial bioenergetics.

Reperfusion leads to a 48% reduction in respiration compared to control hearts [398]. We observed a significant reduction in cardiomyocyte mitochondrial function upon treatment with the fragmented OxPC species. POVPC and PONPC caused a decrease in basal and maximal respiration (Figure 9B and C). Consequently, spare respiratory capacity, a measure of the ability of the cell to respond to increased energy demand or after stress was reduced upon treatment with POVPC and PONPC. We did not observe a decrease in OCR upon oligomycin addition as might be expected when the ATP synthase is inhibited. This might be due to a high rate of proton leak or decreased demand in the isolated, noncontracting cardiomyocytes. This has been observed to occur in isolated adult mouse cardiomyocytes [400]. The proton leak was significantly reduced in cells treated with OxPCs compared to control, which is not in accordance with the study which reported that HNE, which is also an aldehyde, leads to an increase in proton leak [401]. The possible mechanism of OxPC-induced decrease in mitochondrial functional capacity could be through interference with the mitochondrial respiration chain. This is in accordance with previous studies that showed HNE can cause damage to the mitochondrial respiration chain [402-407]. The decline in respiration could potentially be due to decreased mitochondrial cytochrome c oxidase activity. Cytochrome c oxidase is an important factor responsible for the regulation of mitochondrial respiration [408] and a decrease in its activity leads to a diminished mitochondrial respiration in reperfused hearts. HNE causes a decrease of cytochrome c oxidase activity in a concentration dependent manner in the mitochondria isolated from rat heart [409]. As we show here, OxPCs lead to a decrease in electron flow, which would then explain the decrease in proton leak caused by these compounds.

In addition, OxPCs could affect mitochondrial respiration indirectly. Lipid peroxidation and a decrease in PC molecules will increase mitochondrial membrane permeability for calcium and subsequently lead to mitochondrial dysfunction.

The impact of fragmented OxPCs on mitochondrial bioenergetics occurs not only by affecting the electron transport chain, but they also might affect the ability of the cell to adequately use substrates available for ATP production (Figure 10). Upon the addition of oligomycin and FCCP, ECAR is decreased in cells treated with POVPC and PONPC. However, we cannot draw a conclusion that these compounds cause the inability of the cell to compensate by the glycolysis for the ATP production lost when oxidative phosphorylation is inhibited, as the acidification rate depends not only on lactate, produced by anaerobic glycolysis, but also on CO_2, produced by citric acid cycle. The proportion of glycolytic and respiratory acidification depends on the cell type and it has been shown that in adult cardiomyocytes respiration was a major contributor [410]. Upon the addition of Rot/AA and complete inhibition of mitochondrial respiration chain, we did observe a significant decrease in ECAR in PONPC treated cells, which would suggest the impairment of glycolysis, however glycolytic stress test would need to be done in order to further examine the role of OxPCs on the ability of the cells to adequately use substrates available for the ATP production.

When subjected to I/R injury, cardiomyocytes have an increased demand for oxygen [411]. Our results show that OxPCs cause a decrease in mitochondrial spare respiratory capacity which would depress the ability of the mitochondria to respond under stressful conditions. The inability to respond to a stress will ultimately lead to a decrease in ATP production, altered contraction and cell death. This experiment however has its limitations. Isolation of cardiomyocytes and *in vitro* culturing will affect their bioenergetics response, particularly when

they are contracting little or not at all. In addition, the results of OCR and ECAR measurements are normalized according to the protein concentration, which may cause inaccuracies due to the fact that cardiomyocytes have to be plated on laminin coated plates. Further, although the results obtained in this experiment do represent the metabolic changes on cellular levels, however, they do not account for blood flow, the metabolic needs of additional cells, or fuel supply. Therefore, the extrapolation of the results to *in vivo* conditions should be taken with caution.

We have also demonstrated that OxPC-mediated mitochondrial dysfunction can be through the Bnip3 pathway. Bcl-2-like 19kDa-interacting protein (Bnip3) plays a significant role in regulating mitochondrial function in reperfusion injury [388]. The activation of its gene leads to the loss of mitochondrial membrane potential, MPTP opening and cell death [412, 413]. Exposure of cardiomyocytes to POVPC and PONPC induced a significant increase in Bnip3 expression [369]. Pretreatment of the cardiomyocytes with the E06 antibody prevented the increase in Bnip3 expression [369]. In order to further confirm the OxPC mediated cell death through Bnip3, Bnip3 knock-down cells were treated with POVPC (Figure 11.). Compared to wild-type cells, Bnip3 knock-down cells were more resistant to POVPC induced cell death [369].

Cardiomyocyte contraction and heart beating is ensured by mitochondrial production of ATP, which then allows calcium release from sarcoplasmic reticulum into the cytoplasm, where it can interact with troponin [414, 415]. The diminished mitochondrial functional capacity could ultimately lead to contractile dysfunction and occurrence of reperfusion arrhythmias in I/R injury.

Reperfusion arrhythmias represent a major comorbidity of a myocardial infarction. The most common types of reperfusion arrhythmias are ventricular, ranging from premature ventricular contractions, sustained or non-sustained episodes of ventricular tachycardia,

accelerated idioventricular rhythm and ventricular fibrillation. Therefore, it is important to address whether OxPCs affect Ca^{2+} handling in cardiomyocytes. There is evidence in the literature showing that OxPCs cause smooth muscle cell migration by stimulating Ca^{2+} entry through TRPC5 channels [247]. Therefore, we investigated the impact of POVPC and PONPC on Ca^{2+} handling as a potential mechanism for cardiomyocyte damage and cell death. Treatment of isolated cardiomyocytes with 0.1 μM POVPC and PONPC over an hour caused a decrease in net cardiomyocyte contraction (Figure 12A) and Ca^{2+}transients (Figure 12B) ultimately leading to contractile dysfunction. Considering these compounds are produced during I/R injury [272] and that in even in low concentrations they have deleterious effects on Ca^{2+} handling, it is concluded that these OxPCs will generate cardiomyocyte cell death and they might be responsible for reperfusion arrhythmias.

Oxidation of polyunsaturated fatty acids of membrane phospholipids affects selective membrane permeability and interferes with the function of cellular organelles [416]. Pathophysiological concentrations of OxPCs could potentially lead to dramatic electrophysiological alterations of the membrane. Since the cardiac ion channels are embedded in the lipid bilayer, the oxidation of phospholipids will alter their function either by structural changes within the membrane following oxidation, or by electrophilic interaction of aldehydes with proteins. Changes in sarcolemmal lipid composition affect the activity of NCX in ischemia [417]. Alterations, such as accumulation of lysophosphatidyl species during I/R modifies the activity of the exchanger. However the mechanism is still not clear. [418, 419]. There is evidence showing that OxPCs lead to a decrease in lipid order and disintegration of the membrane [174]. Addition of POVPC and PONPC to membranes leads to a decrease in bilayer packing and increased water penetration [180]. As aldehydes, these molecules will have a tendency to react

with proteins within the membrane to form Schiff bases [163], which will lead to disturbances in protein structure and function, including ion channels responsible for maintaining the electrical activity of cardiomyocytes. Current literature supports this hypothesis. Isoketals (IsoK), which are highly reactive y-ketoaldehydes, are formed as a product of isoprostane lipid peroxidation [420], and were found to adduct to protein lysyl residues [421]. They reduced the Na^+ current by binding to Na^+ channels. In addition, the same study showed an oxidant tert-butyl hydroperoxide (t-BHP) induced a reduction in the Na^+ channel current in cardiac myocytes, as a consequence of IsoK increase [421]. In addition, lipid peroxidation products, such as malondialdehyde, inhibit sarcolemmal Na^+ /K^+ -ATPase activity [422]. Its inhibition will lead to a Na^+ overload, which further activates Na^+ /Ca^{2+} exchanger and increases Ca^{2+} influx [423, 424] and Ca^{2+} overload due to SERCA inactivity. Another possible site of OxPC-induced contractile dysfunction can be sarcoplasmic reticulum. It is well established that oxidative stress and lipid peroxidation lead to sarcoplasmic reticulum dysfunction by affecting the activity of SERCA, found in the sarcoplasmic reticulum of the cardiac myocytes. SERCA plays an important role by actively transporting Ca^{2+} from the cytosol into the sarcoplasmic reticulum during myocardial diastole [425]. Oxidative stress depresses SERCA function, contributing to Ca^{2+}overload [426]. In the stunned myocardium, the sarcoplasmic reticulum is not able to transport calcium as a consequence of the reduction in SERCA activity [427]. In addition, exposure of isolated sarcoplasmic reticulum to oxygen radicals leads to a decrease in SERCA activity and Ca^{2+} uptake, whereas antioxidants preserve its function [416, 428]. We show here that upon addition of OxPCs, there is a decrease in Ca^{2+} transients in cardiomyocytes, suggesting that Ca^{2+} is not properly sequestered from the cytosol by SERCA in diastole. It is hypothesized that OxPCs further decrease its activity either by direct interaction with it, or indirectly by changing the

membrane properties of sarcoplasmic reticulum. This is in accordance with our results showing a decrease in net contraction leading to contracture. However, further experiments with isolated sarcoplasmic reticulum vesicles need to be carried out to more definitively identify the role that the sarcoplasmic reticulum plays in OxPC-induced contractile dysfunction.

One of the limitations of this study is the lack of incorporation of the gender data. The experiments in this study were performed in isolated adult rat cardiomyocytes from male rats. As shown previously by Ross et al, there are sex differences in cardiomyocyte contraction at reperfusion, which cannot be attributed to sex hormones [429]. In addition, cells from male rats were shown to be less resistant to I/R injury. The differences between sexes in the phospholipid composition of the membrane bilayer were reported. Males have 27% higher level of PC containing LA than females [430]. Considering that LA containing PC is the precursor for the PONPC which we show in this study has cardiotoxic effect, it is possible that this is the reason for the contractile dysfunction and increase in male cardiomyocytes cell death compared to females in I/R injury.

To summarize to this far in our series of experiments, we have shown that OxPCs, more precisely fragmented aldehydes, cause cardiomyocyte dysfunction by decreasing mitochondrial functional capacity, leading to contractile dysfunction and ultimately leading to cell death. Therefore, the next important part of this study was to examine the exact mechanism of cardiomyocyte cell death induced by OxPCs.

The current evidence in non-cardiac cells indicates that OxPCs induce apoptosis [150, 210, 236]. It is reasonable to hypothesize that this may also be the case in cardiomyocytes because apoptosis and necrosis are two forms of cell death reported to occur in myocardial I/R injury [300-302] . However, in the present study, cleaved caspase 3, as a marker of apoptosis,

was not detected in cardiomyocytes treated with 10 μM OxPCs (Figure 13A). This concentration was chosen as significant cardiomyocyte cell death was observed when cells were treated with 10 μM POVPC and PONPC. Additionally, DNA fragmentation which is the hallmark of apoptosis was not observed upon the addition of OxPCs (Figure 13B). This clearly suggests that apoptosis is not the form of cell death induced by these fragmented species. Alternatively, another form of cell death demonstrated in myocardial I/R injury is necrosis. Western blot analyses of cardiomyocyte treated with PONPC and POVPC showed no change in HMGB 1 expression (Figure 14). HMGB1 is an inflammatory molecule released from the necrotic cells and has been used as a marker of necrotic cell death. These results, therefore, show that OxPC-induced cardiomyocyte death is also not through necrosis. We cannot exclude the occurrence of both apoptosis and necrosis in myocardial I/R at different time point. However, in this study, we do observe cell death induced by OxPCs in concentration in a time dependent manner, which cannot be attributed to apoptosis or necrosis according to abovementioned results.

As an alternative mechanism, non-apoptotic and non-necrotic regulated cell death is a recently emerging field that has implicated oxidized phospholipids as executioners of cell death. Ferroptosis is one of these new non-apoptotic pathways of cell death. Ferroptosis is a newly discovered form of cell death caused by the accumulation of lipid peroxidation products. In this study, we provide evidence that OxPC-mediated cardiomyocyte cell death in I/R injury is through ferroptosis. Several lines of evidence support this hypothesis.

First, lipid peroxidation was crucial for ferroptosis to occur [338]. However, the identity of the species that are lethal was unknown. PUFA rich membrane phospholipids represent the major substrates for ferroptosis [336, 352] as they are highly susceptible to oxidation. There is evidence showing that PE hydroperoxides are the major driver of ferroptosis, however, we have

reason to believe that PC is the class that significantly contributes to ferroptotic cell death in myocardial I/R injury. PC and PE phospholipid class together represent 95% of the phospholipids in the rat heart [149]. Almost 70% of all phospholipids in the rat heart are PC phospholipids [149]. Even though the unsaturation index of PE is higher than in PC, it could be argued that PC is important in ferroptosis as the levels of PC are significantly higher in the heart. In addition PC-OOH as the primary oxidation products are very unstable tending to form secondary products such as species with aldehyde or carboxylic group. Friedman et al. attempted to synthesize the PE analogues of POVPC and showed that upon synthesis, aldehyde groups of these molecules reacted immediately with the amine head group either in intramolecular or intermolecular fashion [253]. This data suggests that secondary products of PE oxidation will not be as toxic as the ones formed from PC as they can interact with the different cellular components leading to the dysfunction or inhibition of some enzymes. Regardless of the large complexity of phospholipid composition in cells, the majority of screening studies of oxidized phospholipids have identified OxPCs the most abundant one.

Secondly, further support for the involvement of OxPCs in ferroptosis in myocardial I/R injury was provided by experiments measuring the activity of GPx4. The inactivation of this enzyme leads to the accumulation of lipid peroxidation products and ferroptosis [338, 343], Following chemical inactivation of GPx4 by RSL3, a marked decrease in protein abundance was noticed, suggesting that GPx4 activity is needed to prevent its instability and degradation [352]. To further examine if cardiomyocytes cell death caused by POVPC and PONPC is due to their effect on GPx4 activity, we synthesized phospholipid hydroperoxide, a substrate specific for GPx4 enzyme, as done previously by Roveri et al [384]. The substrate was then used to assess the activity of the enzyme in control and cells treated with POVPC, PONPC and PSPC. We

found a decrease in Gpx4 activity upon the treatment of cardiomyocytes with POVPC and PONPC (Figure 15). The exact mechanism of their action still needs to be further examined. It can be speculated that the aldehyde groups on POVPC and PONPC bind to amino acids in the enzyme changing its conformation and leading to its inactivity. Our results are in accordance with a previous study by Park et al. showing that in MI GPx4 is inactivated which leads to downregulation of GPx4 and the decreased levels of GPx4 mRNA [363]. Additionally, GPx4 knockdown in a glutathione independent manner leads to mitochondrial morphology disruption and an increase in mitochondrial ROS production [431]. Therefore, OxPC-induced GPx4 inhibition could lead to its downregulation and further increase in ROS production.

In order to further evaluate the role of OxPCs in inducing ferroptosis, we tested whether ferrostatin-1, one of the inhibitors of ferroptosis could prevent OxPC-induced cardiomyocyte death. Ferrostatin-1 is a small molecule that acts as a free radical scavenger [338]. Previously, co-treatment of mouse cardiomyocytes with erastin and ferrostatin-1 led to a decrease in ROS levels and cell death [340]. Ferrostatin-1 has been protective in mouse models of kidney [351], brain [432] and liver [433] I/R injury. In the present study, co-treatment of cardiomyocytes with 1 μM ferrostatin-1 and 10 μM POVPC attenuated cardiomyocyte cell death caused by POVPC on its own (Figure 16). In addition, 1 μM ferrostatin-1 prevented cardiomyocyte death when exposed to I/R challenge *in vitro* (Figure 17). Both, ferrostatin-1 and another lipophilic inhibitor of ferroptosis, liproxstatin, suppressed the accumulation of LOOH [351, 433]. However, the mechanism of their action was not clear. It has been proposed that ferrostatin-1 acts by reducing lipid peroxides to alcohol or by scavenging lipid radicals [433]. According to its chemical structure, ferrostatin-1 is an arylalkylamine. Its amine group will therefore easily interact with aldehyde forming imines. In order to examine the binding of the ferrostatin-1 amine group to the

POVPC and PONPC aldehyde groups as a possible mechanism of its ability to inhibit ferroptosis, we incubated pure PONPC with ferrostatin-1 and performed H NMR analyses to detect the product. The expected product, as observed in Figure 18, has the ferrostatin-1 attached at the aldehyde carbon. Because of this, the aldehyde peak from the original starting material at 9.74 ppm should not appear in the spectrum of the reaction mixture. Using prediction software, MestReNova 12.0 to predict the expected product, this proton should shift to a position near 7.5 ppm. The disappearance of the aldehyde peak at 9.74 ppm and the observation of the new imine proton peak at 7.5 ppm provides convincing evidence that a reaction took place (Figure 20). Another indication that a reaction has taken place is provided by the characteristics of the ferrostatin-1 peaks. The three aromatic peaks of pure ferrostatin-1 are a doublet (d) at 7.44 ppm, a doublet of doublets (dd) at 7.60 ppm, and a doublet at 6.62 ppm, observed from the spectrum of a standard sample. The prediction shows a shift of all three of these peaks when attached to PONPC, the new positions are 7.97 ppm (d), 7.91 ppm (dd), and 7.50 ppm (d), respectively. Because the reaction mixture involved an excess of ferrostatin-1, there will be no disappearance of the aromatic peaks, however, the appearance of the shifted peaks having similar integration of the imine proton strongly supports a completed reaction. When examining the spectrum of the reaction mixture, the peaks of the unreacted ferrostatin-1 are highly visible, and while there is some interference with the shifted peaks, they are still detected. Firstly, there is no peak at 9.74 ppm which is the first indication that a reaction took place consuming the PONPC. The imine peak is visible at 7.46 ppm, however, it slightly overlaps with one of the ferrostatin-1 peaks from the left-over reactants, so more evidence is required. The three shifted peaks from the attached ferrostatin-1 are also evident at 8.10 ppm (d), 8.05 ppm (dd), and 7.47 ppm (d). Because of the overlap of the imine proton peak and the ferrostatin-1 peak, the integration of the aromatic peaks

cannot be confirmed without another point of reference. The CH_2 on the phosphorus group of the PONPC is a clear peak that stands alone and is clearly visible in the reaction mixture at 3.69 ppm. It integrates with 2 protons as expected when compared to the aromatic peaks. Due to this evidence it can be concluded that a reaction took place at the aldehyde position of the PONPC.

The other consideration of importance in this regard concerns the two other carbonyl bonds on the PONPC compound, which could potentially yield many different products. Because the reaction at the aldehyde position was confirmed, it limits the other potential products to include the two or three attached ferrostatin-1 fragments to the PONPC chain, as shown in Figure 19. The predictions for each additional products show a different pattern of the protons. The most notable difference is the increased number of aromatic peaks from the additional ferrostatin-1 molecules. Due to the different positions and electrical environments at each position, the shifts of the aromatic peaks differ from those of the ferrostatin-1 attached at the aldehyde position. This leads to many peaks in that region. When the reaction mixture spectrum is observed, there are no additional peaks in the expected range (6.7 - 7.7 ppm) that have matching integration to the identified peaks. This suggests that no additional ferrostatin-1 molecules were added to the PONPC resulting in the formation of only one product. The major limitation of this experiment is that we have used pure standards, in highly controlled *in vitro* conditions. Further investigation of ferrostatin-1 interaction with OxPCs in physiological conditions is needed.

The localization of ferroptosis within the cell remains a topic of debate. However, there is evidence in the literature that the possible site where ferroptosis occurs is the endoplasmic reticulum. Stockwell and his group have utilized an imaging technique known as Stimulated Raman Scattering (SRS) microscopy coupled with small vibrational tags to visualize ferrostatin-

1 in live cells [356]. They found that ferrostatin-1 accumulates in specific subcellular regions including lysosomes, mitochondria and endoplasmic reticulum, but not plasma membrane and nucleus. They treated a fibrosarcoma cell line (HT-1080 cells) deprived of mitochondria with erastin or RSL3 and a serial dilution of ferrostatin-1, and showed that ferrostatin-1 was more potent following mitophagy, indicating that mitochondria are not required for ferroptosis. Further evidence that ferroptosis does not occur in mitochondria was obtained in a study carried out by the same group showing that ROS generated by the mitochondrial electron transport chain do not contribute to ferroptosis as the cells lacking mitochondrial DNA are still sensitive to ferroptosis [338]. Alternatively, the possible site of ferrostatin-1 localization and action is the sarcoplasmic reticulum. Consistent with this possibility, our results demonstrate that OxPCs affect cardiomyocyte contractile function and ferrostatin-1 binds to OxPCs. Therefore, we wanted to examine if ferrostatin-1 would be able to functionally salvage cardiomyocyte exposed to I/R challenge by having an effect on Ca^{2+} handling and contractile properties. The perfusion of cardiomyocytes with 1 µM ferrostatin-1did not cause any significant changes in diastolic calcium, cardiomyocyte cell length and contraction (Figure 21). However, the addition of ferrostatin-1 at the time of reperfusion led to a decrease in diastolic Ca^{2+} (Figure 22 A), an improvement in Ca^{2+} transients (Figure 22 B), a preservation of cell length (Figure 22 C) and an improvement in the contraction of cardiomyocytes (Figure 22 D) compared to cardiomyocytes subjected to I/R only without the addition of ferrostatin-1. This is consistent with an action on the sarcoplasmic reticulum but further research is needed to examine the exact mechanism through which ferrostatin-1 improved contractile function. According to our results, we can conclude that ferrostatin-1 improves contractile function by binding to OxPCs thus preventing them from having a detrimental effect on the contractile process within cardiomyocytes.

All of the above results clearly show that the OxPCs generated during I/R are responsible for cardiomyocyte cell death and, therefore, could contribute to the final infarct size. However, definitive proof of this aspect of myocardial reperfusion injury is lacking and whether the capture of OxPCs could decrease infarct size and improve myocardial function was unknown. If possible, this novel approach could lead to a new therapy for I/R injury.

One of the potential candidates for the neutralization of OxPCs is the E06 antibody. E06 is a natural murine monoclonal antibody which binds to a PC group of OxPC but not its unoxidized precursor [253]. Current evidence, both *in vitro* and *in vivo* clearly shows that this antibody can ameliorate different cardiovascular pathologies. For example, it has been well established that E06 leads to a decrease in atherosclerosis. It prevents the uptake of OxLDL by macrophages in vitro [186, 274] and attenuates the inflammatory effects of OxPCs in monocytes and endothelial cells [275]. In a transgenic LDL receptor KO mouse model expressing a single chain variable of E06 (E06-scFv) fed high cholesterol diet, there was a significant decrease in atherosclerosis and an increase in plaque stability measured by necrotic core area size and collagen content at 4, 7 and 12 months [212]. In the same animal model, echocardiographic and histologic analysis of aortic valves showed that E06 decreased the valve gradients and calcification. The mean pressure gradient across the aortic valve measured by Doppler echocardiography was 49% lower in animals expressing E06. In addition, the valve calcium composition was reduced by 41.5% in E06 mice. E06 also led to a decrease in systemic inflammation [212].

There has also been some evidence to support the contention that E06 can ameliorate myocardial I/R injury. In neonatal cardiomyocytes the E06 antibody was effective in attenuating cell death caused by POVPC and PONPC [272]. In addition, the present study demonstrated that

when E06 was added at reperfusion, it was able to ameliorate the toxic effects of OxPCs in cardiomyocytes and prevent their cell death during I/R (Figure 23). In an MI mouse model overexpressing E06, significantly decreased infarct size presented as a percentage of area at risk (66%) was observed, compared to controls [272].

For several decades, research has focused on understanding the mechanism underlying I/R injury. Existing therapeutic strategies to date have only been successful in experimental models. The evidence presented here using small animal models of myocardial I/R injury in addition to the limited data currently available in the literature supports the contention that the E06 antibody may offer a brand new therapeutic opportunity to neutralize the elusive mechanism underlying myocardial I/R injury. This attractive possibility represented the rationale for the pilot study we conducted in a preclinical swine model of an MI. Ischemia was induced by balloon occlusion and 0.5 mg of E06 antibody was delivered by an intracoronary catheter at the time of reperfusion. Through TTC staining to estimate the infarct size, we demonstrated that infarct size was decreased in the animals that received E06 compared to the ones that received saline infusion. However, the decrease was not statistically significant, probably due to the small sample size at this point of the study (Figure 25). This pilot data demonstrates the potential of the antibody to reduce infarct size and will support the initiation of additional work to address the statistical shortcomings. This will also support the future implementation of E06 to improve clinical outcomes in STEMI patients. However, further studies are necessary to establish the right dosage of the antibody, the pharmacokinetics of E06 administration in humans, and the chronic systemic effects of the E06 infusion before clinical studies can be initiated.

Chapter VII: Conclusions

In summary, we have shown for the first time the important role of OxPCs in mediating cardiomyocyte cell death during myocardial I/R injury. This study clearly demonstrates that OxPCs generated during reperfusion, fragmented aldehydes specifically, lead to cell death in a concentration and time dependent manner. In isolated cardiomyocytes OxPCs lead to a reduction in mitochondrial functional capacity which will ultimately have a detrimental effect on Ca^{2+} handling leading to contractile dysfunction.

In this study we have also shown for the first time that OxPC mediated cardiomyocyte cell death in I/R injury is through ferroptosis. An inhibitor of ferroptosis, ferrrostatin-1, was able to prevent OxPC-induced cardiomyocyte death. We have provided evidence for the possible mechanism of ferrostatin-1 action, which is by binding OxPCs and preventing them from expressing their detrimental effect in multiple sites within the cell, including sarcoplasmic reticulum, which in turn improves calcium handling in I/R injury.

We have also shown that OxPC-induced cardiomyocyte death can be prevented by the addition of E06 antibody which binds OxPCs but not their unoxidized precursors. We also provide evidence for utilizing the E06 antibody as a therapy for I/R injury. We show that intracoronary delivery of the antibody at the time of reperfusion in a preclinical swine model leads to a decrease in infarct size. These results are promising as they represent an opportunity to be translated into the clinical world as a therapy for myocardial I/R injury. Despite the significance of myocardial I/R injury as a major cause of morbidity in the world today, an effective therapy does not currently exist.

Literature cited

1. Benjamin, E.J., et al., *Heart Disease and Stroke Statistics-2018 Update: A Report From the American Heart Association.* Circulation, 2018. **137**(12): p. e67-e492.
2. Canada, P.H.A.o., *Report from the Canadian chronic disease surveillance system: Heart disease in Canada, 2018.* 2018.
3. Network, E.H., *European Cardiovascular Disease Statistics 2017.* 2017.
4. Frangogiannis, N.G., *Pathophysiology of Myocardial Infarction.* Compr Physiol, 2015. **5**(4): p. 1841-75.
5. Virani, S.S., et al., *Heart Disease and Stroke Statistics-2020 Update: A Report From the American Heart Association.* Circulation, 2020. **141**(9): p. e139-e596.
6. Lewis, E.F., et al., *Predictors of late development of heart failure in stable survivors of myocardial infarction: the CARE study.* J Am Coll Cardiol, 2003. **42**(8): p. 1446-53.
7. Agarwal, S., et al., *Changing Trends of Atherosclerotic Risk Factors Among Patients With Acute Myocardial Infarction and Acute Ischemic Stroke.* Am J Cardiol, 2017. **119**(10): p. 1532-1541.
8. Makki, N., T.M. Brennan, and S. Girotra, *Acute coronary syndrome.* J Intensive Care Med, 2015. **30**(4): p. 186-200.
9. Gregg, R.E. and S. Babaeizadeh, *Detection of culprit coronary lesion location in pre-hospital 12-lead ECG.* J Electrocardiol, 2014. **47**(6): p. 890-4.
10. Writing Group, M., et al., *Heart Disease and Stroke Statistics-2016 Update: A Report From the American Heart Association.* Circulation, 2016. **133**(4): p. e38-360.
11. DeWood, M.A., et al., *Prevalence of total coronary occlusion during the early hours of transmural myocardial infarction.* N Engl J Med, 1980. **303**(16): p. 897-902.
12. Keeley, E.C., J.A. Boura, and C.L. Grines, *Primary angioplasty versus intravenous thrombolytic therapy for acute myocardial infarction: a quantitative review of 23 randomised trials.* Lancet, 2003. **361**(9351): p. 13-20.
13. Cung, T.T., et al., *Cyclosporine before PCI in Patients with Acute Myocardial Infarction.* N Engl J Med, 2015. **373**(11): p. 1021-31.
14. Bochaton, T., et al., *Importance of infarct size versus other variables for clinical outcomes after PPCI in STEMI patients.* Basic Res Cardiol, 2019. **115**(1): p. 4.
15. De Luca, G., et al., *Time delay to treatment and mortality in primary angioplasty for acute myocardial infarction: every minute of delay counts.* Circulation, 2004. **109**(10): p. 1223-5.
16. Damman, P., et al., *Multiple biomarkers at admission significantly improve the prediction of mortality in patients undergoing primary percutaneous coronary intervention for acute ST-segment elevation myocardial infarction.* J Am Coll Cardiol, 2011. **57**(1): p. 29-36.
17. Stebbins, A., et al., *A model for predicting mortality in acute ST-segment elevation myocardial infarction treated with primary percutaneous coronary intervention: results from the Assessment of Pexelizumab in Acute Myocardial Infarction Trial.* Circ Cardiovasc Interv, 2010. **3**(5): p. 414-22.
18. Halkin, A., et al., *Prediction of mortality after primary percutaneous coronary intervention for acute myocardial infarction: the CADILLAC risk score.* J Am Coll Cardiol, 2005. **45**(9): p. 1397-405.
19. Stone, G.W., et al., *Relationship Between Infarct Size and Outcomes Following Primary PCI: Patient-Level Analysis From 10 Randomized Trials.* J Am Coll Cardiol, 2016. **67**(14): p. 1674-83.
20. Huynh, T., et al., *Comparison of primary percutaneous coronary intervention and fibrinolytic therapy in ST-segment-elevation myocardial infarction: bayesian hierarchical meta-analyses of randomized controlled trials and observational studies.* Circulation, 2009. **119**(24): p. 3101-9.
21. Yellon, D.M. and D.J. Hausenloy, *Myocardial reperfusion injury.* N Engl J Med, 2007. **357**(11): p. 1121-35.

22. Kloner, R.A., et al., *Ultrastructural evidence of microvascular damage and myocardial cell injury after coronary artery occlusion: which comes first?* Circulation, 1980. **62**(5): p. 945-52.
23. Reimer, K.A., R.B. Jennings, and A.H. Tatum, *Pathobiology of acute myocardial ischemia: metabolic, functional and ultrastructural studies.* Am J Cardiol, 1983. **52**(2): p. 72A-81A.
24. Heusch, G. and B.J. Gersh, *The pathophysiology of acute myocardial infarction and strategies of protection beyond reperfusion: a continual challenge.* Eur Heart J, 2017. **38**(11): p. 774-784.
25. Callender, T., et al., *Heart failure care in low- and middle-income countries: a systematic review and meta-analysis.* PLoS Med, 2014. **11**(8): p. e1001699.
26. Sharif, D., et al., *Doppler echocardiographic myocardial stunning index predicts recovery of left ventricular systolic function after primary percutaneous coronary intervention.* Echocardiography, 2016. **33**(10): p. 1465-1471.
27. Wdowiak-Okrojek, K., et al., *Recovery of regional systolic and diastolic myocardial function after acute myocardial infarction evaluated by two-dimensional speckle tracking echocardiography.* Clin Physiol Funct Imaging, 2019. **39**(2): p. 177-181.
28. Kloner, R.A., et al., *Medical and cellular implications of stunning, hibernation, and preconditioning: an NHLBI workshop.* Circulation, 1998. **97**(18): p. 1848-67.
29. Laky, D., L. Parascan, and V. Candea, *Myocardial stunning. Morphological studies in acute experimental ischemia and intraoperatory myocardial biopsies.* Rom J Morphol Embryol, 2008. **49**(2): p. 153-8.
30. Crystal, G.J., et al., *Isoflurane late preconditioning against myocardial stunning is associated with enhanced antioxidant defenses.* Acta Anaesthesiol Scand, 2012. **56**(1): p. 39-47.
31. Kals, J., et al., *Antioxidant UPF1 attenuates myocardial stunning in isolated rat hearts.* Int J Cardiol, 2008. **125**(1): p. 133-5.
32. Ambrosio, G. and I. Tritto, *Clinical manifestations of myocardial stunning.* Coron Artery Dis, 2001. **12**(5): p. 357-61.
33. Tatli, E., et al., *Arrhythmias following revascularization procedures in the course of acute myocardial infarction: are they indicators of reperfusion or ongoing ischemia?* ScientificWorldJournal, 2013. **2013**: p. 160380.
34. Majidi, M., et al., *Reperfusion ventricular arrhythmia 'bursts' predict larger infarct size despite TIMI 3 flow restoration with primary angioplasty for anterior ST-elevation myocardial infarction.* Eur Heart J, 2009. **30**(7): p. 757-64.
35. van der Weg, K., et al., *Reperfusion ventricular arrhythmia bursts identify larger infarct size in spite of optimal epicardial and microvascular reperfusion using cardiac magnetic resonance imaging.* Eur Heart J Acute Cardiovasc Care, 2018. **7**(3): p. 246-256.
36. Eitel, I., et al., *Comprehensive prognosis assessment by CMR imaging after ST-segment elevation myocardial infarction.* J Am Coll Cardiol, 2014. **64**(12): p. 1217-26.
37. Bekkers, S.C., et al., *Microvascular obstruction: underlying pathophysiology and clinical diagnosis.* J Am Coll Cardiol, 2010. **55**(16): p. 1649-60.
38. Niccoli, G., et al., *Myocardial no-reflow in humans.* J Am Coll Cardiol, 2009. **54**(4): p. 281-92.
39. de Waha, S., et al., *Relationship between microvascular obstruction and adverse events following primary percutaneous coronary intervention for ST-segment elevation myocardial infarction: an individual patient data pooled analysis from seven randomized trials.* Eur Heart J, 2017. **38**(47): p. 3502-3510.
40. Klug, G., et al., *Prognostic value at 5 years of microvascular obstruction after acute myocardial infarction assessed by cardiovascular magnetic resonance.* J Cardiovasc Magn Reson, 2012. **14**: p. 46.
41. Heusch, G., et al., *Coronary microembolization: from bedside to bench and back to bedside.* Circulation, 2009. **120**(18): p. 1822-36.

42. Kleinbongard, P., et al., *Aspirate from human stented native coronary arteries vs. saphenous vein grafts: more endothelin but less particulate debris.* Am J Physiol Heart Circ Physiol, 2013. **305**(8): p. H1222-9.
43. Kleinbongard, P., et al., *Vasoconstrictor potential of coronary aspirate from patients undergoing stenting of saphenous vein aortocoronary bypass grafts and its pharmacological attenuation.* Circ Res, 2011. **108**(3): p. 344-52.
44. Barrabes, J.A., et al., *Microvascular thrombosis: an exciting but elusive therapeutic target in reperfused acute myocardial infarction.* Cardiovasc Hematol Disord Drug Targets, 2010. **10**(4): p. 273-83.
45. Kloner, R.A., C.E. Ganote, and R.B. Jennings, *The "no-reflow" phenomenon after temporary coronary occlusion in the dog.* J Clin Invest, 1974. **54**(6): p. 1496-508.
46. Manciet, L.H., et al., *Microvascular compression during myocardial ischemia: mechanistic basis for no-reflow phenomenon.* Am J Physiol, 1994. **266**(4 Pt 2): p. H1541-50.
47. Thiele, H., et al., *Intracoronary compared with intravenous bolus abciximab application in patients with ST-elevation myocardial infarction undergoing primary percutaneous coronary intervention: the randomized Leipzig immediate percutaneous coronary intervention abciximab IV versus IC in ST-elevation myocardial infarction trial.* Circulation, 2008. **118**(1): p. 49-57.
48. Bellandi, F., et al., *Increase of myocardial salvage and left ventricular function recovery with intracoronary abciximab downstream of the coronary occlusion in patients with acute myocardial infarction treated with primary coronary intervention.* Catheter Cardiovasc Interv, 2004. **62**(2): p. 186-92.
49. Khan, J.N., et al., *Infarct Size Following Treatment With Second- Versus Third-Generation P2Y12 Antagonists in Patients With Multivessel Coronary Disease at ST-Segment Elevation Myocardial Infarction in the CvLPRIT Study.* J Am Heart Assoc, 2016. **5**(6).
50. Ishihara, M., et al., *Attenuation of the no-reflow phenomenon after coronary angioplasty for acute myocardial infarction with intracoronary papaverine.* Am Heart J, 1996. **132**(5): p. 959-63.
51. Werner, G.S., et al., *Intracoronary verapamil for reversal of no-reflow during coronary angioplasty for acute myocardial infarction.* Catheter Cardiovasc Interv, 2002. **57**(4): p. 444-51.
52. Ota, S., et al., *Impact of nicorandil to prevent reperfusion injury in patients with acute myocardial infarction: Sigmart Multicenter Angioplasty Revascularization Trial (SMART).* Circ J, 2006. **70**(9): p. 1099-104.
53. Li, X.D., et al., *Effect of pre-procedural statin therapy on myocardial no-reflow following percutaneous coronary intervention: a meta analysis.* Chin Med J (Engl), 2013. **126**(9): p. 1755-60.
54. Murry, C.E., R.B. Jennings, and K.A. Reimer, *Preconditioning with ischemia: a delay of lethal cell injury in ischemic myocardium.* Circulation, 1986. **74**(5): p. 1124-36.
55. Zhao, Z.Q., et al., *Inhibition of myocardial injury by ischemic postconditioning during reperfusion: comparison with ischemic preconditioning.* Am J Physiol Heart Circ Physiol, 2003. **285**(2): p. H579-88.
56. Staat, P., et al., *Postconditioning the human heart.* Circulation, 2005. **112**(14): p. 2143-8.
57. Sorensson, P., et al., *Effect of postconditioning on infarct size in patients with ST elevation myocardial infarction.* Heart, 2010. **96**(21): p. 1710-5.
58. Tarantini, G., et al., *Postconditioning during coronary angioplasty in acute myocardial infarction: the POST-AMI trial.* Int J Cardiol, 2012. **162**(1): p. 33-8.
59. Przyklenk, K., et al., *Regional ischemic 'preconditioning' protects remote virgin myocardium from subsequent sustained coronary occlusion.* Circulation, 1993. **87**(3): p. 893-9.

60. Botker, H.E., et al., *Remote ischaemic conditioning before hospital admission, as a complement to angioplasty, and effect on myocardial salvage in patients with acute myocardial infarction: a randomised trial.* Lancet, 2010. **375**(9716): p. 727-34.
61. Dash, R., et al., *Dose-Dependent Cardioprotection of Moderate (32 degrees C) Versus Mild (35 degrees C) Therapeutic Hypothermia in Porcine Acute Myocardial Infarction.* JACC Cardiovasc Interv, 2018. **11**(2): p. 195-205.
62. Kern, K.B., et al., *Importance of Both Early Reperfusion and Therapeutic Hypothermia in Limiting Myocardial Infarct Size Post-Cardiac Arrest in a Porcine Model.* JACC Cardiovasc Interv, 2016. **9**(23): p. 2403-2412.
63. Erlinge, D., et al., *Rapid endovascular catheter core cooling combined with cold saline as an adjunct to percutaneous coronary intervention for the treatment of acute myocardial infarction. The CHILL-MI trial: a randomized controlled study of the use of central venous catheter core cooling combined with cold saline as an adjunct to percutaneous coronary intervention for the treatment of acute myocardial infarction.* J Am Coll Cardiol, 2014. **63**(18): p. 1857-65.
64. Piot, C., et al., *Effect of cyclosporine on reperfusion injury in acute myocardial infarction.* N Engl J Med, 2008. **359**(5): p. 473-81.
65. Van de Werf, F., et al., *Short-term effects of early intravenous treatment with a beta-adrenergic blocking agent or a specific bradycardiac agent in patients with acute myocardial infarction receiving thrombolytic therapy.* J Am Coll Cardiol, 1993. **22**(2): p. 407-16.
66. Ibanez, B., et al., *The cardioprotection granted by metoprolol is restricted to its administration prior to coronary reperfusion.* Int J Cardiol, 2011. **147**(3): p. 428-32.
67. Ibanez, B., et al., *Early metoprolol administration before coronary reperfusion results in increased myocardial salvage: analysis of ischemic myocardium at risk using cardiac magnetic resonance.* Circulation, 2007. **115**(23): p. 2909-16.
68. Ibanez, B., et al., *Effect of early metoprolol on infarct size in ST-segment-elevation myocardial infarction patients undergoing primary percutaneous coronary intervention: the Effect of Metoprolol in Cardioprotection During an Acute Myocardial Infarction (METOCARD-CNIC) trial.* Circulation, 2013. **128**(14): p. 1495-503.
69. Chen, Z.M., et al., *Early intravenous then oral metoprolol in 45,852 patients with acute myocardial infarction: randomised placebo-controlled trial.* Lancet, 2005. **366**(9497): p. 1622-32.
70. Bangalore, S., et al., *Clinical outcomes with beta-blockers for myocardial infarction: a meta-analysis of randomized trials.* Am J Med, 2014. **127**(10): p. 939-53.
71. Selker, H.P., et al., *Out-of-hospital administration of intravenous glucose-insulin-potassium in patients with suspected acute coronary syndromes: the IMMEDIATE randomized controlled trial.* JAMA, 2012. **307**(18): p. 1925-33.
72. Holst, J.J., *The physiology of glucagon-like peptide 1.* Physiol Rev, 2007. **87**(4): p. 1409-39.
73. Wei, Y. and S. Mojsov, *Tissue-specific expression of the human receptor for glucagon-like peptide-I: brain, heart and pancreatic forms have the same deduced amino acid sequences.* FEBS Lett, 1995. **358**(3): p. 219-24.
74. Bose, A.K., et al., *Glucagon-like peptide 1 can directly protect the heart against ischemia/reperfusion injury.* Diabetes, 2005. **54**(1): p. 146-51.
75. Ossum, A., et al., *The cardioprotective and inotropic components of the postconditioning effects of GLP-1 and GLP-1(9-36)a in an isolated rat heart.* Pharmacol Res, 2009. **60**(5): p. 411-7.
76. Sonne, D.P., T. Engstrom, and M. Treiman, *Protective effects of GLP-1 analogues exendin-4 and GLP-1(9-36) amide against ischemia-reperfusion injury in rat heart.* Regul Pept, 2008. **146**(1-3): p. 243-9.
77. Timmers, L., et al., *Exenatide reduces infarct size and improves cardiac function in a porcine model of ischemia and reperfusion injury.* J Am Coll Cardiol, 2009. **53**(6): p. 501-10.

78. Lonborg, J., et al., *Exenatide reduces reperfusion injury in patients with ST-segment elevation myocardial infarction.* Eur Heart J, 2012. **33**(12): p. 1491-9.
79. Treiman, M., et al., *Glucagon-like peptide 1--a cardiologic dimension.* Trends Cardiovasc Med, 2010. **20**(1): p. 8-12.
80. Hanninen, S.L., et al., *Mitochondrial uncoupling downregulates calsequestrin expression and reduces SR Ca2+ stores in cardiomyocytes.* Cardiovasc Res, 2010. **88**(1): p. 75-82.
81. Kaplan, P., et al., *Effect of ischemia and reperfusion on sarcoplasmic reticulum calcium uptake.* Circ Res, 1992. **71**(5): p. 1123-30.
82. Herzog, W.R., et al., *Short-term low dose intracoronary diltiazem administered at the onset of reperfusion reduces myocardial infarct size.* Int J Cardiol, 1997. **59**(1): p. 21-7.
83. Miyamae, M., et al., *Attenuation of postischemic reperfusion injury is related to prevention of [Ca2+]m overload in rat hearts.* Am J Physiol, 1996. **271**(5 Pt 2): p. H2145-53.
84. Bar, F.W., et al., *Results of the first clinical study of adjunctive CAldaret (MCC-135) in patients undergoing primary percutaneous coronary intervention for ST-Elevation Myocardial Infarction: the randomized multicentre CASTEMI study.* Eur Heart J, 2006. **27**(21): p. 2516-23.
85. Meng, H.P. and G.N. Pierce, *Protective effects of 5-(N,N-dimethyl)amiloride on ischemia-reperfusion injury in hearts.* Am J Physiol, 1990. **258**(5 Pt 2): p. H1615-9.
86. Hurtado, C., et al., *Cells expressing unique Na+/Ca2+ exchange (NCX1) splice variants exhibit different susceptibilities to Ca2+ overload.* Am J Physiol Heart Circ Physiol, 2006. **290**(5): p. H2155-62.
87. Lemasters, J.J., et al., *The pH paradox in ischemia-reperfusion injury to cardiac myocytes.* EXS, 1996. **76**: p. 99-114.
88. Hausenloy, D.J. and D.M. Yellon, *The mitochondrial permeability transition pore: its fundamental role in mediating cell death during ischaemia and reperfusion.* J Mol Cell Cardiol, 2003. **35**(4): p. 339-41.
89. Heusch, G., K. Boengler, and R. Schulz, *Inhibition of mitochondrial permeability transition pore opening: the Holy Grail of cardioprotection.* Basic Res Cardiol, 2010. **105**(2): p. 151-4.
90. Meng, H.P., B.B. Lonsberry, and G.N. Pierce, *Influence of perfusate pH on the postischemic recovery of cardiac contractile function: involvement of sodium-hydrogen exchange.* J Pharmacol Exp Ther, 1991. **258**(3): p. 772-7.
91. Qian, T., et al., *Mitochondrial permeability transition in pH-dependent reperfusion injury to rat hepatocytes.* Am J Physiol, 1997. **273**(6 Pt 1): p. C1783-92.
92. Chi, L., et al., *Protection of Myocardial Ischemia-Reperfusion by Therapeutic Hypercapnia: a Mechanism Involving Improvements in Mitochondrial Biogenesis and Function.* J Cardiovasc Transl Res, 2019.
93. Vinten-Johansen, J., *Involvement of neutrophils in the pathogenesis of lethal myocardial reperfusion injury.* Cardiovasc Res, 2004. **61**(3): p. 481-97.
94. Hayward, R., et al., *Recombinant soluble P-selectin glycoprotein ligand-1 protects against myocardial ischemic reperfusion injury in cats.* Cardiovasc Res, 1999. **41**(1): p. 65-76.
95. Ma, X.L., P.S. Tsao, and A.M. Lefer, *Antibody to CD-18 exerts endothelial and cardiac protective effects in myocardial ischemia and reperfusion.* J Clin Invest, 1991. **88**(4): p. 1237-43.
96. Zhao, Z.Q., et al., *Monoclonal antibody to ICAM-1 preserves postischemic blood flow and reduces infarct size after ischemia-reperfusion in rabbit.* J Leukoc Biol, 1997. **62**(3): p. 292-300.
97. Litt, M.R., et al., *Neutrophil depletion limited to reperfusion reduces myocardial infarct size after 90 minutes of ischemia. Evidence for neutrophil-mediated reperfusion injury.* Circulation, 1989. **80**(6): p. 1816-27.
98. Li, Y., et al., *Losartan protects against myocardial ischemia and reperfusion injury via vascular integrity preservation.* FASEB J, 2019: p. fj201900060R.

99. Qin, C.X., et al., *Cardioprotective Actions of the Annexin-A1 N-Terminal Peptide, Ac2-26, Against Myocardial Infarction.* Front Pharmacol, 2019. **10**: p. 269.
100. Sheibani, M., et al., *Sumatriptan protects against myocardial ischaemia-reperfusion injury by inhibition of inflammation in rat model.* Inflammopharmacology, 2019.
101. Ross, A.M., et al., *A randomized, double-blinded, placebo-controlled multicenter trial of adenosine as an adjunct to reperfusion in the treatment of acute myocardial infarction (AMISTAD-II).* J Am Coll Cardiol, 2005. **45**(11): p. 1775-80.
102. Investigators, A.A., et al., *Pexelizumab for acute ST-elevation myocardial infarction in patients undergoing primary percutaneous coronary intervention: a randomized controlled trial.* JAMA, 2007. **297**(1): p. 43-51.
103. Atar, D., et al., *Effect of intravenous FX06 as an adjunct to primary percutaneous coronary intervention for acute ST-segment elevation myocardial infarction results of the F.I.R.E. (Efficacy of FX06 in the Prevention of Myocardial Reperfusion Injury) trial.* J Am Coll Cardiol, 2009. **53**(8): p. 720-9.
104. Juranek, I. and S. Bezek, *Controversy of free radical hypothesis: reactive oxygen species--cause or consequence of tissue injury?* Gen Physiol Biophys, 2005. **24**(3): p. 263-78.
105. Allen, R.G. and M. Tresini, *Oxidative stress and gene regulation.* Free Radic Biol Med, 2000. **28**(3): p. 463-99.
106. Dillard, C.J., et al., *Effects of exercise, vitamin E, and ozone on pulmonary function and lipid peroxidation.* J Appl Physiol Respir Environ Exerc Physiol, 1978. **45**(6): p. 927-32.
107. Carvajal, K., M. El Hafidi, and G. Banos, *Myocardial damage due to ischemia and reperfusion in hypertriglyceridemic and hypertensive rats: participation of free radicals and calcium overload.* J Hypertens, 1999. **17**(11): p. 1607-16.
108. Arroyo, C.M., et al., *Identification of free radicals in myocardial ischemia/reperfusion by spin trapping with nitrone DMPO.* FEBS Lett, 1987. **221**(1): p. 101-4.
109. Eaton, P. and H. Clements-Jewery, *Peroxynitrite: in vivo cardioprotectant or arrhythmogen?* Br J Pharmacol, 2008. **155**(7): p. 972-3.
110. Friedl, H.P., et al., *Ischemia-reperfusion in humans. Appearance of xanthine oxidase activity.* Am J Pathol, 1990. **136**(3): p. 491-5.
111. Vasquez-Vivar, J., et al., *Superoxide generation by endothelial nitric oxide synthase: the influence of cofactors.* Proc Natl Acad Sci U S A, 1998. **95**(16): p. 9220-5.
112. Chalupsky, K. and H. Cai, *Endothelial dihydrofolate reductase: critical for nitric oxide bioavailability and role in angiotensin II uncoupling of endothelial nitric oxide synthase.* Proc Natl Acad Sci U S A, 2005. **102**(25): p. 9056-61.
113. Loukogeorgakis, S.P., et al., *Role of NADPH oxidase in endothelial ischemia/reperfusion injury in humans.* Circulation, 2010. **121**(21): p. 2310-6.
114. Braunersreuther, V., et al., *Role of NADPH oxidase isoforms NOX1, NOX2 and NOX4 in myocardial ischemia/reperfusion injury.* J Mol Cell Cardiol, 2013. **64**: p. 99-107.
115. Hare, J.M. and W.S. Colucci, *Role of nitric oxide in the regulation of myocardial function.* Prog Cardiovasc Dis, 1995. **38**(2): p. 155-66.
116. Xie, Y.W. and M.S. Wolin, *Role of nitric oxide and its interaction with superoxide in the suppression of cardiac muscle mitochondrial respiration. Involvement in response to hypoxia/reoxygenation.* Circulation, 1996. **94**(10): p. 2580-6.
117. Pacher, P., J.S. Beckman, and L. Liaudet, *Nitric oxide and peroxynitrite in health and disease.* Physiol Rev, 2007. **87**(1): p. 315-424.
118. Yasmin, W., K.D. Strynadka, and R. Schulz, *Generation of peroxynitrite contributes to ischemia-reperfusion injury in isolated rat hearts.* Cardiovasc Res, 1997. **33**(2): p. 422-32.

119. McCord, J.M. and R.S. Roy, *The pathophysiology of superoxide: roles in inflammation and ischemia.* Can J Physiol Pharmacol, 1982. **60**(11): p. 1346-52.
120. Xia, Y. and J.L. Zweier, *Direct measurement of nitric oxide generation from nitric oxide synthase.* Proc Natl Acad Sci U S A, 1997. **94**(23): p. 12705-10.
121. Ferrari, R., et al., *Occurrence of oxidative stress during reperfusion of the human heart.* Circulation, 1990. **81**(1): p. 201-11.
122. Tanaka-Esposito, C., Q. Chen, and E.J. Lesnefsky, *Blockade of electron transport before ischemia protects mitochondria and decreases myocardial injury during reperfusion in aged rat hearts.* Transl Res, 2012. **160**(3): p. 207-16.
123. Murphy, M.P., *How mitochondria produce reactive oxygen species.* Biochem J, 2009. **417**(1): p. 1-13.
124. Burwell, L.S., et al., *Direct evidence for S-nitrosation of mitochondrial complex I.* Biochem J, 2006. **394**(Pt 3): p. 627-34.
125. Methner, C., et al., *Mitochondria selective S-nitrosation by mitochondria-targeted S-nitrosothiol protects against post-infarct heart failure in mouse hearts.* Eur J Heart Fail, 2014. **16**(7): p. 712-7.
126. Stewart, S., E.J. Lesnefsky, and Q. Chen, *Reversible blockade of electron transport with amobarbital at the onset of reperfusion attenuates cardiac injury.* Transl Res, 2009. **153**(5): p. 224-31.
127. Nathan, A.T. and M. Singer, *The oxygen trail: tissue oxygenation.* Br Med Bull, 1999. **55**(1): p. 96-108.
128. Macdonald, J., H.F. Galley, and N.R. Webster, *Oxidative stress and gene expression in sepsis.* Br J Anaesth, 2003. **90**(2): p. 221-32.
129. McCully, J.D., et al., *Injection of isolated mitochondria during early reperfusion for cardioprotection.* Am J Physiol Heart Circ Physiol, 2009. **296**(1): p. H94-H105.
130. Emani, S.M., et al., *Autologous mitochondrial transplantation for dysfunction after ischemia-reperfusion injury.* J Thorac Cardiovasc Surg, 2017. **154**(1): p. 286-289.
131. Poole, L.B., *The basics of thiols and cysteines in redox biology and chemistry.* Free Radic Biol Med, 2015. **80**: p. 148-57.
132. Ambrosio, G., et al., *Oxygen radicals generated at reflow induce peroxidation of membrane lipids in reperfused hearts.* J Clin Invest, 1991. **87**(6): p. 2056-66.
133. Fahy, E., et al., *Lipid classification, structures and tools.* Biochim Biophys Acta, 2011. **1811**(11): p. 637-47.
134. Magtanong, L., P.J. Ko, and S.J. Dixon, *Emerging roles for lipids in non-apoptotic cell death.* Cell Death Differ, 2016. **23**(7): p. 1099-109.
135. Romaschin, A.D., et al., *Subcellular distribution of peroxidized lipids in myocardial reperfusion injury.* Am J Physiol, 1990. **259**(1 Pt 2): p. H116-23.
136. Dixon, I.M., et al., *Alterations in cardiac membrane Ca2+ transport during oxidative stress.* Mol Cell Biochem, 1990. **99**(2): p. 125-33.
137. Dixon, I.M., T. Hata, and N.S. Dhalla, *Sarcolemmal Na(+)-K(+)-ATPase activity in congestive heart failure due to myocardial infarction.* Am J Physiol, 1992. **262**(3 Pt 1): p. C664-71.
138. Netticadan, T., et al., *Status of Ca2+/calmodulin protein kinase phosphorylation of cardiac SR proteins in ischemia-reperfusion.* Am J Physiol, 1999. **277**(3): p. C384-91.
139. Osada, M., et al., *Modification of ischemia-reperfusion-induced changes in cardiac sarcoplasmic reticulum by preconditioning.* Am J Physiol, 1998. **274**(6): p. H2025-34.
140. Donoso, P., et al., *Modulation of cardiac ryanodine receptor activity by ROS and RNS.* Front Biosci (Landmark Ed), 2011. **16**: p. 553-67.
141. Blaustein, A., et al., *Myocardial glutathione depletion impairs recovery after short periods of ischemia.* Circulation, 1989. **80**(5): p. 1449-57.

142. Le, C.T., et al., *Buthionine sulfoximine reduces the protective capacity of myocytes to withstand peroxide-derived free radical attack.* J Mol Cell Cardiol, 1993. **25**(5): p. 519-28.
143. Werns, S.W., et al., *Myocardial glutathione depletion impairs recovery of isolated blood-perfused hearts after global ischaemia.* J Mol Cell Cardiol, 1992. **24**(11): p. 1215-20.
144. Konz, K.H., et al., *Diastolic dysfunction of perfused rat hearts induced by hydrogen peroxide. Protective effect of selenium.* J Mol Cell Cardiol, 1989. **21**(8): p. 789-95.
145. Yoshida, T., et al., *Transgenic mice overexpressing glutathione peroxidase are resistant to myocardial ischemia reperfusion injury.* J Mol Cell Cardiol, 1996. **28**(8): p. 1759-67.
146. Brasier, A.R., *The nuclear factor-kappaB-interleukin-6 signalling pathway mediating vascular inflammation.* Cardiovasc Res, 2010. **86**(2): p. 211-8.
147. Rodrigo, R., et al., *Oxidative stress-related biomarkers in essential hypertension and ischemia-reperfusion myocardial damage.* Dis Markers, 2013. **35**(6): p. 773-90.
148. Philippova, M., et al., *Oxidised phospholipids as biomarkers in human disease.* Swiss Med Wkly, 2014. **144**: p. w14037.
149. Mitchell, T.W., et al., *Differences in membrane acyl phospholipid composition between an endothermic mammal and an ectothermic reptile are not limited to any phospholipid class.* J Exp Biol, 2007. **210**(Pt 19): p. 3440-50.
150. Fruhwirth, G.O., A. Loidl, and A. Hermetter, *Oxidized phospholipids: from molecular properties to disease.* Biochim Biophys Acta, 2007. **1772**(7): p. 718-36.
151. Fernandis, A.Z. and M.R. Wenk, *Membrane lipids as signaling molecules.* Curr Opin Lipidol, 2007. **18**(2): p. 121-8.
152. Falkenburger, B.H., et al., *Phosphoinositides: lipid regulators of membrane proteins.* J Physiol, 2010. **588**(Pt 17): p. 3179-85.
153. Wisastra, R. and F.J. Dekker, *Inflammation, Cancer and Oxidative Lipoxygenase Activity are Intimately Linked.* Cancers (Basel), 2014. **6**(3): p. 1500-21.
154. Ashraf, M.Z., N.S. Kar, and E.A. Podrez, *Oxidized phospholipids: biomarker for cardiovascular diseases.* Int J Biochem Cell Biol, 2009. **41**(6): p. 1241-4.
155. Greig, F.H., S. Kennedy, and C.M. Spickett, *Physiological effects of oxidized phospholipids and their cellular signaling mechanisms in inflammation.* Free Radic Biol Med, 2012. **52**(2): p. 266-80.
156. Mugge, A., *The role of reactive oxygen species in atherosclerosis.* Z Kardiol, 1998. **87**(11): p. 851-64.
157. Guarnieri, C., F. Flamigni, and C.M. Caldarera, *Role of oxygen in the cellular damage induced by re-oxygenation of hypoxic heart.* J Mol Cell Cardiol, 1980. **12**(8): p. 797-808.
158. Jezek, P. and L. Hlavata, *Mitochondria in homeostasis of reactive oxygen species in cell, tissues, and organism.* Int J Biochem Cell Biol, 2005. **37**(12): p. 2478-503.
159. Singh, R., S. Devi, and R. Gollen, *Role of free radical in atherosclerosis, diabetes and dyslipidaemia: larger-than-life.* Diabetes Metab Res Rev, 2015. **31**(2): p. 113-26.
160. Anderson, E.J., L.A. Katunga, and M.S. Willis, *Mitochondria as a source and target of lipid peroxidation products in healthy and diseased heart.* Clin Exp Pharmacol Physiol, 2012. **39**(2): p. 179-93.
161. Winterbourn, C.C., *Toxicity of iron and hydrogen peroxide: the Fenton reaction.* Toxicol Lett, 1995. **82-83**: p. 969-74.
162. Esterbauer, H. and H. Zollner, *Methods for determination of aldehydic lipid peroxidation products.* Free Radic Biol Med, 1989. **7**(2): p. 197-203.
163. Ravandi, A., et al., *Preparation of Schiff base adducts of phosphatidylcholine core aldehydes and aminophospholipids, amino acids, and myoglobin.* Lipids, 1997. **32**(9): p. 989-1001.
164. Dixon, S.J., et al., *Pharmacological inhibition of cystine-glutamate exchange induces endoplasmic reticulum stress and ferroptosis.* Elife, 2014. **3**: p. e02523.

165. Marnett, L.J., *Peroxyl free radicals: potential mediators of tumor initiation and promotion.* Carcinogenesis, 1987. **8**(10): p. 1365-73.
166. Pratt, D.A., K.A. Tallman, and N.A. Porter, *Free radical oxidation of polyunsaturated lipids: New mechanistic insights and the development of peroxyl radical clocks.* Acc Chem Res, 2011. **44**(6): p. 458-67.
167. Reis, A. and C.M. Spickett, *Chemistry of phospholipid oxidation.* Biochim Biophys Acta, 2012. **1818**(10): p. 2374-87.
168. Bochkov, V., et al., *Pleiotropic effects of oxidized phospholipids.* Free Radic Biol Med, 2017. **111**: p. 6-24.
169. Wittwer, J. and M. Hersberger, *The two faces of the 15-lipoxygenase in atherosclerosis.* Prostaglandins Leukot Essent Fatty Acids, 2007. **77**(2): p. 67-77.
170. Kuhn, H., S. Banthiya, and K. van Leyen, *Mammalian lipoxygenases and their biological relevance.* Biochim Biophys Acta, 2015. **1851**(4): p. 308-30.
171. Aldrovandi, M., et al., *Human platelets generate phospholipid-esterified prostaglandins via cyclooxygenase-1 that are inhibited by low dose aspirin supplementation.* J Lipid Res, 2013. **54**(11): p. 3085-97.
172. Clark, S.R., et al., *Esterified eicosanoids are acutely generated by 5-lipoxygenase in primary human neutrophils and in human and murine infection.* Blood, 2011. **117**(6): p. 2033-43.
173. Khandelia, H. and O.G. Mouritsen, *Lipid gymnastics: evidence of complete acyl chain reversal in oxidized phospholipids from molecular simulations.* Biophys J, 2009. **96**(7): p. 2734-43.
174. Jurkiewicz, P., et al., *Biophysics of lipid bilayers containing oxidatively modified phospholipids: insights from fluorescence and EPR experiments and from MD simulations.* Biochim Biophys Acta, 2012. **1818**(10): p. 2388-402.
175. Sabatini, K., et al., *Characterization of two oxidatively modified phospholipids in mixed monolayers with DPPC.* Biophys J, 2006. **90**(12): p. 4488-99.
176. Beranova, L., et al., *Oxidation changes physical properties of phospholipid bilayers: fluorescence spectroscopy and molecular simulations.* Langmuir, 2010. **26**(9): p. 6140-4.
177. Volinsky, R., et al., *Oxidized phosphatidylcholines facilitate phospholipid flip-flop in liposomes.* Biophys J, 2011. **101**(6): p. 1376-84.
178. Angeletti, C. and J.W. Nichols, *Dithionite quenching rate measurement of the inside-outside membrane bilayer distribution of 7-nitrobenz-2-oxa-1,3-diazol-4-yl-labeled phospholipids.* Biochemistry, 1998. **37**(43): p. 15114-9.
179. Lis, M., et al., *The effect of lipid oxidation on the water permeability of phospholipids bilayers.* Phys Chem Chem Phys, 2011. **13**(39): p. 17555-63.
180. Ayee, M.A., et al., *Molecular-Scale Biophysical Modulation of an Endothelial Membrane by Oxidized Phospholipids.* Biophys J, 2017. **112**(2): p. 325-338.
181. Stemmer, U. and A. Hermetter, *Protein modification by aldehydophospholipids and its functional consequences.* Biochim Biophys Acta, 2012. **1818**(10): p. 2436-45.
182. Moumtzi, A., et al., *Import and fate of fluorescent analogs of oxidized phospholipids in vascular smooth muscle cells.* J Lipid Res, 2007. **48**(3): p. 565-82.
183. Stafforini, D.M., S.M. Prescott, and T.M. McIntyre, *Human plasma platelet-activating factor acetylhydrolase. Purification and properties.* J Biol Chem, 1987. **262**(9): p. 4223-30.
184. Stremler, K.E., et al., *Human plasma platelet-activating factor acetylhydrolase. Oxidatively fragmented phospholipids as substrates.* J Biol Chem, 1991. **266**(17): p. 11095-103.
185. Liu, J., et al., *Circulating platelet-activating factor is primarily cleared by transport, not intravascular hydrolysis by lipoprotein-associated phospholipase A2/ PAF acetylhydrolase.* Circ Res, 2011. **108**(4): p. 469-77.

186. Horkko, S., et al., *Monoclonal autoantibodies specific for oxidized phospholipids or oxidized phospholipid-protein adducts inhibit macrophage uptake of oxidized low-density lipoproteins.* J Clin Invest, 1999. **103**(1): p. 117-28.
187. Bochkov, V., et al., *Novel immune assay for quantification of plasma protective capacity against oxidized phospholipids.* Biomark Med, 2016. **10**(8): p. 797-810.
188. Bochkov, V.N., et al., *Protective role of phospholipid oxidation products in endotoxin-induced tissue damage.* Nature, 2002. **419**(6902): p. 77-81.
189. Code, C., et al., *Activation of phospholipase A2 by 1-palmitoyl-2-(9'-oxo-nonanoyl)-sn-glycero-3-phosphocholine in vitro.* Biochim Biophys Acta, 2010. **1798**(8): p. 1593-600.
190. Moellering, D.R., et al., *Induction of glutathione synthesis by oxidized low-density lipoprotein and 1-palmitoyl-2-arachidonyl phosphatidylcholine: protection against quinone-mediated oxidative stress.* Biochem J, 2002. **362**(Pt 1): p. 51-9.
191. Leitinger, N., et al., *Structurally similar oxidized phospholipids differentially regulate endothelial binding of monocytes and neutrophils.* Proc Natl Acad Sci U S A, 1999. **96**(21): p. 12010-5.
192. Oskolkova, O.V., et al., *Oxidized phospholipids are more potent antagonists of lipopolysaccharide than inducers of inflammation.* J Immunol, 2010. **185**(12): p. 7706-12.
193. Kim, M.J., et al., *Suppression of Toll-like receptor 4 activation by endogenous oxidized phosphatidylcholine, KOdiA-PC by inhibiting LPS binding to MD2.* Inflamm Res, 2013. **62**(6): p. 571-80.
194. Erridge, C., et al., *Oxidized phospholipid inhibition of toll-like receptor (TLR) signaling is restricted to TLR2 and TLR4: roles for CD14, LPS-binding protein, and MD2 as targets for specificity of inhibition.* J Biol Chem, 2008. **283**(36): p. 24748-59.
195. Cherepanova, O.A., et al., *Oxidized phospholipids induce type VIII collagen expression and vascular smooth muscle cell migration.* Circ Res, 2009. **104**(5): p. 609-18.
196. Cole, A.L., et al., *Oxidized phospholipid-induced endothelial cell/monocyte interaction is mediated by a cAMP-dependent R-Ras/PI3-kinase pathway.* Arterioscler Thromb Vasc Biol, 2003. **23**(8): p. 1384-90.
197. Imai, Y., et al., *Identification of oxidative stress and Toll-like receptor 4 signaling as a key pathway of acute lung injury.* Cell, 2008. **133**(2): p. 235-49.
198. Starosta, V., et al., *Differential regulation of endothelial cell permeability by high and low doses of oxidized 1-palmitoyl-2-arachidonyl-sn-glycero-3-phosphocholine.* Am J Respir Cell Mol Biol, 2012. **46**(3): p. 331-41.
199. Qin, J., et al., *Oxidized phosphatidylcholine is a marker for neuroinflammation in multiple sclerosis brain.* J Neurosci Res, 2007. **85**(5): p. 977-84.
200. Ikura, Y., et al., *Localization of oxidized phosphatidylcholine in nonalcoholic fatty liver disease: impact on disease progression.* Hepatology, 2006. **43**(3): p. 506-14.
201. Yang, L., et al., *Chronic alcohol exposure increases circulating bioactive oxidized phospholipids.* J Biol Chem, 2010. **285**(29): p. 22211-20.
202. Berliner, J., *Introduction. Lipid oxidation products and atherosclerosis.* Vascul Pharmacol, 2002. **38**(4): p. 187-91.
203. Watson, A.D., et al., *Structural identification by mass spectrometry of oxidized phospholipids in minimally oxidized low density lipoprotein that induce monocyte/endothelial interactions and evidence for their presence in vivo.* J Biol Chem, 1997. **272**(21): p. 13597-607.
204. Frey, B., et al., *Increase in fragmented phosphatidylcholine in blood plasma by oxidative stress.* J Lipid Res, 2000. **41**(7): p. 1145-53.
205. Ravandi, A., et al., *Phospholipids and oxophospholipids in atherosclerotic plaques at different stages of plaque development.* Lipids, 2004. **39**(2): p. 97-109.

206. van Dijk, R.A., et al., *Differential expression of oxidation-specific epitopes and apolipoprotein(a) in progressing and ruptured human coronary and carotid atherosclerotic lesions.* J Lipid Res, 2012. **53**(12): p. 2773-90.
207. Gharavi, N.M., et al., *Role of the Jak/STAT pathway in the regulation of interleukin-8 transcription by oxidized phospholipids in vitro and in atherosclerosis in vivo.* J Biol Chem, 2007. **282**(43): p. 31460-8.
208. Greig, F.H., et al., *Differential effects of chlorinated and oxidized phospholipids in vascular tissue: implications for neointima formation.* Clin Sci (Lond), 2015. **128**(9): p. 579-92.
209. Pidkovka, N.A., et al., *Oxidized phospholipids induce phenotypic switching of vascular smooth muscle cells in vivo and in vitro.* Circ Res, 2007. **101**(8): p. 792-801.
210. Stemmer, U., et al., *Toxicity of oxidized phospholipids in cultured macrophages.* Lipids Health Dis, 2012. **11**: p. 110.
211. Davis, B., et al., *Electrospray ionization mass spectrometry identifies substrates and products of lipoprotein-associated phospholipase A2 in oxidized human low density lipoprotein.* J Biol Chem, 2008. **283**(10): p. 6428-37.
212. Que, X., et al., *Oxidized phospholipids are proinflammatory and proatherogenic in hypercholesterolaemic mice.* Nature, 2018. **558**(7709): p. 301-306.
213. Tsimikas, S., et al., *Oxidized phospholipids, Lp(a) lipoprotein, and coronary artery disease.* N Engl J Med, 2005. **353**(1): p. 46-57.
214. Rajendran, P., et al., *The vascular endothelium and human diseases.* Int J Biol Sci, 2013. **9**(10): p. 1057-69.
215. Vanhoutte, P.M., *Endothelial control of vasomotor function: from health to coronary disease.* Circ J, 2003. **67**(7): p. 572-5.
216. Pober, J.S. and W.C. Sessa, *Evolving functions of endothelial cells in inflammation.* Nat Rev Immunol, 2007. **7**(10): p. 803-15.
217. Bombeli, T., M. Mueller, and A. Haeberli, *Anticoagulant properties of the vascular endothelium.* Thromb Haemost, 1997. **77**(3): p. 408-23.
218. Wu, K.K., K. Frasier-Scott, and H. Hatzakis, *Endothelial cell function in hemostasis and thrombosis.* Adv Exp Med Biol, 1988. **242**: p. 127-33.
219. Ghosh, A., et al., *Role of free fatty acids in endothelial dysfunction.* J Biomed Sci, 2017. **24**(1): p. 50.
220. Davignon, J. and P. Ganz, *Role of endothelial dysfunction in atherosclerosis.* Circulation, 2004. **109**(23 Suppl 1): p. III27-32.
221. Mudau, M., et al., *Endothelial dysfunction: the early predictor of atherosclerosis.* Cardiovasc J Afr, 2012. **23**(4): p. 222-31.
222. Birukova, A.A., et al., *Fragmented oxidation products define barrier disruptive endothelial cell response to OxPAPC.* Transl Res, 2013. **161**(6): p. 495-504.
223. Gugiu, B.G., et al., *Protein targets of oxidized phospholipids in endothelial cells.* J Lipid Res, 2008. **49**(3): p. 510-20.
224. Lee, S., et al., *Role of phospholipid oxidation products in atherosclerosis.* Circ Res, 2012. **111**(6): p. 778-99.
225. Romanoski, C.E., et al., *Network for activation of human endothelial cells by oxidized phospholipids: a critical role of heme oxygenase 1.* Circ Res, 2011. **109**(5): p. e27-41.
226. Li, R., et al., *Identification of prostaglandin E2 receptor subtype 2 as a receptor activated by OxPAPC.* Circ Res, 2006. **98**(5): p. 642-50.
227. Rezaie-Majd, A., et al., *Simvastatin reduces expression of cytokines interleukin-6, interleukin-8, and monocyte chemoattractant protein-1 in circulating monocytes from hypercholesterolemic patients.* Arterioscler Thromb Vasc Biol, 2002. **22**(7): p. 1194-9.

228. Gargalovic, P.S., et al., *The unfolded protein response is an important regulator of inflammatory genes in endothelial cells.* Arterioscler Thromb Vasc Biol, 2006. **26**(11): p. 2490-6.
229. Wang, N., et al., *Interleukin 8 is induced by cholesterol loading of macrophages and expressed by macrophage foam cells in human atheroma.* J Biol Chem, 1996. **271**(15): p. 8837-42.
230. Ricote, M., et al., *Expression of the peroxisome proliferator-activated receptor gamma (PPARgamma) in human atherosclerosis and regulation in macrophages by colony stimulating factors and oxidized low density lipoprotein.* Proc Natl Acad Sci U S A, 1998. **95**(13): p. 7614-9.
231. Lee, H., et al., *Role for peroxisome proliferator-activated receptor alpha in oxidized phospholipid-induced synthesis of monocyte chemotactic protein-1 and interleukin-8 by endothelial cells.* Circ Res, 2000. **87**(6): p. 516-21.
232. Bochkov, V.N., et al., *Oxidized phospholipids stimulate tissue factor expression in human endothelial cells via activation of ERK/EGR-1 and Ca(++)/NFAT.* Blood, 2002. **99**(1): p. 199-206.
233. Ma, Q., *Role of nrf2 in oxidative stress and toxicity.* Annu Rev Pharmacol Toxicol, 2013. **53**: p. 401-26.
234. Kuosmanen, S.M., et al., *NRF2 regulates endothelial glycolysis and proliferation with miR-93 and mediates the effects of oxidized phospholipids on endothelial activation.* Nucleic Acids Res, 2017.
235. Rikitake, Y., et al., *Inhibition of endothelium-dependent arterial relaxation by oxidized phosphatidylcholine.* Atherosclerosis, 2000. **152**(1): p. 79-87.
236. Yan, F.X., et al., *The oxidized phospholipid POVPC impairs endothelial function and vasodilation via uncoupling endothelial nitric oxide synthase.* J Mol Cell Cardiol, 2017. **112**: p. 40-48.
237. Moore, K.J., F.J. Sheedy, and E.A. Fisher, *Macrophages in atherosclerosis: a dynamic balance.* Nat Rev Immunol, 2013. **13**(10): p. 709-21.
238. Pegorier, S., et al., *Oxidized phospholipid: POVPC binds to platelet-activating-factor receptor on human macrophages. Implications in atherosclerosis.* Atherosclerosis, 2006. **188**(2): p. 433-43.
239. Huber, J., et al., *Specific monocyte adhesion to endothelial cells induced by oxidized phospholipids involves activation of cPLA2 and lipoxygenase.* J Lipid Res, 2006. **47**(5): p. 1054-62.
240. Podrez, E.A., et al., *A novel family of atherogenic oxidized phospholipids promotes macrophage foam cell formation via the scavenger receptor CD36 and is enriched in atherosclerotic lesions.* J Biol Chem, 2002. **277**(41): p. 38517-23.
241. Huber, J., et al., *Oxidized membrane vesicles and blebs from apoptotic cells contain biologically active oxidized phospholipids that induce monocyte-endothelial interactions.* Arterioscler Thromb Vasc Biol, 2002. **22**(1): p. 101-7.
242. Yeon, S.H., et al., *Oxidized phosphatidylcholine induces the activation of NLRP3 inflammasome in macrophages.* J Leukoc Biol, 2017. **101**(1): p. 205-215.
243. Di Gioia, M., et al., *Endogenous oxidized phospholipids reprogram cellular metabolism and boost hyperinflammation.* Nat Immunol, 2020. **21**(1): p. 42-53.
244. Tavakoli, S., et al., *Characterization of Macrophage Polarization States Using Combined Measurement of 2-Deoxyglucose and Glutamine Accumulation: Implications for Imaging of Atherosclerosis.* Arterioscler Thromb Vasc Biol, 2017. **37**(10): p. 1840-1848.
245. Kwak, B.R., et al., *Altered pattern of vascular connexin expression in atherosclerotic plaques.* Arterioscler Thromb Vasc Biol, 2002. **22**(2): p. 225-30.
246. Johnstone, S.R., et al., *Oxidized phospholipid species promote in vivo differential cx43 phosphorylation and vascular smooth muscle cell proliferation.* Am J Pathol, 2009. **175**(2): p. 916-24.
247. Al-Shawaf, E., et al., *Short-term stimulation of calcium-permeable transient receptor potential canonical 5-containing channels by oxidized phospholipids.* Arterioscler Thromb Vasc Biol, 2010. **30**(7): p. 1453-9.

248. Hansen, N.U., et al., *Type VIII collagen is elevated in diseases associated with angiogenesis and vascular remodeling.* Clin Biochem, 2016. **49**(12): p. 903-8.
249. Matter, C.M., et al., *Increased balloon-induced inflammation, proliferation, and neointima formation in apolipoprotein E (ApoE) knockout mice.* Stroke, 2006. **37**(10): p. 2625-32.
250. Ali, Z.A., et al., *Increased in-stent stenosis in ApoE knockout mice: insights from a novel mouse model of balloon angioplasty and stenting.* Arterioscler Thromb Vasc Biol, 2007. **27**(4): p. 833-40.
251. Clarke, M.C., et al., *Chronic apoptosis of vascular smooth muscle cells accelerates atherosclerosis and promotes calcification and medial degeneration.* Circ Res, 2008. **102**(12): p. 1529-38.
252. Fruhwirth, G.O., et al., *The oxidized phospholipids POVPC and PGPC inhibit growth and induce apoptosis in vascular smooth muscle cells.* Biochim Biophys Acta, 2006. **1761**(9): p. 1060-9.
253. Friedman, P., et al., *Correlation of antiphospholipid antibody recognition with the structure of synthetic oxidized phospholipids. Importance of Schiff base formation and aldol condensation.* J Biol Chem, 2002. **277**(9): p. 7010-20.
254. Chen, R., et al., *Platelet activation by low concentrations of intact oxidized LDL particles involves the PAF receptor.* Arterioscler Thromb Vasc Biol, 2009. **29**(3): p. 363-71.
255. Gopfert, M.S., et al., *Structural identification of oxidized acyl-phosphatidylcholines that induce platelet activation.* J Vasc Res, 2005. **42**(2): p. 120-32.
256. Abumrad, N.A. and I.J. Goldberg, *CD36 actions in the heart: Lipids, calcium, inflammation, repair and more?* Biochim Biophys Acta, 2016. **1861**(10): p. 1442-9.
257. Podrez, E.A., et al., *Identification of a novel family of oxidized phospholipids that serve as ligands for the macrophage scavenger receptor CD36.* J Biol Chem, 2002. **277**(41): p. 38503-16.
258. Podrez, E.A., et al., *Platelet CD36 links hyperlipidemia, oxidant stress and a prothrombotic phenotype.* Nat Med, 2007. **13**(9): p. 1086-95.
259. Yutzey, K.E., et al., *Calcific aortic valve disease: a consensus summary from the Alliance of Investigators on Calcific Aortic Valve Disease.* Arterioscler Thromb Vasc Biol, 2014. **34**(11): p. 2387-93.
260. Stewart, B.F., et al., *Clinical factors associated with calcific aortic valve disease. Cardiovascular Health Study.* J Am Coll Cardiol, 1997. **29**(3): p. 630-4.
261. Roberts, W.C., *The senile cardiac calcification syndrome.* Am J Cardiol, 1986. **58**(6): p. 572-4.
262. Pomerance, A., *Pathogenesis of aortic stenosis and its relation to age.* Br Heart J, 1972. **34**(6): p. 569-74.
263. Sathyamurthy, I. and S. Alex, *Calcific aortic valve disease: is it another face of atherosclerosis?* Indian Heart J, 2015. **67**(5): p. 503-6.
264. Capoulade, R., et al., *Oxidized Phospholipids, Lipoprotein(a), and Progression of Calcific Aortic Valve Stenosis.* J Am Coll Cardiol, 2015. **66**(11): p. 1236-1246.
265. Kamstrup, P.R., A. Tybjaerg-Hansen, and B.G. Nordestgaard, *Elevated lipoprotein(a) and risk of aortic valve stenosis in the general population.* J Am Coll Cardiol, 2014. **63**(5): p. 470-7.
266. Arsenault, B.J., et al., *Impact of high-dose atorvastatin therapy and clinical risk factors on incident aortic valve stenosis in patients with cardiovascular disease (from TNT, IDEAL, and SPARCL).* Am J Cardiol, 2014. **113**(8): p. 1378-82.
267. Thanassoulis, G., et al., *Genetic associations with valvular calcification and aortic stenosis.* N Engl J Med, 2013. **368**(6): p. 503-12.
268. Leibundgut, G., et al., *Determinants of binding of oxidized phospholipids on apolipoprotein (a) and lipoprotein (a).* J Lipid Res, 2013. **54**(10): p. 2815-30.
269. Bergmark, C., et al., *A novel function of lipoprotein [a] as a preferential carrier of oxidized phospholipids in human plasma.* J Lipid Res, 2008. **49**(10): p. 2230-9.

270. Torzewski, M., et al., *Lipoprotein(a) Associated Molecules are Prominent Components in Plasma and Valve Leaflets in Calcific Aortic Valve Stenosis.* JACC Basic Transl Sci, 2017. **2**(3): p. 229-240.
271. Taleb, A., J.L. Witztum, and S. Tsimikas, *Oxidized phospholipids on apoB-100-containing lipoproteins: a biomarker predicting cardiovascular disease and cardiovascular events.* Biomark Med, 2011. **5**(5): p. 673-94.
272. Yeang, C., et al., *Reduction of Myocardial Ischemia-Reperfusion Injury by Inactivating Oxidized Phospholipids.* Cardiovasc Res, 2018.
273. Ganguly, R., et al., *Alpha linolenic acid decreases apoptosis and oxidized phospholipids in cardiomyocytes during ischemia/reperfusion.* Mol Cell Biochem, 2018. **437**(1-2): p. 163-175.
274. Shaw, P.X., et al., *Natural antibodies with the T15 idiotype may act in atherosclerosis, apoptotic clearance, and protective immunity.* J Clin Invest, 2000. **105**(12): p. 1731-40.
275. Chang, M.K., et al., *Apoptotic cells with oxidation-specific epitopes are immunogenic and proinflammatory.* J Exp Med, 2004. **200**(11): p. 1359-70.
276. Bochkov, V.N., et al., *Generation and biological activities of oxidized phospholipids.* Antioxid Redox Signal, 2010. **12**(8): p. 1009-59.
277. Tsimikas, S., et al., *Temporal increases in plasma markers of oxidized low-density lipoprotein strongly reflect the presence of acute coronary syndromes.* J Am Coll Cardiol, 2003. **41**(3): p. 360-70.
278. Tsimikas, S., et al., *Percutaneous coronary intervention results in acute increases in oxidized phospholipids and lipoprotein(a): short-term and long-term immunologic responses to oxidized low-density lipoprotein.* Circulation, 2004. **109**(25): p. 3164-70.
279. Kiechl, S., et al., *Oxidized phospholipids, lipoprotein(a), lipoprotein-associated phospholipase A2 activity, and 10-year cardiovascular outcomes: prospective results from the Bruneck study.* Arterioscler Thromb Vasc Biol, 2007. **27**(8): p. 1788-95.
280. Tsimikas, S., et al., *Oxidation-specific biomarkers, lipoprotein(a), and risk of fatal and nonfatal coronary events.* J Am Coll Cardiol, 2010. **56**(12): p. 946-55.
281. Wu, R., et al., *Autoantibodies to OxLDL are decreased in individuals with borderline hypertension.* Hypertension, 1999. **33**(1): p. 53-9.
282. Penny, W.F., et al., *Improvement of coronary artery endothelial dysfunction with lipid-lowering therapy: heterogeneity of segmental response and correlation with plasma-oxidized low density lipoprotein.* J Am Coll Cardiol, 2001. **37**(3): p. 766-74.
283. Tsimikas, S., et al., *High-dose atorvastatin reduces total plasma levels of oxidized phospholipids and immune complexes present on apolipoprotein B-100 in patients with acute coronary syndromes in the MIRACL trial.* Circulation, 2004. **110**(11): p. 1406-12.
284. Silaste, M.L., et al., *Changes in dietary fat intake alter plasma levels of oxidized low-density lipoprotein and lipoprotein(a).* Arterioscler Thromb Vasc Biol, 2004. **24**(3): p. 498-503.
285. Tsimikas, S., et al., *Oxidized phospholipids predict the presence and progression of carotid and femoral atherosclerosis and symptomatic cardiovascular disease: five-year prospective results from the Bruneck study.* J Am Coll Cardiol, 2006. **47**(11): p. 2219-28.
286. Rodenburg, J., et al., *Oxidized low-density lipoprotein in children with familial hypercholesterolemia and unaffected siblings: effect of pravastatin.* J Am Coll Cardiol, 2006. **47**(9): p. 1803-10.
287. Inami, S., et al., *Tea catechin consumption reduces circulating oxidized low-density lipoprotein.* Int Heart J, 2007. **48**(6): p. 725-32.
288. Ky, B., et al., *The influence of pravastatin and atorvastatin on markers of oxidative stress in hypercholesterolemic humans.* J Am Coll Cardiol, 2008. **51**(17): p. 1653-62.
289. Choi, S.H., et al., *Relationship between biomarkers of oxidized low-density lipoprotein, statin therapy, quantitative coronary angiography, and atheroma: volume observations from the*

REVERSAL (Reversal of Atherosclerosis with Aggressive Lipid Lowering) study. J Am Coll Cardiol, 2008. **52**(1): p. 24-32.
290. Tsimikas, S., et al., *Relationship of oxidized phospholipids on apolipoprotein B-100 particles to race/ethnicity, apolipoprotein(a) isoform size, and cardiovascular risk factors: results from the Dallas Heart Study.* Circulation, 2009. **119**(13): p. 1711-9.
291. Budoff, M.J., et al., *Aged garlic extract supplemented with B vitamins, folic acid and L-arginine retards the progression of subclinical atherosclerosis: a randomized clinical trial.* Prev Med, 2009. **49**(2-3): p. 101-7.
292. Ahmadi, N., et al., *Relation of oxidative biomarkers, vascular dysfunction, and progression of coronary artery calcium.* Am J Cardiol, 2010. **105**(4): p. 459-66.
293. Faghihnia, N., et al., *Changes in lipoprotein(a), oxidized phospholipids, and LDL subclasses with a low-fat high-carbohydrate diet.* J Lipid Res, 2010. **51**(11): p. 3324-30.
294. Byun, Y.S., et al., *Relationship of oxidized phospholipids on apolipoprotein B-100 to cardiovascular outcomes in patients treated with intensive versus moderate atorvastatin therapy: the TNT trial.* J Am Coll Cardiol, 2015. **65**(13): p. 1286-1295.
295. Leibundgut, G., et al., *Acute and long-term effect of percutaneous coronary intervention on serially-measured oxidative, inflammatory, and coagulation biomarkers in patients with stable angina.* J Thromb Thrombolysis, 2016. **41**(4): p. 569-80.
296. Yeang, C., et al., *Effect of therapeutic interventions on oxidized phospholipids on apolipoprotein B100 and lipoprotein(a).* J Clin Lipidol, 2016. **10**(3): p. 594-603.
297. van der Valk, F.M., et al., *Oxidized Phospholipids on Lipoprotein(a) Elicit Arterial Wall Inflammation and an Inflammatory Monocyte Response in Humans.* Circulation, 2016. **134**(8): p. 611-24.
298. Byun, Y.S., et al., *Oxidized Phospholipids on Apolipoprotein B-100 and Recurrent Ischemic Events Following Stroke or Transient Ischemic Attack.* J Am Coll Cardiol, 2017. **69**(2): p. 147-158.
299. Galluzzi, L., et al., *Essential versus accessory aspects of cell death: recommendations of the NCCD 2015.* Cell Death Differ, 2015. **22**(1): p. 58-73.
300. Lee, P., et al., *Fas pathway is a critical mediator of cardiac myocyte death and MI during ischemia-reperfusion in vivo.* Am J Physiol Heart Circ Physiol, 2003. **284**(2): p. H456-63.
301. Ohtsuka, T., et al., *Clinical implications of circulating soluble Fas and Fas ligand in patients with acute myocardial infarction.* Coron Artery Dis, 1999. **10**(4): p. 221-5.
302. Fertin, M., et al., *Circulating levels of soluble Fas ligand and left ventricular remodeling after acute myocardial infarction (from the REVE-2 study).* J Cardiol, 2012. **60**(2): p. 93-7.
303. Nilsson, L., et al., *Soluble TNF receptors are associated with infarct size and ventricular dysfunction in ST-elevation myocardial infarction.* PLoS One, 2013. **8**(2): p. e55477.
304. Krown, K.A., et al., *Tumor necrosis factor alpha-induced apoptosis in cardiac myocytes. Involvement of the sphingolipid signaling cascade in cardiac cell death.* J Clin Invest, 1996. **98**(12): p. 2854-65.
305. Asgeri, M., et al., *Dual effects of tumor necrosis factor alpha on myocardial injury following prolonged hypoperfusion of the heart.* Immunol Invest, 2015. **44**(1): p. 23-35.
306. Monden, Y., et al., *Tumor necrosis factor-alpha is toxic via receptor 1 and protective via receptor 2 in a murine model of myocardial infarction.* Am J Physiol Heart Circ Physiol, 2007. **293**(1): p. H743-53.
307. Kehmeier, E.S., et al., *TNF-alpha, myocardial perfusion and function in patients with ST-segment elevation myocardial infarction and primary percutaneous coronary intervention.* Clin Res Cardiol, 2012. **101**(10): p. 815-27.
308. Padfield, G.J., et al., *Cardiovascular effects of tumour necrosis factor alpha antagonism in patients with acute myocardial infarction: a first in human study.* Heart, 2013. **99**(18): p. 1330-5.

309. Condorelli, G., et al., *Heart-targeted overexpression of caspase3 in mice increases infarct size and depresses cardiac function.* Proc Natl Acad Sci U S A, 2001. **98**(17): p. 9977-82.
310. Liu, Q., *Lentivirus mediated interference of Caspase-3 expression ameliorates the heart function on rats with acute myocardial infarction.* Eur Rev Med Pharmacol Sci, 2014. **18**(13): p. 1852-8.
311. Agosto, M., et al., *Serum caspase-3 p17 fragment is elevated in patients with ST-segment elevation myocardial infarction: a novel observation.* J Am Coll Cardiol, 2011. **57**(2): p. 220-1.
312. Fliss, H. and D. Gattinger, *Apoptosis in ischemic and reperfused rat myocardium.* Circ Res, 1996. **79**(5): p. 949-56.
313. de Moissac, D., et al., *Caspase activation and mitochondrial cytochrome C release during hypoxia-mediated apoptosis of adult ventricular myocytes.* J Mol Cell Cardiol, 2000. **32**(1): p. 53-63.
314. Chen, M., et al., *Bid is cleaved by calpain to an active fragment in vitro and during myocardial ischemia/reperfusion.* J Biol Chem, 2001. **276**(33): p. 30724-8.
315. Edinger, A.L. and C.B. Thompson, *Death by design: apoptosis, necrosis and autophagy.* Curr Opin Cell Biol, 2004. **16**(6): p. 663-9.
316. Nikoletopoulou, V., et al., *Crosstalk between apoptosis, necrosis and autophagy.* Biochim Biophys Acta, 2013. **1833**(12): p. 3448-3459.
317. Luedde, M., et al., *RIP3, a kinase promoting necroptotic cell death, mediates adverse remodelling after myocardial infarction.* Cardiovasc Res, 2014. **103**(2): p. 206-16.
318. Smith, C.C., et al., *Necrostatin: a potentially novel cardioprotective agent?* Cardiovasc Drugs Ther, 2007. **21**(4): p. 227-33.
319. Oerlemans, M.I., et al., *Inhibition of RIP1-dependent necrosis prevents adverse cardiac remodeling after myocardial ischemia-reperfusion in vivo.* Basic Res Cardiol, 2012. **107**(4): p. 270.
320. Miao, B. and A. Degterev, *Methods to analyze cellular necroptosis.* Methods Mol Biol, 2009. **559**: p. 79-93.
321. Vanden Berghe, T., et al., *Necroptosis, necrosis and secondary necrosis converge on similar cellular disintegration features.* Cell Death Differ, 2010. **17**(6): p. 922-30.
322. Zhang, D.W., et al., *RIP3, an energy metabolism regulator that switches TNF-induced cell death from apoptosis to necrosis.* Science, 2009. **325**(5938): p. 332-6.
323. Cho, Y.S., et al., *Phosphorylation-driven assembly of the RIP1-RIP3 complex regulates programmed necrosis and virus-induced inflammation.* Cell, 2009. **137**(6): p. 1112-23.
324. Sun, X., et al., *RIP3, a novel apoptosis-inducing kinase.* J Biol Chem, 1999. **274**(24): p. 16871-5.
325. Dondelinger, Y., et al., *MLKL compromises plasma membrane integrity by binding to phosphatidylinositol phosphates.* Cell Rep, 2014. **7**(4): p. 971-81.
326. Hildebrand, J.M., et al., *Activation of the pseudokinase MLKL unleashes the four-helix bundle domain to induce membrane localization and necroptotic cell death.* Proc Natl Acad Sci U S A, 2014. **111**(42): p. 15072-7.
327. Wang, H., et al., *Mixed lineage kinase domain-like protein MLKL causes necrotic membrane disruption upon phosphorylation by RIP3.* Mol Cell, 2014. **54**(1): p. 133-146.
328. Han, J., C.Q. Zhong, and D.W. Zhang, *Programmed necrosis: backup to and competitor with apoptosis in the immune system.* Nat Immunol, 2011. **12**(12): p. 1143-9.
329. Vanden Berghe, T., et al., *Regulated necrosis: the expanding network of non-apoptotic cell death pathways.* Nat Rev Mol Cell Biol, 2014. **15**(2): p. 135-47.
330. Xie, T., et al., *Structural insights into RIP3-mediated necroptotic signaling.* Cell Rep, 2013. **5**(1): p. 70-8.
331. Vaseva, A.V., et al., *p53 opens the mitochondrial permeability transition pore to trigger necrosis.* Cell, 2012. **149**(7): p. 1536-48.

332. Hou, H., et al., *The role of RIP3 in cardiomyocyte necrosis induced by mitochondrial damage of myocardial ischemia-reperfusion.* Acta Biochim Biophys Sin (Shanghai), 2018. **50**(11): p. 1131-1140.
333. Zhang, T., et al., *CaMKII is a RIP3 substrate mediating ischemia- and oxidative stress-induced myocardial necroptosis.* Nat Med, 2016. **22**(2): p. 175-82.
334. Zhu, P., et al., *Ripk3 promotes ER stress-induced necroptosis in cardiac IR injury: A mechanism involving calcium overload/XO/ROS/mPTP pathway.* Redox Biol, 2018. **16**: p. 157-168.
335. Dmitriev, Y.V., et al., *Study of cardioprotective effects of necroptosis inhibitors on isolated rat heart subjected to global ischemia-reperfusion.* Bull Exp Biol Med, 2013. **155**(2): p. 245-8.
336. Stockwell, B.R., et al., *Ferroptosis: A Regulated Cell Death Nexus Linking Metabolism, Redox Biology, and Disease.* Cell, 2017. **171**(2): p. 273-285.
337. Doll, S. and M. Conrad, *Iron and ferroptosis: A still ill-defined liaison.* IUBMB Life, 2017. **69**(6): p. 423-434.
338. Dixon, S.J., et al., *Ferroptosis: an iron-dependent form of nonapoptotic cell death.* Cell, 2012. **149**(5): p. 1060-72.
339. Yagoda, N., et al., *RAS-RAF-MEK-dependent oxidative cell death involving voltage-dependent anion channels.* Nature, 2007. **447**(7146): p. 864-8.
340. Baba, Y., et al., *Protective effects of the mechanistic target of rapamycin against excess iron and ferroptosis in cardiomyocytes.* Am J Physiol Heart Circ Physiol, 2018. **314**(3): p. H659-H668.
341. Kim, J.Y., et al., *Human cystine/glutamate transporter: cDNA cloning and upregulation by oxidative stress in glioma cells.* Biochim Biophys Acta, 2001. **1512**(2): p. 335-44.
342. Feng, Y., et al., *Liproxstatin-1 protects the mouse myocardium against ischemia/reperfusion injury by decreasing VDAC1 levels and restoring GPX4 levels.* Biochem Biophys Res Commun, 2019.
343. Yang, W.S., et al., *Regulation of ferroptotic cancer cell death by GPX4.* Cell, 2014. **156**(1-2): p. 317-331.
344. Ursini, F., et al., *Purification from pig liver of a protein which protects liposomes and biomembranes from peroxidative degradation and exhibits glutathione peroxidase activity on phosphatidylcholine hydroperoxides.* Biochim Biophys Acta, 1982. **710**(2): p. 197-211.
345. Yang, W.S. and B.R. Stockwell, *Synthetic lethal screening identifies compounds activating iron-dependent, nonapoptotic cell death in oncogenic-RAS-harboring cancer cells.* Chem Biol, 2008. **15**(3): p. 234-45.
346. Wang, H., et al., *Characterization of ferroptosis in murine models of hemochromatosis.* Hepatology, 2017. **66**(2): p. 449-465.
347. Yang, W.S., et al., *Peroxidation of polyunsaturated fatty acids by lipoxygenases drives ferroptosis.* Proc Natl Acad Sci U S A, 2016. **113**(34): p. E4966-75.
348. Dixon, S.J. and B.R. Stockwell, *The role of iron and reactive oxygen species in cell death.* Nat Chem Biol, 2014. **10**(1): p. 9-17.
349. Torii, S., et al., *An essential role for functional lysosomes in ferroptosis of cancer cells.* Biochem J, 2016. **473**(6): p. 769-77.
350. Linkermann, A., et al., *Synchronized renal tubular cell death involves ferroptosis.* Proc Natl Acad Sci U S A, 2014. **111**(47): p. 16836-41.
351. Friedmann Angeli, J.P., et al., *Inactivation of the ferroptosis regulator Gpx4 triggers acute renal failure in mice.* Nat Cell Biol, 2014. **16**(12): p. 1180-91.
352. Kagan, V.E., et al., *Oxidized arachidonic and adrenic PEs navigate cells to ferroptosis.* Nat Chem Biol, 2017. **13**(1): p. 81-90.

353. Bulluck, H., et al., *Residual Myocardial Iron Following Intramyocardial Hemorrhage During the Convalescent Phase of Reperfused ST-Segment-Elevation Myocardial Infarction and Adverse Left Ventricular Remodeling.* Circ Cardiovasc Imaging, 2016. **9**(10).
354. Gammella, E., S. Recalcati, and G. Cairo, *Dual Role of ROS as Signal and Stress Agents: Iron Tips the Balance in favor of Toxic Effects.* Oxid Med Cell Longev, 2016. **2016**: p. 8629024.
355. Gao, M., et al., *Glutaminolysis and Transferrin Regulate Ferroptosis.* Mol Cell, 2015. **59**(2): p. 298-308.
356. Gaschler, M.M., et al., *Determination of the Subcellular Localization and Mechanism of Action of Ferrostatins in Suppressing Ferroptosis.* ACS Chem Biol, 2018. **13**(4): p. 1013-1020.
357. Doll, S., et al., *ACSL4 dictates ferroptosis sensitivity by shaping cellular lipid composition.* Nat Chem Biol, 2017. **13**(1): p. 91-98.
358. Golej, D.L., et al., *Long-chain acyl-CoA synthetase 4 modulates prostaglandin E(2) release from human arterial smooth muscle cells.* J Lipid Res, 2011. **52**(4): p. 782-93.
359. Imai, H. and Y. Nakagawa, *Biological significance of phospholipid hydroperoxide glutathione peroxidase (PHGPx, GPx4) in mammalian cells.* Free Radic Biol Med, 2003. **34**(2): p. 145-69.
360. Cao, J.Y. and S.J. Dixon, *Mechanisms of ferroptosis.* Cell Mol Life Sci, 2016. **73**(11-12): p. 2195-209.
361. Yang, W.S. and B.R. Stockwell, *Ferroptosis: Death by Lipid Peroxidation.* Trends Cell Biol, 2016. **26**(3): p. 165-176.
362. Imai, H., et al., *Lipid Peroxidation-Dependent Cell Death Regulated by GPx4 and Ferroptosis.* Curr Top Microbiol Immunol, 2017. **403**: p. 143-170.
363. Park, T.J., et al., *Quantitative proteomic analyses reveal that GPX4 downregulation during myocardial infarction contributes to ferroptosis in cardiomyocytes.* Cell Death Dis, 2019. **10**(11): p. 835.
364. Writing Group, M., et al., *Executive Summary: Heart Disease and Stroke Statistics--2016 Update: A Report From the American Heart Association.* Circulation, 2016. **133**(4): p. 447-54.
365. Berliner, J.A., et al., *Atherosclerosis: basic mechanisms. Oxidation, inflammation, and genetics.* Circulation, 1995. **91**(9): p. 2488-96.
366. Berliner, J.A. and A.D. Watson, *A role for oxidized phospholipids in atherosclerosis.* N Engl J Med, 2005. **353**(1): p. 9-11.
367. White, C.W., et al., *A cardioprotective preservation strategy employing ex vivo heart perfusion facilitates successful transplant of donor hearts after cardiocirculatory death.* J Heart Lung Transplant, 2013. **32**(7): p. 734-43.
368. White, C.W., et al., *A whole blood-based perfusate provides superior preservation of myocardial function during ex vivo heart perfusion.* J Heart Lung Transplant, 2015. **34**(1): p. 113-21.
369. Yeang, C., et al., *Reduction of Myocardial Ischemia-Reperfusion Injury by Inactivating Oxidized Phospholipids.* Cardiovasc Res, 2018.
370. Valko, M., et al., *Redox- and non-redox-metal-induced formation of free radicals and their role in human disease.* Arch Toxicol, 2016. **90**(1): p. 1-37.
371. Halliwell, B. and C.E. Cross, *Oxygen-derived species: their relation to human disease and environmental stress.* Environ Health Perspect, 1994. **102 Suppl 10**: p. 5-12.
372. Grivennikova, V.G. and A.D. Vinogradov, *Generation of superoxide by the mitochondrial Complex I.* Biochim Biophys Acta, 2006. **1757**(5-6): p. 553-61.
373. Kakhlon, O. and Z.I. Cabantchik, *The labile iron pool: characterization, measurement, and participation in cellular processes(1).* Free Radic Biol Med, 2002. **33**(8): p. 1037-46.
374. Gujja, P., et al., *Iron overload cardiomyopathy: better understanding of an increasing disorder.* J Am Coll Cardiol, 2010. **56**(13): p. 1001-12.

375. Dev, S. and J.L. Babitt, *Overview of iron metabolism in health and disease.* Hemodial Int, 2017. **21 Suppl 1**: p. S6-S20.
376. Sullivan, J.L., *Iron and the sex difference in heart disease risk.* Lancet, 1981. **1**(8233): p. 1293-4.
377. Kuo, K.L., et al., *Iron sucrose accelerates early atherogenesis by increasing superoxide production and upregulating adhesion molecules in CKD.* J Am Soc Nephrol, 2014. **25**(11): p. 2596-606.
378. Sullivan, J.L., *Iron in arterial plaque: modifiable risk factor for atherosclerosis.* Biochim Biophys Acta, 2009. **1790**(7): p. 718-23.
379. Tuomainen, T.P., et al., *Association between body iron stores and the risk of acute myocardial infarction in men.* Circulation, 1998. **97**(15): p. 1461-6.
380. Fang, X., et al., *Ferroptosis as a target for protection against cardiomyopathy.* Proc Natl Acad Sci U S A, 2019. **116**(7): p. 2672-2680.
381. Ahmed Elbaggari, J.C., Kevin McDonald, and Anthony Alburo, *Evaluation of the Criterion Stain Free gel imaging system for use in western blotting applications*, in *Bio-Rad Bulletin 5781*. 2008.
382. Lukas, A. and G.R. Ferrier, *Interaction of ischemia and reperfusion with subtoxic concentrations of acetylstrophanthidin in isolated cardiac ventricular tissues: effects on mechanisms of arrhythmia.* J Mol Cell Cardiol, 1986. **18**(11): p. 1143-56.
383. Maddaford, T.G., et al., *A model of low-flow ischemia and reperfusion in single, beating adult cardiomyocytes.* Am J Physiol, 1999. **277**(2 Pt 2): p. H788-98.
384. Roveri, A., M. Maiorino, and F. Ursini, *Enzymatic and immunological measurements of soluble and membrane-bound phospholipid-hydroperoxide glutathione peroxidase.* Methods Enzymol, 1994. **233**: p. 202-12.
385. Gang, H., et al., *PDK2-mediated alternative splicing switches Bnip3 from cell death to cell survival.* J Cell Biol, 2015. **210**(7): p. 1101-15.
386. Tsimikas, S., et al., *Human oxidation-specific antibodies reduce foam cell formation and atherosclerosis progression.* J Am Coll Cardiol, 2011. **58**(16): p. 1715-27.
387. Kuda, O., et al., *Sulfo-N-succinimidyl oleate (SSO) inhibits fatty acid uptake and signaling for intracellular calcium via binding CD36 lysine 164: SSO also inhibits oxidized low density lipoprotein uptake by macrophages.* J Biol Chem, 2013. **288**(22): p. 15547-55.
388. Gang, H., et al., *A novel hypoxia-inducible spliced variant of mitochondrial death gene Bnip3 promotes survival of ventricular myocytes.* Circ Res, 2011. **108**(9): p. 1084-92.
389. Agmon, E., et al., *Modeling the effects of lipid peroxidation during ferroptosis on membrane properties.* Sci Rep, 2018. **8**(1): p. 5155.
390. Conrad, M., et al., *Regulation of lipid peroxidation and ferroptosis in diverse species.* Genes Dev, 2018. **32**(9-10): p. 602-619.
391. Febbraio, M., D.P. Hajjar, and R.L. Silverstein, *CD36: a class B scavenger receptor involved in angiogenesis, atherosclerosis, inflammation, and lipid metabolism.* J Clin Invest, 2001. **108**(6): p. 785-91.
392. Endemann, G., et al., *CD36 is a receptor for oxidized low density lipoprotein.* J Biol Chem, 1993. **268**(16): p. 11811-6.
393. Sun, M., et al., *Light-induced oxidation of photoreceptor outer segment phospholipids generates ligands for CD36-mediated phagocytosis by retinal pigment epithelium: a potential mechanism for modulating outer segment phagocytosis under oxidant stress conditions.* J Biol Chem, 2006. **281**(7): p. 4222-30.
394. Abumrad, N.A., et al., *Cloning of a rat adipocyte membrane protein implicated in binding or transport of long-chain fatty acids that is induced during preadipocyte differentiation. Homology with human CD36.* J Biol Chem, 1993. **268**(24): p. 17665-8.
395. Baillie, A.G., C.T. Coburn, and N.A. Abumrad, *Reversible binding of long-chain fatty acids to purified FAT, the adipose CD36 homolog.* J Membr Biol, 1996. **153**(1): p. 75-81.

396. Silverstein, R.L., *Type 2 scavenger receptor CD36 in platelet activation: the role of hyperlipemia and oxidative stress.* Clin Lipidol, 2009. **4**(6): p. 767.
397. Drahota, Z., et al., *Succinimidyl oleate, established inhibitor of CD36/FAT translocase inhibits complex III of mitochondrial respiratory chain.* Biochem Biophys Res Commun, 2010. **391**(3): p. 1348-51.
398. Paradies, G., et al., *Lipid peroxidation and alterations to oxidative metabolism in mitochondria isolated from rat heart subjected to ischemia and reperfusion.* Free Radic Biol Med, 1999. **27**(1-2): p. 42-50.
399. Zhao, Q., et al., *Complex Regulation of Mitochondrial Function During Cardiac Development.* J Am Heart Assoc, 2019. **8**(13): p. e012731.
400. Readnower, R.D., et al., *Standardized bioenergetic profiling of adult mouse cardiomyocytes.* Physiol Genomics, 2012. **44**(24): p. 1208-13.
401. Azzu, V., N. Parker, and M.D. Brand, *High membrane potential promotes alkenal-induced mitochondrial uncoupling and influences adenine nucleotide translocase conformation.* Biochem J, 2008. **413**(2): p. 323-32.
402. Benderdour, M., et al., *Cardiac mitochondrial NADP+-isocitrate dehydrogenase is inactivated through 4-hydroxynonenal adduct formation: an event that precedes hypertrophy development.* J Biol Chem, 2003. **278**(46): p. 45154-9.
403. Chen, J., G.I. Henderson, and G.L. Freeman, *Role of 4-hydroxynonenal in modification of cytochrome c oxidase in ischemia/reperfused rat heart.* J Mol Cell Cardiol, 2001. **33**(11): p. 1919-27.
404. Choksi, K.B., et al., *Oxidatively damaged proteins of heart mitochondrial electron transport complexes.* Biochim Biophys Acta, 2004. **1688**(2): p. 95-101.
405. Humphries, K.M. and L.I. Szweda, *Selective inactivation of alpha-ketoglutarate dehydrogenase and pyruvate dehydrogenase: reaction of lipoic acid with 4-hydroxy-2-nonenal.* Biochemistry, 1998. **37**(45): p. 15835-41.
406. Humphries, K.M., Y. Yoo, and L.I. Szweda, *Inhibition of NADH-linked mitochondrial respiration by 4-hydroxy-2-nonenal.* Biochemistry, 1998. **37**(2): p. 552-7.
407. Lashin, O.M., et al., *Decreased complex II respiration and HNE-modified SDH subunit in diabetic heart.* Free Radic Biol Med, 2006. **40**(5): p. 886-96.
408. Kadenbach, B., *Regulation of respiration and ATP synthesis in higher organisms: hypothesis.* J Bioenerg Biomembr, 1986. **18**(1): p. 39-54.
409. Kaplan, P., et al., *Oxidative modifications of cardiac mitochondria and inhibition of cytochrome c oxidase activity by 4-hydroxynonenal.* Redox Rep, 2007. **12**(5): p. 211-8.
410. Mdaki, K.S., et al., *Age Related Bioenergetics Profiles in Isolated Rat Cardiomyocytes Using Extracellular Flux Analyses.* PLoS One, 2016. **11**(2): p. e0149002.
411. Smith, D.R., D. Stone, and V.M. Darley-Usmar, *Stimulation of mitochondrial oxygen consumption in isolated cardiomyocytes after hypoxia-reoxygenation.* Free Radic Res, 1996. **24**(3): p. 159-66.
412. Regula, K.M., K. Ens, and L.A. Kirshenbaum, *Inducible expression of BNIP3 provokes mitochondrial defects and hypoxia-mediated cell death of ventricular myocytes.* Circ Res, 2002. **91**(3): p. 226-31.
413. Wang, E.Y., et al., *p53 mediates autophagy and cell death by a mechanism contingent on Bnip3.* Hypertension, 2013. **62**(1): p. 70-7.
414. Eisner, D.A., et al., *Calcium and Excitation-Contraction Coupling in the Heart.* Circ Res, 2017. **121**(2): p. 181-195.
415. Mughal, W., et al., *Myocardin regulates mitochondrial calcium homeostasis and prevents permeability transition.* Cell Death Differ, 2018. **25**(10): p. 1732-1748.

416. Thompson, J.A. and M.L. Hess, *The oxygen free radical system: a fundamental mechanism in the production of myocardial necrosis.* Prog Cardiovasc Dis, 1986. **28**(6): p. 449-62.
417. Bersohn, M.M., K.D. Philipson, and R.S. Weiss, *Lysophosphatidylcholine and sodium-calcium exchange in cardiac sarcolemma: comparison with ischemia.* Am J Physiol, 1991. **260**(3 Pt 1): p. C433-8.
418. McHowat, J., et al., *Recent insights pertaining to sarcolemmal phospholipid alterations underlying arrhythmogenesis in the ischemic heart.* J Cardiovasc Electrophysiol, 1993. **4**(3): p. 288-310.
419. Carmeliet, E., *Cardiac ionic currents and acute ischemia: from channels to arrhythmias.* Physiol Rev, 1999. **79**(3): p. 917-1017.
420. Brame, C.J., et al., *Identification of extremely reactive gamma-ketoaldehydes (isolevuglandins) as products of the isoprostane pathway and characterization of their lysyl protein adducts.* J Biol Chem, 1999. **274**(19): p. 13139-46.
421. Fukuda, K., et al., *Oxidative mediated lipid peroxidation recapitulates proarrhythmic effects on cardiac sodium channels.* Circ Res, 2005. **97**(12): p. 1262-9.
422. Kramer, J.H., I.T. Mak, and W.B. Weglicki, *Differential sensitivity of canine cardiac sarcolemmal and microsomal enzymes to inhibition by free radical-induced lipid peroxidation.* Circ Res, 1984. **55**(1): p. 120-4.
423. Grinwald, P.M., *Calcium uptake during post-ischemic reperfusion in the isolated rat heart: influence of extracellular sodium.* J Mol Cell Cardiol, 1982. **14**(6): p. 359-65.
424. Renlund, D.G., et al., *Perfusate sodium during ischemia modifies post-ischemic functional and metabolic recovery in the rabbit heart.* J Mol Cell Cardiol, 1984. **16**(9): p. 795-801.
425. Komin, N., et al., *Multiscale Modeling Indicates That Temperature Dependent [Ca2+]i Spiking in Astrocytes Is Quantitatively Consistent with Modulated SERCA Activity.* Neural Plast, 2015. **2015**: p. 683490.
426. Hess, M.L. and N.H. Manson, *Molecular oxygen: friend and foe. The role of the oxygen free radical system in the calcium paradox, the oxygen paradox and ischemia/reperfusion injury.* J Mol Cell Cardiol, 1984. **16**(11): p. 969-85.
427. Krause, S.M., W.E. Jacobus, and L.C. Becker, *Alterations in cardiac sarcoplasmic reticulum calcium transport in the postischemic "stunned" myocardium.* Circ Res, 1989. **65**(2): p. 526-30.
428. Rowe, G.T., et al., *Hydrogen peroxide and hydroxyl radical mediation of activated leukocyte depression of cardiac sarcoplasmic reticulum. Participation of the cyclooxygenase pathway.* Circ Res, 1983. **53**(5): p. 584-91.
429. Ross, J.L. and S.E. Howlett, *Age and ovariectomy abolish beneficial effects of female sex on rat ventricular myocytes exposed to simulated ischemia and reperfusion.* PLoS One, 2012. **7**(6): p. e38425.
430. Grant, R.L., S.; Legg, G.; Burdge, G., *Gender differences in the PUFA-fatty acid composition of membrane*
phospholipids in rats. Proceedings of the Nutrition Society, 2008.
431. Jelinek, A., et al., *Mitochondrial rescue prevents glutathione peroxidase-dependent ferroptosis.* Free Radic Biol Med, 2018. **117**: p. 45-57.
432. Tuo, Q.Z., et al., *Tau-mediated iron export prevents ferroptotic damage after ischemic stroke.* Mol Psychiatry, 2017. **22**(11): p. 1520-1530.
433. Skouta, R., et al., *Ferrostatins inhibit oxidative lipid damage and cell death in diverse disease models.* J Am Chem Soc, 2014. **136**(12): p. 4551-6.